TECHNICAL, ECONOMICAL, AND ENVIRONMENTAL FEASIBILITY OF AIR SOURCE HEAT PUMP FOR RESIDENTIAL HOUSES IN COLD CLIMATE - CANADA

By

King Tung
B. Engineering (Mechanical and Industrial Engineering) 2014
Ryerson University

A thesis submitted to
Ryerson University

in partial fulfilment of
the requirements for the degree of

Master of Applied Science

in the program of
Mechanical and Industrial Engineering

Toronto, Ontario, Canada, 2020

Author's Declaration

I, King Tung, hereby declare that I am the sole author of this thesis. This is a true copy of the thesis, including any required final revisions, as accepted by my examiners.

I authorize Ryerson University to lend this thesis to other institutions or individuals for the purpose of scholarly research.

I further authorize Ryerson University to reproduce this thesis by photocopying or by other means, in total or in part, at the request of other institutions or individuals for the purpose of scholarly research.

I understand that my thesis may be made electronically available to the public.

TECHNICAL, ECONOMICAL, AND ENVIRONMENTAL FEASIBILITY OF AIR SOURCE HEAT PUMP IN COLD CLIMATE FOR RESIDENTIAL HOUSES - CANADA

Master of Applied Science, 2020
King Tung
Mechanical Engineering, Ryerson University

Abstract

With increasing concern towards global warming and the deadline of the Paris Agreement 2030 coming up, Canada is struggling to meet the desired greenhouse gas emission reductions. As new energy-efficient technology emerges, heating systems in Canada starts to move away from natural gas heating systems to efficient electrical heating systems such as air source heat pump. Though there are many studies related to reducing space heating, there are few studies performed on transitional technologies that are designed to slowly shift from natural gas-dependent society to an electrically powered society. This study analyses a smart switching system for a natural gas and air source heat pump dual system, and a cold climate air source heat pump water heater. These systems can significantly reduce greenhouse gas (GHG) emissions compared to a typical natural gas-fired heater. With these technologies Canada's residential sector could potentially meet Canada's Paris Agreement goals.

Acknowledgements

I am extremely grateful for the many people that have enabled me to undertake this research. This study was an ambitious and long undertaking. It would not have happened without the support from a vast number of people. Which is why this acknowledgment is necessarily long.

Firstly, I would like to thank my principal supervisor, Dr. Alan Fung. Your unwavering support and encouragement was often what pushed me to strive for more. Thank you for the unyielding belief in my ability which allowed me to be more creative and flexible with the study. Dr. Wey Leong, you provided invaluable introductions, advice and suggestions. Both of you guided me through this process, reassuring me when I needed it and offering consultation and friendship. Thank you.

Throughout this journey at Ryerson University there have been numerous people who have been pivotal to this enjoyable experience. I would like to thank my colleagues, fellow master and PhD students for many conversations, offering advice and support. A special mention must go to Farshad Kimiaghalam, Navid Ekrami, Danilo Yu, Annie Chow, and Anna Wang. I must also acknowledge the support and assistance provided by the Department of Mechanical and Industrial Engineering, particularly the administration staff, Lynn Reynolds, Jessica Miniaci, Lisa Holling, Lauren Sena, and Francine Belnavis, without you, we would all struggle with the simplest of tasks. I would also like to extend my thank to Karen Farjardo, previously our graduate program administrator, for always being warm and cheery whenever I needed her help. Finally, yet importantly, I would like to also thank the technical officers of the Mechanical and Industrial Engineering department, Grace He, Andrew Heim, Joseph Amankrah, and Roy Churaman, for assisting me with labs and giving me guidance.

Union Gas Limited and the team members have all provided information, feedback and invaluable discussion which helped shape the research. Union Gas also assisted financially for this project, providing funding for the equipment used and grants for the students involved. In addition, Wayne Dube and Karen Spring, were generous and patient with us during the project allowing for the testing and energy monitoring to take place in their lovely home. Thank you for the accommodation and good company during the interview phase. There would be no thesis without all the colleagues who were willing to spend time to help with the project proposal, the initial house audit and the sensors set-up team. Thank you! The support team from Obvious Inc helped saved countless hours, by calibrating all the sensors for the entirety of the data collection system. I am very grateful for the support they have given. Also, I would like to thank MITACS for providing funding for this innovative project.

To all the many people I met at the eSim Conference in Montreal, ESCC Conference in Mykonos, and ASim Conference in Hong Kong, I am so grateful for the warm welcome to your city. I appreciate the support and reward from IBPSA for the student travel award to fund me on the travel. Not only was everyone at the conference supportive, they gave me encouraging words and many recommendations for the study. I would also like to thank Ryerson's International Conference & Research Support Fund and Ryerson Mechanical and Industrial Engineering Department for providing financial support for the travels. These experiences with experts from other universities were invaluable.

A small portion of the project was supported by iGEN Technologies. Thank you for providing the new mini-cogeneration heater for this unique chance of testing and analysing it. Thank you for providing financial support and technical support. Although the project was short, the technical support from my fellow colleague, Shivam Saxena, provided me with guidance and insight that was transferred to this thesis. This project allowed me to extend the smart switching project to a cogeneration system. I am very grateful for NSERC Engage Grant and the Ontario Centre of Excellence for providing funding to support my study.

Mitsubishi Electric Canada provided support with state of the art equipment for testing and also provided with financial and technical support to finish this project. Without their water heating system and their support, this project would not have been completed. Aidan Brookson and Ricardo Brown were both extremely helpful. Without their expertise and their help, I would have been clueless on where to start. The financial support from the Ontario Centre of Excellence providing funding to support my study of this unique project.

It was an honour to receive the Queen Elizabeth II Graduate Scholarship in Science and Technology. I am very grateful to be selected for this scholarship. It was a great encouragement to know that hard work was recognized by such a prestigious scholarship program.

Last – and most definitely not least - I would like to thank my wonderful family. I am incredibly fortunate to have a mother, father, sister and other relatives who believed I could do this. Through all the encouragement you have provided over these last two years, I was able to face all the challenges and win over them. It was always appreciated, and I am very grateful to you for providing me a loving home especially when you were going through significant life events. Thank you for your patience and love. You all mean the world to me.

Table of Contents

List of Figures

List of Tables

Abbreviations

ACH: Air Changes per Hour

AHU: Air Handling Unit

APP: Advantage Pricing Plan

ASH: Archetype Sustainable House

ASHP: Air Source Heat Pump

ASHPWH: Air Source Heat Pump Water Heater

ASHRAE: American Society of Heating, Refrigerating and Air-Conditioning

CAD: Computer Aided Design

CCHT: Canadian Centre for Housing Technology

COP: Coefficient of Performance

DAQ: Data Acquisition

DHW: Domestic Hot Water

DWHR: Drain Water Heat Recovery

ERV: Energy Recovery Ventilator

GHG: Greenhouse Gas

GHGPPA: Greenhouse Gas Pollution Pricing Act

HDD: Heating Degree Days

HX: Heat exchanger

HST: Harmonized Sales Tax

HVAC: Heating, Ventilation and Air Conditioning

IEA: International Energy Agency

IESO: Independent Electricity System Operator

LSHSDFSS: Load Shifting Smart Dual Fuel Switching System

MATLAB: Matrix Laboratory software

NBC: National Building Code

NG: Natural Gas

NRCan: Natural Resource Canada

NZEH: Net Zero Energy House

OBC: Ontario Building Code

OCE: Ontario Center of Excellence

PST: Provincial Sales Tax

PV: Photovoltaic

RH: Relative Humidity

RMSE: Root Mean Square Error

SCM: Switching Control Model

SCOP: Seasonal Coefficient of Performance

SDFSS: Smart Dual Fuel Switching System

SEER: Seasonal Energy Efficiency Ratio

TMY: Typical Meteorological Year

TOU: Time-Of-Use

TRCA: Toronto and Region Conservation Authority

TRNSYS: Transient System Simulation Tool

UNFCCC: United Nations Framework Convention on Climate Change

Nomenclature

Cap_{Min} = *Capacity for the temperature using the minimum capacity curve (W)*

Cap_{Max} = *Capacity for the temperature using the maximum capacity curve (W)*

$COP = Coefficient\ of\ performance\ for\ ASHP$

COP_{Min} = *COP for that temperature using the minimum COP curve*

COP_{Max} = *COP for the temperature using the maximum COP curve*

$C_p = Specific\ heat\ capacity\ of\ the\ fluid\ (kj/kg°C)$

$C_T = Total\ annual\ operating\ cost\ (\$)$

$D_E = GHG\ density\ for\ electricity\ consumption\ (kg/kWh)$

$D_{NG} = GHG\ density\ for\ natural\ gas\ (kg/m^3)$

$E = ASHP\ electricity\ consumption\ (kWh)$

$e_c = Hourly\ cost\ of\ electricity\ (\$)$

$e_e = \ Effective\ electricity\ cost\ (\$)$

$E_{in} = Electricity\ Input\ (kWh)$

$GHG_e = Hourly\ GHG\ emission\ from\ electricity\ consumption\ (kg)$

$GHG_n = Hourly\ GHG\ emission\ from\ natural\ gas\ consumption\ (kg)$

$GHG_{Total} = Total\ Greenhouse\ Gas\ Emissions\ (kg)$

$H = Space\ heating\ demand\ (kWh)$

$\dot{m} = mass\ flowrate\ of\ the\ fluid\ (kg/min)$

$N = Furnace\ natural\ gas\ consumption\ (m^3)$

$n_c = Hourly\ cost\ of\ natural\ gas\ (\$)$

$n_e = Effective\ natural\ gas\ cost\ (\$)$

$\eta_n = Efficiency\ of\ natural\ gas\ furnace\ (\%)$

$\rho = Density\ of\ the\ fluid\ (kg/m^3)$

$P_e = Marginal\ pricing\ of\ electricity\ per\ kWh\ (\$/kWh)$

$P_n = Marginal\ price\ of\ natural\ gas\ per\ m^3 (\$/m^3)$

$P_{Tax} = Price\ of\ the\ carbon\ tax\ (\$/tonne)$

$Q = Heat\ supplied\ by\ ASHPWH\ (kWh)$

$\Delta T = Temperature\ (°C)$

$U_n = Natural\ gas\ energy\ density\ (kWh/m^3)$

$\dot{V} = Volumetric\ flow\ rate\ (L/min)$

Chapter 1 – Introduction

The global energy demand was on an increase where the primary energy consumption and CO_2 emission have grown by 49% and 43%, respectively, from 1984-2004 [1]. A primary energy source is considered source energy that is un-transmitted such as natural gas and coal. Fossil fuels are not the only examples of primary energy, and it also includes renewable energy and nuclear energy, which is not considered fossil fuel but would still be considered primary energy. If the trend continues to grow at the current rates, the effects of global warming will be more evident. According to Pérez-Lombard et al. [1], the emerging nations are consuming more energy at a growth of 3.2% and will exceed the consumption rate of developed countries by the year 2020. Due to this frightening data, we need to be vigilant in the near future by reducing greenhouse gas (GHG) emissions and total energy consumption.

Climate change continues to have a massive impact on the world today, causing tremendous negative environmental impacts. The effects of climate change affected even the Himalayan glaciers, causing an estimated loss of 174 gigatonnes of water from the glaciers [2]. A new agreement, Paris Agreement, proposed by the United Nation Framework Convention on Climate Change (UNFCCC) was implemented to attempt to halt the global average temperature from increasing and reducing the greenhouse gas emissions [3]. The Paris Agreement aims to limit global warming to 1.5°C-2°C above the pre-industrial levels [4]. In response to the Paris Agreement, Canada developed the Pan-Canadian Framework on Clean Growth and Climate Change. The main feature of the framework was to implement a tariff for carbon pollution, a more stringent energy efficiency standard, actions to help adapt to climate change and also investing in clean technology, innovation, and jobs [5].

The residential sector is the third-largest source of greenhouse gas (GHG) emissions in Canada, accounting for 14% of the GHG emissions in 2016 [6]. Within the residential sector, space heating amounts to over 60% of the GHG emission. The most significant emission reduction in this sector can be achieved by transitioning from fossil fuel-dependent furnaces to a fully electric heating system. Such transition will require a shift in demand from natural gas to electricity. A recent paper from the journal of Renewable and Sustainable Energy Reviews, presented by Nejat et al. [7], found that the residential sector represents 27% of the global energy consumption and 17% of the global CO_2 emissions. It was also found that the global residential energy consumption grew by 14% from the year 2000 to 2011. This high growth was mostly due to the developing countries where the population growth is the primary driver of the increase in energy consumption. Nejat et al. [7] also showed that the three highest global energy consumption was in the transportation, industry, and residential sectors in descending order. In order to reduce GHG emissions, the energy consumption within these three sectors must be reduced. Energy consumption from transportation is tough to reduce since large

commercial emitters such as shipping tankers and airplanes emissions are included in the count. A feasible option is to reduce residential energy consumption and industrial energy consumption by introducing energy-efficient technology. Figure 1.1 shows the total GHG emissions of different sectors in Canada concerning the different sectors.

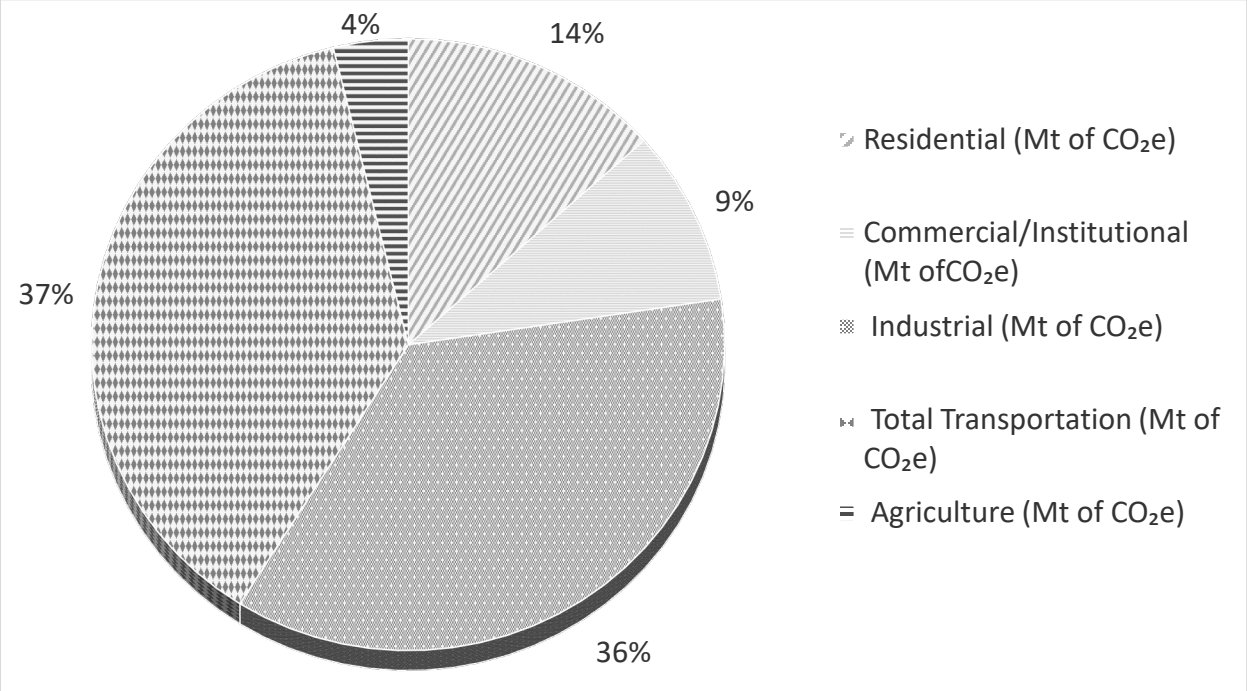

Figure 1.1: Total GHG Emissions in Canada [8]

Figure 1.1 shows the breakdown of GHG emission in Canada. The residential sector emits 14% of the total GHG emission in Canada. Though the residential sector does not produce the highest amount of GHG emission, the residential sector is still the third-largest contributor to Canada's GHG emission.

Canada, along with many other countries, came together to sign the Paris agreement to reduce the GHG emission to 30% below 2005 levels by 2030 [9]. In order to meet this target, all five major sectors illustrated in Figure 1.1 must significantly reduce the GHG emission. According to Natural Resources Canada in 2016, 66% of the Canadian housing stock was built in 1995 or prior [10]. A majority of these houses were built before the Ontario Building Code Act of 1992 (OBC) where standards and restrictions for the envelope were following a less stringent National Building Code (NBC) of Canada [11]. Though the OBC improves the performance of new houses built after the realization of it, the vintage houses built to older NBC or OBC standards do not need to meet new OBC codes. This resulted in many houses with higher heating and cooling demands than houses meeting the current OBC codes. Having new technologies such as the efficient air source heat pump (ASHP) to meet the high heating demand instead of natural gas furnace would reduce the GHG emission significantly.

Starting from the year 2003, Ontario strived to reduce coal-fired generating stations. The five-main coal power plants located at Lakeview, Nanticoke, Lambton, Thunder Bay, and Atikokan was slowly decommissioned and was successfully removed from the electrical grid in 2014 [12]. The Ontario electrical grid was officially off coal in 2014 and was replaced with mainly nuclear, natural gas, hydro-electric and other non-hydro renewables. In 2014, 60% of the electrical grid supply was from nuclear energy, 24% was from hydro-electric, 9% was from natural gas, and 7% was from non-hydro renewables [12]. The natural gas is mainly used to achieve peak demands during peak hours [13]. Ontario's grid is relatively clean compared to the previous coal-fired plants. With this recent change, electricity is an environmentally friendly energy alternative for private transportation, industrial and residential heating and cooling systems. Though coal-fired power plants were phased out, natural gas-fired peaking power plants are still used in order to meet the high peaks during peak demand times. This causes the GHG intensity of electricity to increase during the peak hours. Though the source of electricity is cleaner than before, there is still an urgency to reduce the overall GHG emission by reducing electricity consumption.

Figure 1.2 shows the breakdown of residential energy consumption. The space heating GHG emissions are the highest portion of the overall residential GHG emissions. This is due to the high amount of fossil fuel consumption for space heating [14]. A similar situation for domestic water heating is also evident, which is the second-highest GHG emitter.

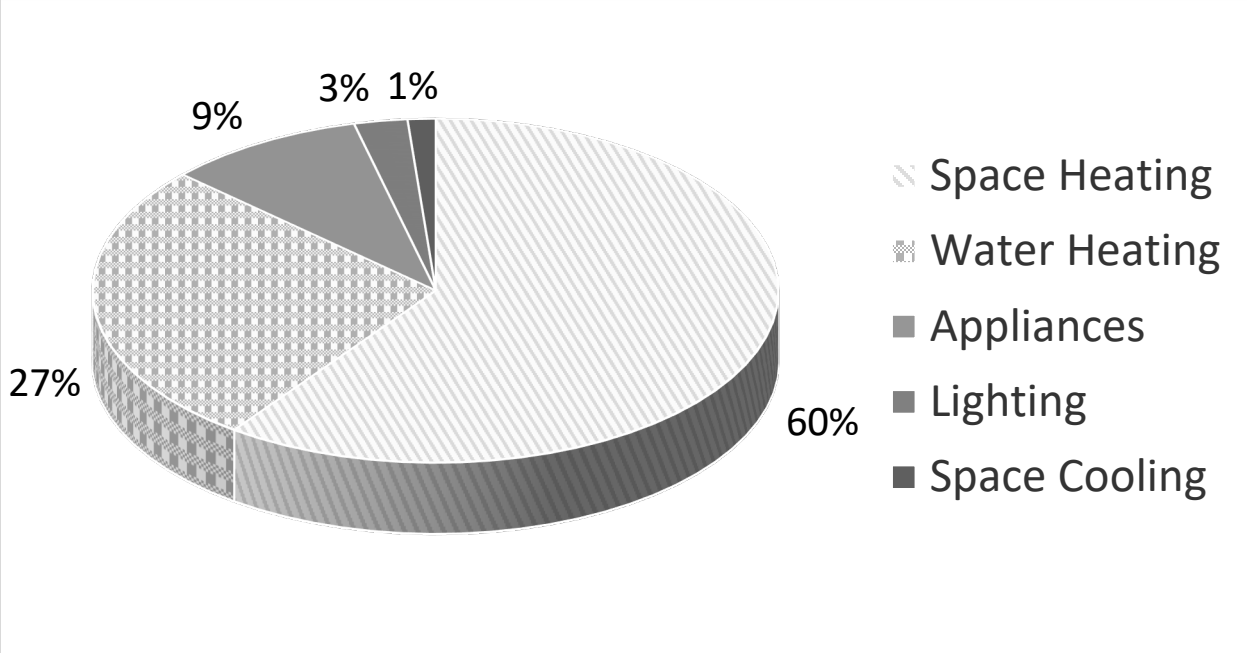

Figure 1.2: Breakdown of Residential GHG Emissions [8]

Domestic hot water is the second-highest energy consumer for residential end-use [15]. Though space heating consumption holds 60% of the total residential energy consumption, water heating consists of 27% of the end-

use energy demand. By minimizing the two significant sources of GHG emission, the overall GHG emission from the residential sector could be significantly reduced.

There are several adopted methods of reducing energy consumption. One of the most common practice is to meet energy guidelines such as the new Ontario Building Code, R2000 and EnergyStar [16–18]. The voluntary guidelines, R2000, and EnergyStar aim to reduce energy consumption in the residential sector. Though these guidelines are relatively effective, a net-zero energy home (NZEH) built to a net-zero standard will be much more efficient. A NZEH is a house that consumes as much energy as it produces over a year [19]. A NZEH is an excellent method in overall reducing energy consumption however, the current Canadian residential housing stock shows that most houses use natural gas for heating. It is unreasonable to expect a drastic change in the building envelope for the full Canadian housing stock. A change in heating fuel would be a more cost-effective alternative to envelope improvements for carbon emission reduction.

According to NRCan, over 64% of the heating demand for Canada's heating was met with natural gas or heating oil [14]. A transitional technology is needed to slowly convert the fossil fuel-dependent heating system to a more environmentally friendly electrical system. One method to reduce the GHG emission is to convert residential natural gas-consuming equipment to electrically powered alternatives. Several types of household equipments that utilize natural gas (NG) can be replaced with an equivalent or superior electrical counterpart. Currently, the most commonly used heating energy sources in Ontario is natural gas [20]. Two primary electricity sources of heating in Ontario are electrical resistance heating and electric air-source heat pump (ASHP) heating [21].

In specific locations, the switch to electricity might be counter-intuitive since some locations still utilize coal as the primary source of electricity. Due to the cleaner electrical grid in Ontario, implementing electrical heating is an excellent alternative for natural gas residential furnaces. Electrical resistance heating uses electricity as the primary energy source and converts the energy into heat. This process is exceptionally efficient where all the electricity converts into heat. ASHP, on the other hand, uses electricity to "pump" heat from one location to another location. Due to this ability to move heat around rather than to generate it, heat pumps can provide more useful thermal energy than required to operate the heat pump. This effectively produces more useful heat than the heat pump's energy consumption. Residential houses are starting to adopt heat pumps for space heating to reduce the operational cost and reduce the environmental impact.

Long term forecast of electricity and natural gas demand in Ontario performed in 2018 showed that there is a slight decline in demand from 2018 to 2020 [22]. A further prediction performed by the IESO showed the overall increase prediction for several different scenarios [23, 24]. This forecast was likely performed with

the pretense that there are no drastic changes in the pricing schemes, additional imposed tax, and new efficient technologies.

The Canadian federal government committed to encouraging low carbon alternatives and the growth of clean technology that reduces GHG emissions [25]. The government announced that the new target is to reduce the GHG emission by 80% by 2050, relative to 2005 GHG levels. By 2017, the GHG emission reduction has reached 28% from 2005 levels [26]. The next primary target, as highlighted in the Paris Agreement, is to reduce GHG emission by 30% by 2030 [27]. Though Canada is actively adopting clean technology, more intensive plans will be needed in order to meet the 2050 goal. As a result of this additional pricing on carbon, fossil fuels such as natural gas will not be as economical compared to today's standards. This pricing change might encourage the community to conserve energy and put efforts in conservation.

1.1 Background to the study

In the Ontario residential sector, there are limited options available for electrical heating alternatives. Two main categories reviewed in this thesis are electrical resistance heating and electrical air-source heat pump (ASHP) heating. ASHP is much more efficient when compared to an electrical resistance heater. Some heat pumps can provide six times more heat than the energy required for operation. This study addressed an experimental heat pump switching system using ASHP as the primary heating source with the furnace as supplementary heating, and an air-source heat pump water heater (ASHPWH) which utilizes a cold-climate air source heat pump.

The primary concerns with implementing such ASHP is the increase in electricity demand. If all the NG furnace were to be replaced with electrical resistance or ASHP, the electrical grid would not be able to provide enough energy for the increase of demand. Currently, the electrical grid is using NG generator plants to meet peak load electric demands. It is a reasonable prediction that having all the HVAC system in Ontario switch to ASHP will cause a detrimental increase in demand to the power grid. To combat this problem, a smooth transitional stage was required before fully converting to full electric heating.

Few studies have explicitly looked at technologies that would be considered transitional technology. One similar studies looked at a load shifting smart dual fuel switching system with electrical and natural gas as a source for space heating. This past study was a predecessor where the simulation investigated several types of switching systems, including Smart Dual Fuel Switching System, Load Shifting and Load Shifting Smart Dual Fuel Switching System [28]. The current literature is heavily reliant on using an air source heat pump (ASHP) as the primary source for heating. This was because an ASHP is extremely efficient where instead generating heat using electricity, it moves heat from one source to another. This efficient technology can potentially output heat a few times as much electricity used to operate the system. Using an ASHP for load

shifting can effectively take advantage of the ASHP efficiency to pre-heat or pre-cool the house. This load shifting technology can be considered a transitional method for the shift from a natural gas dominated heating, ventilation and air conditioning (HVAC) system to a more environmentally friendly electricity dominated system powered by renewable energy source.

To provide a smooth transitional stage, both the natural gas furnace and the electrical ASHP should be used simultaneously in order to provide a flexible heating option. Alibabaei et al. [28], performed a study on a load switching smart dual fuel switching system which was capable of switching the fuel source from the traditional NG to the more efficient ASHP when the pre-set requirement conditions are met and use load shifting strategies to offset peak demands. With this load shifting algorithm, the electrical grid can control the heating source using load shifting. This system allows the electrical grid to make the decision, during high peak demand times, to switch heating operation from ASHP to NG furnace. This shifting algorithm lowers the burden of the electricity grid and will remedy the concern of exceeding the demands. This could reduce the need for natural gas power plants for peak hours. In addition to load shifting, the load shifting smart dual fuel switching system (LSHSDFSS) can switch the fuel source from NG to ASHP depending on the time of use pricing cost.

Since Ontario follows a time-of-use pricing scheme for electricity, the LSHSDFSS can pick the optimal times when the heat pump will operate; and, for higher electricity costs, the natural gas furnace will operate. This allows the homeowner to gain the cost benefits of the LSHSDFSS and reduce GHG emissions. This encourages researchers to develop such HVAC systems to provide a better alternative to a traditional natural gas furnace and also to inform the community of the benefits of such developments.

Domestic hot water (DHW) heating, the second-largest source of carbon emission in Canada, should also be analyzed as a significant contribution to the GHG emission. In literature, a heat pump is generally used as an environmentally friendly alternative for a natural gas furnace or an electric water heater. By using such an energy-efficient alternative, the energy consumption was reduced, and the carbon emission will also, in effect, be reduced. Since heat pumps generally utilize electricity to meet heating demands, it replaces the need for natural gas and also effectively remove the carbon emission from natural gas in a residential home. There are a few types of system configurations that utilize heat pump as its source of heating.

There are several types of heat pump water heaters that are currently available in the market. However, the performance of the current technology was only economically beneficial in milder temperatures such as the winter in many European climates. In colder climate, the heat pump water heater was not able to extract enough heat from the outdoor air to heat domestic hot water efficiently. Bursill and Cruickshank performed an experimental study on an ASHP water heater using indoor air as the heating source [29]. The results of the study show that there was a COP of 1.7-2 when the water set-point temperature was set to 60°C. This

shows that the heat pump wass an efficient alternative to a natural gas boiler with 80% efficiency. However, since Cruickshank's study was performed indoors where the heat was extracted from the indoor ambient air. This will lower the performance of the space heating system in place of higher performance for the ASHPWH.

Similarly, Amirirad et al. [30] performed a study on an ASHPWH for the residential sector in cold Canadian climate at the Toronto Region Conservation Authority (TRCA) Archetype Sustainable House (ASH) located in Vaughan, Ontario. The study result showed that there were a substantial GHG reduction and a 55% electricity consumption when the ASHPWH was compared with an electric resistance water heater [31]. However, the ASHPWH used in this study was an indoor unit which uses the indoor ambient air as a heating source. This results in an overall increase in space heating during the winter. The slight heating demand increase could result in potential performance reduction by increasing the heating load that the heat pump was required to meet. However, as an alternative to natural gas furnaces, this system is currently an excellent candidate for reducing carbon emissions.

As an alternative to the indoor ASHPWH, an outdoor heat pump unit could be of used to mitigate the impact to indoor heating demand. Similar to the ASHP for space heating, the ASHPWH utilizes the outdoor air and extracts usable heat from the outdoor ambient air, and the fluid was moved to a refrigerant to water heat exchange unit. With the heat exchanger unit implemented, the heat generally allocated for space heating will now be used to heat the domestic hot water. The domestic hot water storage tank stores the water for later use. A similar combination is currently available in European countries with milder winters. This system was extremely efficient when the outdoor air temperature was relatively high, such as the outdoor air in summer.

However, the performance of the system was significantly reduced during the harsh winter in the cold climate regions. Such systems are mainly marketed towards milder winter climates such as in Europe. ASHP designed to be used in European climates could not meet the required heating capacity in cold climates. A cold climate ASHP specifically designed to have a higher capacity in a colder climate must be used in place of European systems. A backup system was also installed which will turn on the secondary electrical heating system when the air source heat pump cannot provide enough heat. The secondary energy source will only operate when the outdoor temperature is too low for the heat pump to function efficiently. In warmer climates, the secondary heating source is not as crucial. However, in colder climate, the secondary heating source is a crucial feature to ensure the residence have hot water during cold days.

1.1.1 Justification for the research

The research in this thesis is to analyze technology that mitigates environmental pollutant by implementing low GHG intensity technology to replace higher GHG emitters. The topics discussed in this thesis focuses on reducing environmental impacts from the residential sector. This study explores two different applications of ASHP in residential sector and its economic and environmental impacts. The study consists of simulations and analysis with computer simulation, mathematical models, and experimental results. The work done in this thesis is building upon a few previous studies.

The first heat pump application investigated was the Smart Dual Fuel Switching System. The Smart Dual Fuel Switching System was based on Alibabaei et al. [9] study on a model predictive controller, load shifting strategy plan and the initial idea of the SDFSS [32]. The pricing of electricity and natural gas was changed, and the SDFSS in this thesis takes advantage of the difference in cost. This prior study did not have extensive experimental backing and was not analyzed with different scenarios that could extend to other cold climate locations.

The ASHPWH project was based on Amirirad et al. [31] study on an ASHPWH which utilizes the indoor basement air as the heat source as a solution to the frigid climate. This study showed that during the winter season, the heating demand was increased, adding additional load to the space heating system. If the space heating was met by an ASHP, this additional load could increase the overall cost and GHG emission. This second part of the study was to implement an outdoor cold climate ASHP to an ASHPWH with an indoor hydrobox unit and determine the energy consumption, GHG emission reduction, and the operating costs.

Overall, these studies are either not experimentally verified, not performed on an icy climate, or the switching control system does not provide an impactful economic return. The current literature does not take into account the foreseeable changes in policies and how it impacts the effectiveness of the control systems. This study aims to fill this research gap by first introducing the smart dual fuel switching system model and the required parameters. Next, the overall benchmark calibrated model and the experimental results will be presented. The calibrated simulation model was used to demonstrate the flexibility of the smart dual fuel switching control system for several sensitivity analyses. The goal of the study was to answer the main question "*How effective was the smart dual fuel switching system in different cold climate cities, and how does it perform in future high-carbon pricing scheme from a greenhouse gas emission and economic perspective?*".

In this study, the main focus was to simulate the cloud-integrated Smart Dual Fuel Switching System (SDFSS). This system acts like a transitional technology that helps bridge the gap between a full natural gas-fired heating system to a more environmentally friendly electrical alternative. The benchmark of the study

was to simulate a residential house that was located in Strathroy, Ontario. The simulation aims to show the benefit of having a transitional technology compared to having the manufacturer control system or conventional natural gas furnace only heating system.

The SDFSS uses different parameters to predict the operational cost and GHG emission for the scenario. In this study, the base case scenario uses the outdoor temperature, natural gas, and electricity utility pricing, equipment performance and the date and time of the scenario. These parameters are constantly changing, affecting the overall hourly cost. SDFSS is flexible where changes can be made immediately, and the system can also potentially take advantage of more parameters.

Using the two different applications of the ASHP, net-zero energy houses and net zero-emission houses could be more approachable to the average residential owner.

1.1.2 Significance of the thesis

Due to the approaching Paris agreement deadline, efforts have been made by the Canadian Federal government to reduce the GHG emission. The Canadian Federal Government has imposed carbon pricing on fossil fuel to disincentivize the use of fossil fuel [33]. This added cost on fossil fuel will lessen the pricing difference between natural gas and electricity, allowing electricity to be a competitive cost source for heating. This also incentivizes the reduction of GHG emission, which will promote technologies such as ASHP.

This research investigates two applications for ASHP in cold climate locations such as Canada. The two chapters (Chapter 2-3) are based on two case studies. The findings contribute to current knowledge of smart fuel switching control systems and ASHPWH, in particular, addressing the gaps including:

1) Overall effectiveness, the flexibility of the SDFSS accounting for several foreseeable parameters
2) Potential for a cold climate ASHPWH with the outdoor unit in cold climates
3) Overall environmental and economic impacts of both ASHP systems in comparison with typical natural gas equipment

The first case study performed was based on a residential house in Strathroy, Ontario. The residential house was occupied by a retired couple and sensors were installed to monitor the energy consumption. This house was also built to meet net-zero standards at the time of development. Using such an efficient house, the performance of the SDFSS was analyzed to investigate its performance. The objective of the case study was to collect information to simulate the SDFSS on a calibrated model and use it to extend its result to simulate other situations.

The second case study was performed at the TRCA ASH. The ASHPWH was installed and tested at the TRCA ASH for half a year. The data obtained was used to improve the simulation model. Energy consumption, operating costs, and GHG emissions are simulated to show the performance of the ASHP. The simulation model will allow the results to translate to other cold climate regions.

The GHG reduction of both these technologies can substantially reduce the overall GHG emissions in the residential sector. The reduced operating cost from the SDFSS can incentivize residential homeowners to convert older natural gas equipment to a full electric heating system. The flexibility of the SDFSS can be extremely beneficial and also allows the system to adapt to most changes in parameters. In addition to that, the combination of the two technologies can be used to control the electrical peak. By using the connectivity of the SDFSS cloud system, the ASHPWH could utilize extra electricity from the electrical grid during off-peak hours. The SDFSS cloud system could also potentially allow utility companies to schedule its own load demand response plans for peak load management. This not only helps the utilities managing the electricity grid system but it also potentially reduces the need for peaking natural gas-fired power plants, ultimately eliminating the GHG intensity from the grid.

This study is significant because it potentially has an impact on the GHG emission problem on a national level. The two application for ASHP was an accessible solution which could be implemented by typical residential homeowners. It was ambitious in its focus on two case study in such a short period. This study allows for more full scope and a broader perspective on ASHP as a sustainable alternative for the residential sector. This study has provided a potential solution which was extended to other location in Canada and could be further extended to other cold climate regions.

1.2 Research aims

The aims of the thesis were developed from the gaps in the literature for fuel switching based system. Specifically, this study aims to explore the environmental benefits of implementing ASHP in residential houses and describes the potential for operating cost and GHG emission reductions. The following question guides the flow of the thesis:

1. What can be done to lower the GHG emission without overloading the electrical grid?
2. What is its role in the path of sustainability?
3. What are the environmental benefits?
4. What are the economic benefits?

This thesis was divided into two ASHP configurations:

1. Smart Dual Fuel Switching System (SDFSS)

In this study, the main focus was to simulate the cloud-integrated Smart Dual Fuel Switching System (SDFSS). This system acts like a transitional technology that helps bridge the gap between a full natural gas-fired heating system to a more environmentally friendly electrical alternative. The benchmark of the study was to simulate a residential house that was located in Strathroy, Ontario. The simulation aims to show the benefit of having a transitional technology compared to having the manufacturer control system or conventional natural gas furnace only heating system.

2. Air Source Heat Pump Water Heater (ASHPWH)

The primary purpose of this study was to experimentally analyze the air source heat pump water heater in the Canadian climate. This is important as the system was initially designed for the European market and the winters experienced in the European region is milder in comparison to the Canadian winters. The main goal of the study was to experimentally evaluate the impact of the air source heat pump water heater in Toronto and to analyze the potential energy cost savings and greenhouse gas emission reduction. This analysis was also extended to other major Canadian cities.

1.3 Structure of the thesis

This thesis consists of four chapters including the first chapter, the introduction chapter (Chapter 1), two chapters presenting the results from the two case studies (Chapter 2 – 3), a discussion chapter (Chapter 5) analyzing the results and a conclusion chapter (Chapter 5).

Chapter 1 introduces the research topic and the background of the study by summarizing what was already known in the topic of smart switching systems and air source heat pump water heaters, identifying the gaps related to the application of the ASHP and the significance of the study, introduces the case study, and define the research aims.

Chapter 2 provides an extensive analysis of the smart dual fuel switching system and its impact in cold climates. This chapter presents the parameters used and explains the methods of the case study. The results are then presented at the end of the chapter. The results include a sensitivity analysis that explores several different parameters.

Chapter 3 examines the simulation of an ASHPWH in Toronto, Montreal, Halifax, Edmonton, and Vancouver. The methods and parameters used for the experiments are explained for this case study. The experimental results were also analyzed and illustrated to show the performance of the ASHPWH.

Chapter 4 combines and integrate the significant findings of chapters 2 and 3, highlighting the contribution of the research.

Chapter 5 concludes the thesis with implications from the research with potential future work. Additionally, it explores the possibility and implications for meeting the Paris Agreement.

Chapter 2 – Residential Smart Dual Fuel Switching System (SDFSS) for Simultaneous Reduction of Energy Cost and GHG Emission

2.1 Methods

A comprehensive overview of the two simulation models used in this study was investigated in this section. This section describes the combined Transient System Simulation Tool (TRNSYS) house model and Switching Control Model (SCM) to assess the technical and economical operation of the switching system for the selected house [18]. Next, six different scenarios and four sensitivity analyses are defined and described. Lastly, a detailed description of the parameters for the sensitivity analyses was also included.

2.1.1 Simulation models

Two computer models are used to simulate natural gas consumption, electricity consumption, operating cost, and the GHG emission for six different heating systems. The heating demand was first simulated with the TRNSYS house model. Next, the overall results for each scenario are simulated with each SCM, which accounts for the inputs and parameters mentioned in the study. For the sensitivity analysis, the model was re-initiated with each of the changed parameters. In the post-analysis, the results of the different scenarios and sensitivity analyses are compared. The energy cost savings and GHG emission reduction compared to the natural gas-fired heating only system was calculated. In this study, the simulation models ran for the year 2018.

2.1.1.1 TRNSYS house model

The TRNSYS house model was a simulation model that calculates the heating demand for the given parameters (Section 2.2.1). The model was built based on the NZEH located in Strathroy, Ontario. The house specifications were obtained from the builders and developers; additionally, a comprehensive energy audit was also performed to validate the house performance. Additional energy end-use was collected from the installed sensors during the experimentation period to validate the model.

Based on the detailed information gathered, a computer-aided design (CAD) simulation model was created on TRNSYS-SketchUp. The house information, including dimension, infiltration, wall insulation, window characteristics, and occupant behaviour was necessary to build an accurate house model. Next, additional modules were added to simulate the surrounding environments and other components in the house. The full TRNSYS model was built to mainly simulate the annual space heating demand using the input parameters set. The output results are used as an input to the SCM.

The TRNSYS model in this study was calibrated using experimental data collected. In the experiment, the benchmark house was considered a NZEH at the time of conception and development and will be referred to as the NZEH in this study. The NZEH was a newly constructed house with two floors, main floor, and basement, which collectively account for 2586 ft^2 of conditioned living space. The residents are a retired couple with two dogs. This house was also fitted with both an air source heat pump (rated at 3.3 COP and 21 SEER) and an efficient natural gas furnace (89% efficiency) for space heating and cooling. To offset the electricity consumption, a photovoltaic (PV) system (8.745 kWp installed capacity), enthalpy recovery ventilation system (ERV) with sensible recovery efficiency of 75% at 0°C, and a drain water heat recovery system (DWHR) rated at 53.3% efficiency was also installed. For the domestic water heating, a high efficiency instantaneous natural gas hot water boiler was installed.

To gather information for the computer simulation, a full ASHRAE level II energy audit was performed on the house in November 2017. The energy audit included verification of envelope dimensions, plug load audit, lighting audit, combustion test, and blower door depressurization test. This information was collected, analyzed and, used to construct the benchmark TRNSYS model.

An experimental test was performed on the NZEH to experimentally validate the effects of different switching systems. A data acquisition (DAQ) system was installed based on the required parameters and requirements of the SDFSS. The natural gas furnace only operation was tested for two weeks, and an additional two weeks of standard manufacturer heat pump switching was tested.

The data collected was for every two-minute intervals, and during the analysis, the data was consolidated to hourly intervals. The sensors installed at the Strathroy NZEH was as followed:

Table 2.1: List of Sensors

Electricity Consumption/Generation Sensors	Natural Gas Consumption Sensors	Indoor Parameters	Outdoor Parameters
Air source heat pump (W) (0.5% Error)	Natural gas fired furnace (m^3) ($0.05m^3$ per pulse)	Main floor temperature (°C) (±0.3°C)	Ambient outdoor air temperature (°C) (±0.3°C)
Air handling unit (W) (0.5% Error)	Instantaneous domestic hot water boiler (m^3) ($0.05m^3$ per pulse)	Basement temperature (°C) (±0.5°C)	Global horizontal radiation (W/m^2) (±5%)
Enthalpy recovery ventilator (W) (0.5% Error)	Whole house natural gas consumption (m^3) ($0.05m^3$ per pulse)	Supply air temperature (°C) (±1.0°C)	
Whole house consumption (W) (1% Error)		Return air temperature (°C) (±1.0°C)	
Photovoltaic system (W) (0.5% Error)		Main floor relative humidity (%) (±2%)	
		Basement relative humidity (%) (±1%)	

The electricity consumption data was collected using current transducer type sensors, and the natural gas consumption was collected using a utility company approved diaphragm gas meter. Indoor temperature and humidity were collected using a mounted wall sensor in the basement, and a wireless indoor temperature and humidity sensor for the main floor. The air supply and return temperature were collected using thermocouples installed in the ducts. The outdoor weather parameters were collected using a weather station. These sensors collect data from the location and were uploaded over-the-air to a cloud server. Daily consumption and daily operating cost of each of the different test scenarios were calculated for comparison with the experimental model.

2.1.1.2 Switching control model

The SCM was an Excel-based model for different space heating system scenarios. The model simulated the effects of the heating system for the year of 2018 depending on the six scenarios: (1) SDFSS configuration, (2) manufacturer fuel switching at -5°C, (3) manufacturer fuel switching at -15°C, (4) natural gas-fired heating only (5) 100% electricity resistance baseboard only, and (6) ASHP with 100% resistance baseboard with -15°C manufacturer switching. A mathematical model was developed for each of the different heating system scenarios to control fuel switching using the input data. The input data are based on public sources, and the input data will be further discussed in Section 2.2.

The SDFSS model consists of a few essential mathematical and optimization models that determine the optimal switching point for a dual fuel system. Since the mathematical model is dependent on several parameters, the different parameters are also illustrated and presented. The parameters include the hourly

GHG emission for the Ontario electricity generation needed to be estimated and calculated. The following equations show the hourly cost for electricity consumption if the residential heating system were to operate *(Equation 1)* and the hourly cost for the natural gas consumption if the natural gas furnace were to operate independently *(Equation 2)*.

$$e_c = E \times \mathrm{P}_e \qquad \textit{(Equation 1)}$$

Where: $e_c = Hourly\ cost\ of\ electricity$ (\$)

$E = ASHP\ electricity\ consumption\ (kWh)$

$P_e = Marginal\ pricing\ of\ electricity\ per\ kWh\ (\$/kWh)$

$$n_c = N \times P_n \qquad \textit{(Equation 2)}$$

Where: $n_c = Hourly\ cost\ of\ natural\ gas$ (\$)

$N = Furnace\ natural\ gas\ consumption\ (m^3)$

$P_n = Marginal\ price\ of\ natural\ gas\ per\ m^3 (\$/m^3)$

The ASHP electricity consumption and the furnace natural gas consumption can be derived as follows:

$$E = \frac{H}{COP} \qquad \textit{(Equation 3)}$$

Where: $H = Space\ heating\ demand\ (kWh)$

$COP = Coefficient\ of\ performance\ for\ ASHP$

$$N = \frac{H}{U_n} \times \frac{1}{\eta_n} \qquad \textit{(Equation 4)}$$

Where: $U_n = Natural\ gas\ energy\ density\ (kWh/m^3)$

$\eta_n = Efficiency\ of\ natural\ gas\ furnace$ (%)

The two costs (natural gas and electricity) were simulated and compared on an hourly basis. The following constraint (Equation 5) must be satisfied for the HVAC system to use the electrical ASHP heating as the cost would be lower than the natural gas furnace. This inequality constraint incorporates (Equation 1) to (Equation 4).

$$\frac{H}{COP} \times \mathrm{P}_e < \frac{H}{U_n} \times \frac{1}{\eta_n} \times \mathrm{P}_n \qquad \textit{(Equation 5)}$$

Depending on the fuel selected, the hourly energy cost will be different. To calculate the total electricity consumption, the hourly cost for both electricity and natural gas are summed together. The total annual operational cost was described as following:

$$C_T = \sum e_e + \sum n_e \qquad \textit{(Equation 6)}$$

Where: $C_T = Total\ annual\ operating\ cost$

$e_e = Effective\ electricity\ cost$

$n_e = Effective\ natural\ gas\ cost$

The effective electricity cost (e_e) is the hourly cost of electricity during the hours the ASHP was used. The effective hourly cost of natural gas (n_e) is the hourly cost of natural gas when used. The total cost (C_T) is the summation of all the effective costs.

Since this study also takes into account the hourly GHG emissions, this calculation was also performed similarly to the operational costs. (Equation 7) calculates the hourly GHG emission for natural gas consumption. Similarly, (Equation 8) calculates the hourly GHG emission for electricity consumption.

$$GHG_n = D_{NG} \times N \qquad \textit{(Equation 7)}$$

Where: $GHG_n = Hourly\ GHG\ emission\ from\ natural\ gas\ consumption\ (kg)$

$D_{NG} = GHG\ density\ for\ natural\ gas\ (kg/m^3)$

$$GHG_e = D_E \times E \qquad \textit{(Equation 8)}$$

Where: $GHG_e = Hourly\ GHG\ emission\ from\ electricity\ consumption\ (kg)$

$D_E = GHG\ density\ for\ electricity\ consumption\ (kg/kWh)$

If the ASHP was being used instead of the natural gas furnace, there will be no GHG emission from the consumption of natural gas. Similarly, if the natural gas furnace was used instead of the ASHP, the GHG emission from the consumption of electricity will be zero.

(Equation 9) calculates the total greenhouse gas emissions from both natural gas and electricity consumption.

$$GHG_{Total} = \sum GHG_n + \sum GHG_e \qquad \textit{(Equation 9)}$$

Where: $GHG_{Total} = Total\ Greenhouse\ Gas\ Emissions$

The total greenhouse gas emissions are also calculated for the individual fuel sources to provide a comparison of the different options used in this project.

2.1.1.3 Combining the models

The TRNSYS house models and SCMs are used in tandem to simulate the effects of a house using different HVAC systems. This involves running the models sequentially using the same input parameters; however, the output of the TRNSYS house model was an additional input for the SCM. An extra step was required to organize the output data from the TRNSYS house model for the SCM. The TRNSYS model can provide the heating demand for the benchmark house. This heating demand was then used as an input parameter in the TRNSYS mathematical model.

2.1.2 Scenarios

Six scenarios were considered in this studied (mentioned in section 2.1.1.2). These scenarios were chosen because they explore a range of different HVAC systems. The study focuses on the province of Ontario, Canada, since it has a relatively clean electricity grid but still heavily relies on natural gas for heating [11].

The base-case scenario was configured to reflect the current electricity time-of-use pricing plan and exclusion of the carbon tax. The house and location selected for the benchmark scenario are based on an existing occupied residential house located at Strathroy, Ontario used for a case study. According to the builder's specifications and pre-built simulations, this house was considered a net-zero energy house. This extremely efficient house was occupied by a retired couple living a sedentary lifestyle.

All costs and pricing structures are expressed in Canadian dollar ($ CAD) since this study was mainly focused on the Canadian infrastructure. However, the methodology presented was applicable for any residential house located in a cold climate using similar forced air hybrid heating system. Fuel prices are adopted from the respective regional distribution companies because this study also explores the effects of the SDFSS in different cities in Ontario where both local climate and retail energy prices are different. The fuel prices used was in the form of marginal prices which means the transportation and regulatory charges were accounted with the commodity prices. However, fixed charges such as monthly account fees were excluded.

Using the benchmark model, four sensitivity analyses are also explored in this study: (1) inclusion of federal carbon pricing, (2) different cities in Ontario, Canada, (3) different housing envelopes and (4) different time-of-use (TOU) electricity pricing plan.

2.1.3 Sensitivity analyses

The four sensitivity analyses are performed on the benchmark model to identify the impacts of changing each important parameter specified. Currently, the per-unit energy price of natural gas was much lower than the per-unit energy price for electricity. These four analyses investigate the impacts of these parameters on the overall annual space heating energy consumption, associated cost, and GHG emissions. These sensitivity analyses highlight the flexibility of the SDFSS and its capabilities when different parameters are varied. The natural gas consumption, electricity consumption, operating cost and GHG emission of each scenario are summarized for comparison.

2.1.3.1 Carbon pricing

In order for this study to account for the future carbon pricing imposed by the federal government, this sensitivity analysis on carbon pricing was included to take into account of future additional charges for natural gas from 2019 to 2022. According to the Canadian Department of Finance, the year 2019 has a carbon pricing inclusion of 3.91¢/m^3 natural gas consumed [33, 35]. There are annual carbon pricing increases by $10/tonne until the carbon pricing reaches $50/tonne in 2022.

The inclusion of carbon pricing shows the impacts of indirectly increasing the cost of natural gas. Assuming that the electricity commodity price was not affected by the carbon pricing, due to the limited usage of fossil fuel (natural gas) in Ontario's grid, the price of natural gas will increase closer to electricity pricing. This shows the potential of SDFSS compared with the alternative control systems. The effects of this, coupled with the efficiency of the ASHP, has the potential to further reduce the operating cost of a fully electrical heating system in the future.

Carbon prices are collected based on federal fuel charge rates [35]. The pricing scheme implies that the additional cost was only imposed on direct natural gas consumption and not directly to the electricity pricing on the consumer side. In this study, the additional carbon pricing does not take into account the electricity GHG emission. Overall, a range of carbon price levels considered which only affects the natural gas consumption for heating. During this sensitivity analysis, the overall hourly energy cost will be affected by the carbon tax if natural gas was being consumed. The carbon tax was added into (Equation 2) to create (Equation 10):

$$n_c = N \times P_n + \frac{GHG_n}{1000} \times C_{Tax} \quad \textit{(Equation 10)}$$

Where: $C_{Tax} = \text{Price of the carbon tax (\$/tonne)}$

(Equation 5) was also modified to reflect (Equation 10) to calculate the most cost-effective fuel source for the hour.

2.1.3.2 Different Canadian cities

Four additional cities in Ontario was selected for the sensitivity analysis. The Ontario electrical grid is relatively clean compared to the other provinces in Canada and would benefit in the GHG emission reduction aspect [36]. Two separate scenarios within this sensitivity analysis are explored: (1) ignoring fuel pricing for different region, and (2) replacing the fuel pricing to match respective region. The first scenario aims to show the impact of different outdoor temperature. The second scenario aims to show the real effects when the fuel pricing difference was accounted for.

The first scenario aims to show the impact of different outdoor climates on the house and its heating systems. Since the performance of the ASHP was heavily dependent on outdoor ambient temperature, different climate zones within Ontario will not only change the heating demand; it will also change the COP of the heat pump [37]. The results of the first scenario can also serve as a benchmark for location with similar climates to the selected Ontario cities.

Due to different local conditions in different regions, the electricity and natural gas prices differ from region to region [38–42]. Since this was the case, it was important to also analyze the effects of each regional energy pricing. This analysis was mainly to explore the effects of each region's energy prices in a more realistic comparison.

2.1.3.3 Different house envelopes

The new houses used for the sensitivity analysis was based on previously performed studies in Canada. House models for two other houses different from the one used in the benchmark house model was explored. The first house used for this scenario was the Archetype Sustainable House (ASH) operated by the Toronto and Region Conservation Authority (TRCA) located at Vaughan, Ontario [43, 44]. The second house was a Twin House located in Ottawa commissioned by the Canadian Centre for Housing Technology (CCHT) [45]. These houses were previously studied and mathematical models, developed using the original TRNSYS

simulation models with the outdoor temperature as the independent variable, was used to estimate the hourly space heating demand.

Each of the two house models, TRCA ASH and CCHT, was broken down into linear mathematical equations to represent the house's hourly space heating demand. The mathematical model was used as an input for the SCM and electricity consumption, natural gas consumption, operation cost, and GHG emission.

Hourly space heating demand in this study was a crucial component for the SCM. The heating demand determines how much the heating system needs to work and was proportional to the natural gas and electricity consumption. This scenario analyses different space heating requirements and explores the effects of different scenarios on natural gas consumption and electrical consumption, and the associated operating cost, and GHG emission.

2.1.3.4 New time-of-use pricing

The Ontario electrical grid experiences different demands during different times of the day. The current Ontario electricity time-of-use pricing plan was developed to discourage residential houses to use electricity during the standard work hours by increasing the commodity price drastically [46].

Alectra-Powerstream Utilities tested a new pricing scheme, Advantage Power Pricing (APP), where the peak electricity pricing was drastically increased while a new pricing tier, super off-peak, was added [47]. This new tier was meant to provide electricity at a much lower cost from midnight until morning. This will incentivize residential houses to use electricity as a fuel source for space heating by reducing the operating cost during the night.

2.1.3.5 Overall process flow diagram

The switching system follows a process flow which takes into account numerous different parameters. Figure 2.1 shows the different parameters that were used for the model. In the base-case scenario, the NZEH was used for the house heating demand.

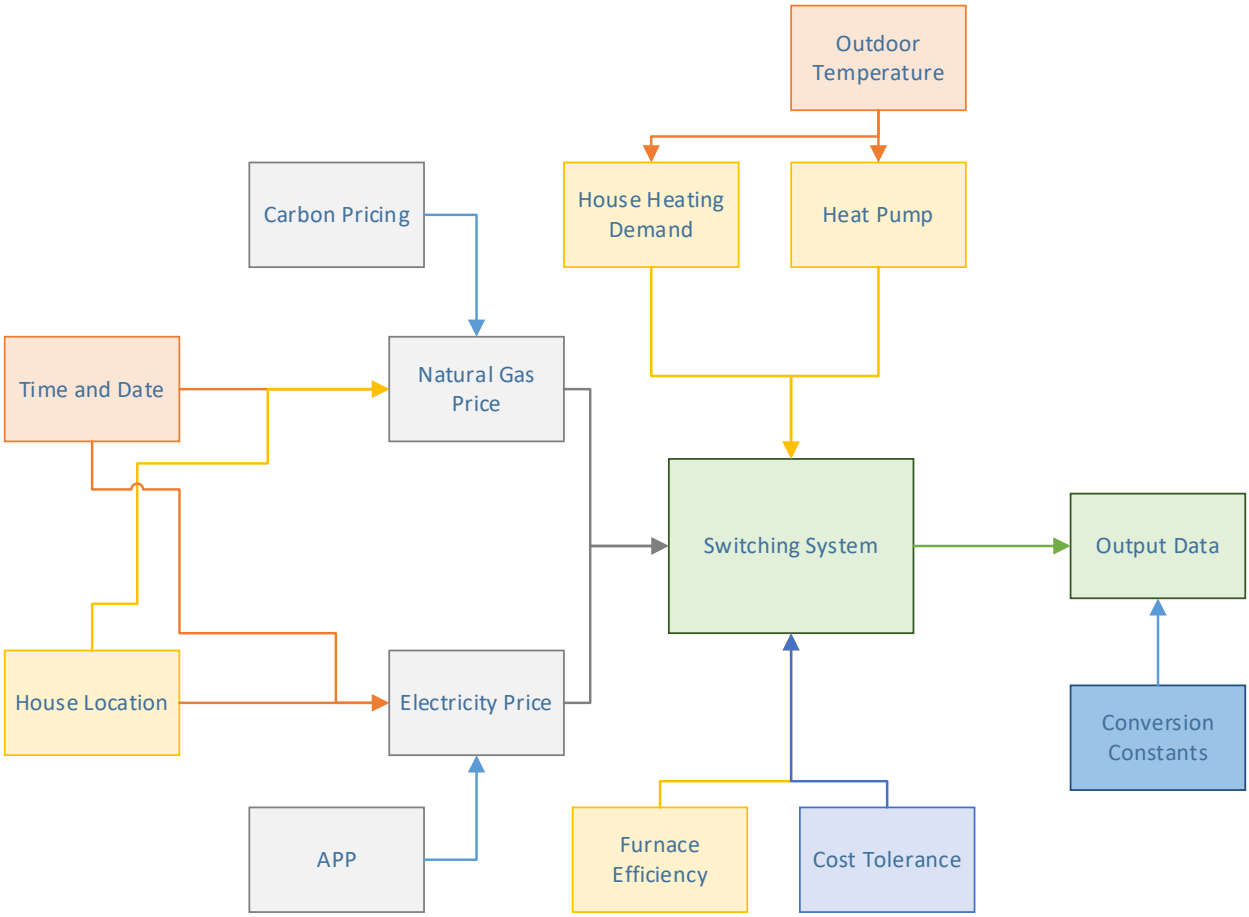

Figure 2.1: Flow chart illustrating the simulation model

The input data are identified and explained in Section 2.2 in further details.

2.2 Input data

This section provides an overview of the input parameters for the simulation models. The input data for the TRNSYS simulation was identified first, and the input data for the SCM was discussed in the subsequent chapter.

2.2.1 TRNSYS model parameters

The parameters for the NZEH was crucial to the simulation since it was the benchmark scenario for the validation of the model. The house model was created in early 2018 and was used in this study [48]. The house parameters used to create the model are listed in Table 2.2. The infiltration rate was modified to calibrate the model.

Table 2.2: List of house parameters

House Parameters		Weather Data	Heating Schedule	ERV
Insulation	Occupants	Temperature	Heating Schedule	Return and Supply Air
Infiltration	Heating Set-point	Humidity		
Windows	Lighting Schedule	Solar Radiation		

The house specifications and design values are summarized in Table 2.3:

Table 2.3: House specifications and design values

House Specifications	Design Values
Main Floor Wall	R34 Nominal
Basement Wall	R34 Nominal
Basement Floor	R10 Nominal
Ceiling	R60 Nominal
Infiltration Rate at 50Pa	0.526 ACH
Main Floor Windows	Triple Glazed Low-e Solar Glass R-value: 4.73 Nominal
Basement Windows	Triple Glazed Low-e Solar Glass R-value: 3.55 Nominal
Heating Set-point Temperature	23°C
Occupants	2 Retired
Lighting Schedule	Standard Work-Lighting Schedule
Annual Plug Load Consumption	4457 kWh
Annual Lighting Electricity Consumption	609 kWh

The wall, ceiling, and window specifications were obtained from the developer specifications. The infiltration rate was recorded from the depressurization test performed during the energy audit. The set-point temperature, occupant number, and lighting schedules were obtained from the occupant interview. The plug load consumption was measured from the energy audit and was then estimated for the year. Similarly, during the energy audit, the power rating for the lighting fixtures was accounted for and an estimated annual consumption was calculated to be 609 kWh.

Typical weather data files are generally available in the format of a TMY (Typical Meteorological Year) file [49]. These files are common types of weather files mainly constructed for simulation purposes. The file

consists of 30 years of organized average data which provides a more consistent weather profile compared to weather data for a single year. The NZEH was physically located in Strathroy; however, the required weather data was not readily available. The weather data selected was for London, Ontario, which is 35 km east of Strathroy. This weather data consists of three main components used in the simulation: (1) outdoor temperature, (2) humidity, (3) global horizontal solar radiation (4), Wind parameters. All three parameters played a role in the simulation of the heating period and were configured accordingly. Figure 2.2 shows the outdoor temperature of London, Ontario.

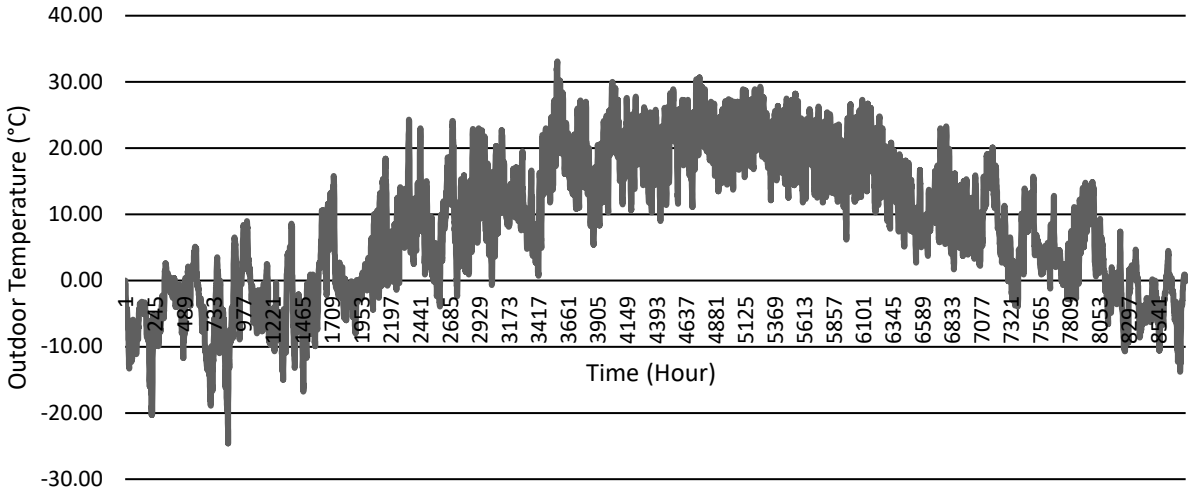

Figure 2.2: London outdoor temperature for a typical year using 30-year TMY data

The London weather data showed that the maximum outdoor temperature was found to be 33.1°C, and the minimum outdoor temperature was found to be -24.6°C. The TRNSYS model used hourly time steps for the simulation and a year of simulation consist of 8760 hours. The heating season was set from 0 hours to the 3408 hours (January 1st to May 22nd) and from 6575 hours to 8760 hours (October 1st to December 31st) [50]. This heating season selected was generally used for simulations. In practice, the heating season was slightly different since it was dependant on the outdoor temperature and the occupant temperature tolerance.

Since the NZEH have an ERV, the TRNSYS model will need to include modules that will simulate how the ERV will operate in practice. The exhaust air from the house simulation first enters the return air plenum module. Next, the ERV module utilizes the output from the plenum humidity and temperature. The intake supply air was mixed with the exhaust air in the ERV, and the resulting pre-heated supply air was directed into the house model.

These parameters are all combined within the TRNSYS model. The TRNSYS model was used to simulate the hourly space heating demand for the NZEH. The results from this model were used as an input for the SCM. Figure 2.3 shows the schematic for the TRNSYS model.

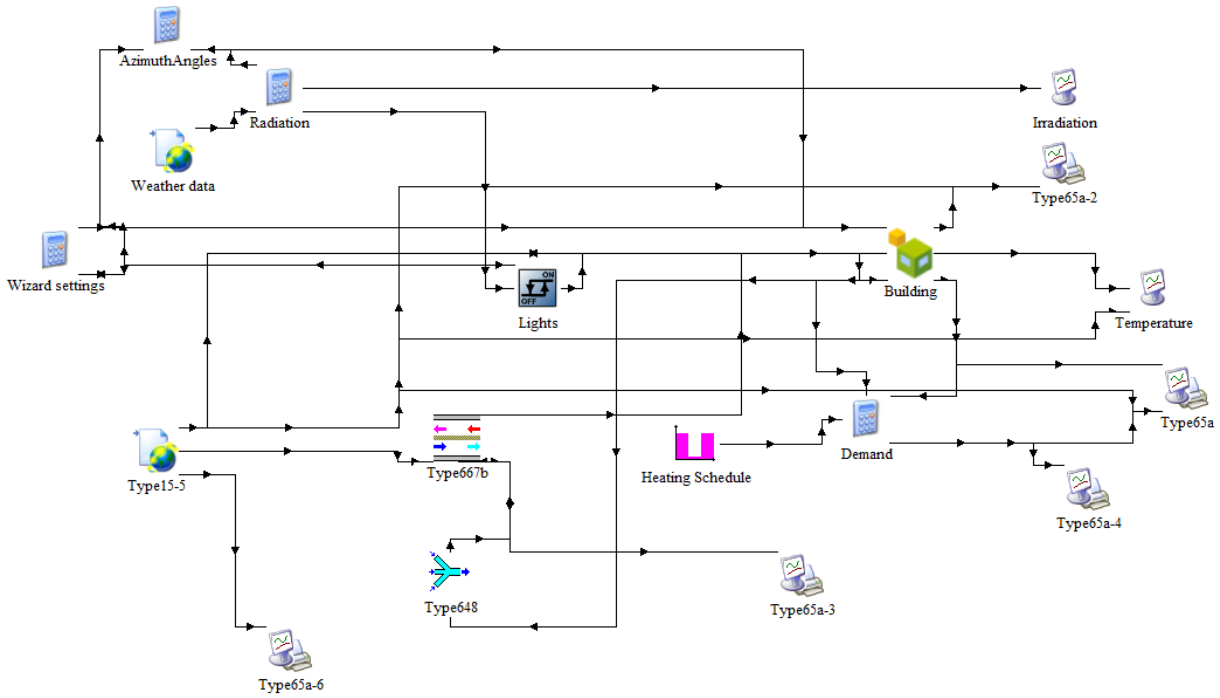

Figure 2.3: TRNSYS Schematic for the London NZEH

The model shows the connection between different TRNSYS modules. The building modelled utilizes the parameters from Table 2.3

2.2.2 Switching control model parameters

The SCM utilizes several parameters in order to determine the cost for different fuel options. The SCM can calculate the electricity consumption, natural gas consumption, annual operating cost and GHG emission for several different fuel combinations including the SDFSS. For the calculations, several temporal parameters are needed including ones that are location based, equipment based, and pricing based. The parameters required are listed in Table 2.4.

Table 2.4: List of switching parameters

Location Based	Heat Pump Specification	Furnace Specification	Fuel Pricing
City	Capacity curve	Capacity	Electricity time-of-use pricing
Temperature	COP curve	Efficiency	Natural gas pricing
	Limit temperature	NG energy density	
	GHG emissions from electricity	GHG emission from NG	

One of the most critical parameters in the simulation was the outdoor temperature. One of the main systems used in this study was an air source heat pump. Since the performance of the ASHP was heavily dependent on outdoor ambient temperature, the information from the reference city's weather data was gathered for the year 2018. Hourly temperature data was collected from Environment Canada and was prepared for the SCM. Though the outdoor humidity does not substantially affect the COP of the ASHP, it was still collected. In this study, solar radiation was ignored to create a simplistic model that could be easily implemented in future studies.

As mentioned, the performance of an ASHP was dependant on the outdoor temperature. However, each heat pump will perform differently depending on different outdoor temperatures and space heating demands. The heat pump capacity and COP for specific temperatures are obtained from the manufacturer's specifications. The information was then used to develop performance curves for both the capacity and COP for the heat pump. Figure 2.4 shows the heat pump capacity curve for different outdoor temperature.

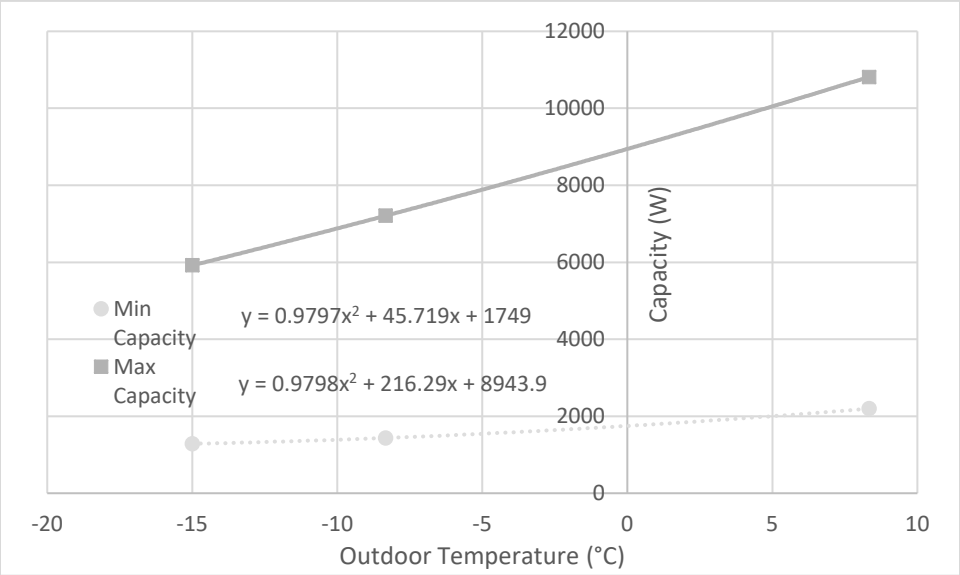

Figure 2.4: Heat pump capacity at different outdoor temperatures

Figure 2.5 shows the respective COP value for the capacity. The minimum capacity COP curve shows the COP value corresponding to the capacity curve.

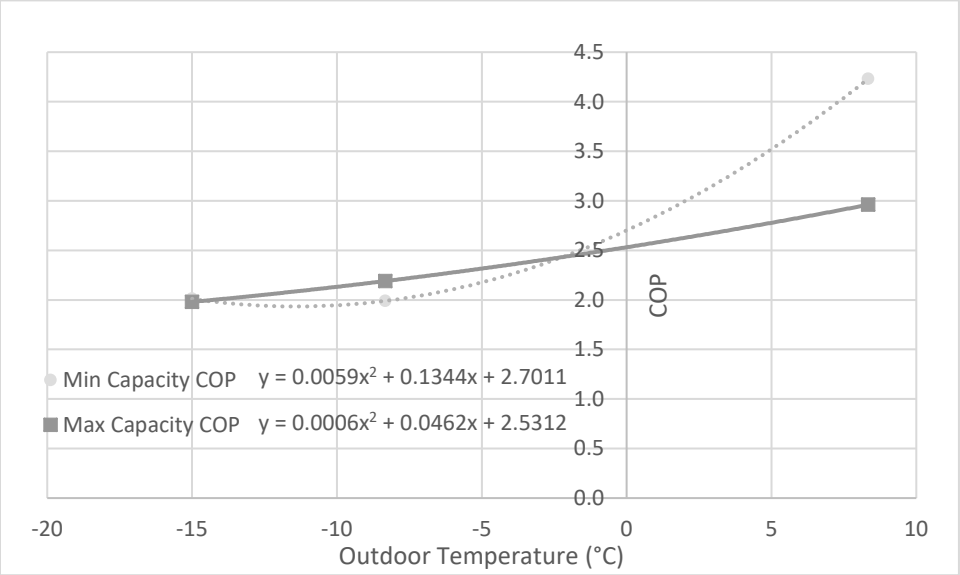

Figure 2.5: Heat pump COP curve at different outdoor temperatures

Since the ASHP used for this study was a modulating heat pump, the COP was theoretically continually changing depending on the outdoor temperature, and the capacity should match the required heating demand of the house. In this study, the heat pump was expected to provide the exact hourly heating demand to the house. This assumes that the heat pump will modulate its capacity to provide precisely the amount of heat required.

The ASHP has a maximum capacity and a minimum capacity curve with the maximum COP and minimum COP curves associated with them. The simulated hourly space heating demand from the TRNSYS model was used to determine the heating demand ratio from the maximum capacity for the given outdoor temperature. The ratio was used on the COP curve to determine the associated COP for the required capacity and outdoor temperature. The mathematical model to find the actual COP was illustrated.

$$\frac{COP_{Actual}-COP_{Min}}{H-Cap_{Min}} = \frac{COP_{Max}-COP_{Min}}{Cap_{Max}-Cap_{Min}} \qquad \textit{(Equation 11)}$$

Where: $COP_{Actual} = Actual\ COP\ for\ the\ temperature$

$H = Space\ heating\ demand$

$Cap_{Min} = Capacity\ for\ the\ temperature\ using\ the\ minimum\ capacity\ curve$

$Cap_{Max} = Capacity\ for\ the\ temperature\ using\ the\ maximum\ capacity\ curve$

$COP_{Min} = COP\ for\ that\ temperature\ using\ the\ minimum\ COP\ curve$

$COP_{Max} = COP\ for\ the\ temperature\ using\ the\ maximum\ COP\ curve$

Using *(Equation 11)*, the equation was rearranged for the actual COP.

$$COP_{Actual} = (H - Cap_{Min})\frac{(COP_{Max}-COP_{Min})}{(Cap_{Max}-Cap_{Min})} + COP_{Min} \qquad \textit{(Equation 12)}$$

The natural gas-fired furnace was similar in functionality as the heat pump. The manufacturer claimed that the furnace was fully modulating and was able to provide heating with a wide range of capacity. The efficiency of the furnace was found to be an average of 89% with the combustion analyzer during the energy audit. The test was performed multiple times to verify efficiency. Since the performance of the natural gas furnace was not highly dependent on the outdoor temperature, the heating demand was calculated by using the performance of the furnace and the natural gas consumption by the furnace. The heating capacity was then compared with the maximum and minimum heating capacity of the ASHP to ensure the ASHP can meet the heating requirement. The equivalent energy was calculated using the energy density of natural gas and was used along with the equipment efficiency to calculate the natural gas consumption. The GHG emissions were calculated with a similar method by taking account of the GHG emission factor from NG.

The time-of-use electricity pricing was obtained from the local utility company for the reference region. In the case of the benchmark model, the house was located at Strathroy, Ontario, the marginal electricity and natural gas pricings were broken down accordingly. Different TOU schedules were presented in Figure 2.6:

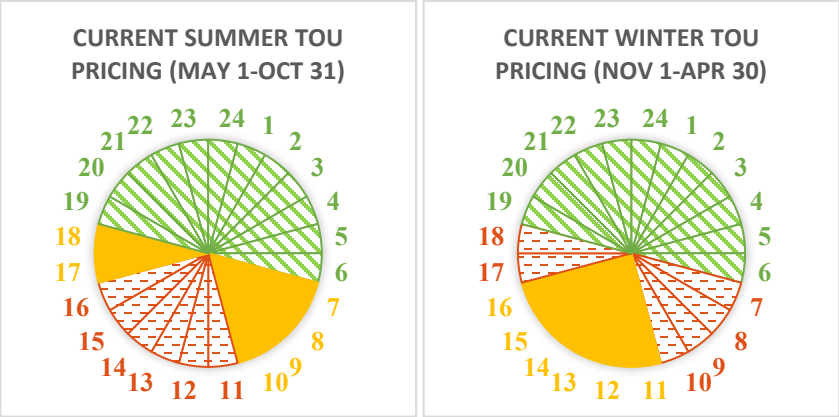

Figure 2.6: Time-of-use Schedules

The green, yellow, and red portion shows the hours for the off-peak, mid-peak and on-peak period respectively. The off-peak hours start from 7 pm to 7 am the next day. The on-peak for winter seasons starts at 7 am and ends at 11 am and resumes from 5 pm to 7 pm. The mid-peak hours for the winter seasons starts at 11 am and ends at 5 pm. The winter seasons have similar times with the exception that on-peak and mid-peak hours are reversed. Table 2.5 illustrates the current TOU electricity pricing schedule.

Table 2.5: Wholesale Ontario electricity time-of-use price for 2018

Price Tiers	Current Price
On-Peak	13.2 ¢/kWh
Mid-Peak	9.5 ¢/kWh
Off-Peak	6.5 ¢/kWh

This pricing was the commodity price of electricity alone and does not include costs such as transportation and distribution charges and other regulatory charges. The price of electricity was consistent for all cities within Ontario; however, the other surcharges vary from different distributors. Table 2.6 shows the electricity breakdown of taking account the other fees, including the delivery costs and service charges. The fixed charges such as monthly charges are not included in the marginal costs.

Table 2.6: Electricity price breakdown for April 2018 [38]

Charges	Rates
Distribution Charge	$0.0052/kWh
Retail Transmission Network Service Rate	$0.0068/kWh
Retail Transmission Connection Service Rate	$0.0052/kWh
Wholesale Market Service Rate	$0.0036/kWh
Global Adjustment Rate	$0.0017/kWh
Rural or Remote Electricity Rate Protection Charge	$0.0003/kWh
HST	13%
PST Rebate	-8%

Average hourly GHG emission factors for electricity were retrieved and derived from IESO data. The different electricity generation and its emission factor were used to estimate the average hourly GHG generation rate. The hourly GHG emission fluctuates depending on the hour.

Since the surcharge pricing are calculated per unit of electricity used, the simulation needs to factor in these costs as well. Table 2.7 shows the marginal price of electricity. The marginal price was substantially increased and will affect the simulation results. The different price tiers are also evident as well. The off-peak price was much lower than the on-peak price counterpart. This was a big difference in price and would affect the simulation results. The prices for holidays and weekends are considered fully off-peak tier and would follow the off-peak marginal pricing scheme.

Table 2.7: Marginal retail TOU electricity prices for the Strathroy

Off-Peak Marginal Price	Mid-Peak Marginal Price	On-Peak Marginal Price
$0.092/kWh	$0.124/kWh	$0.163/kWh

Similarly, the marginal price of natural gas was also calculated with additional surcharges. The price breakdown for natural gas was different from the price breakdown of electricity. Table 2.8 shows the pricing breakdown for natural gas.

Table 2.8: Price breakdown for Natural gas April 2018 [51]

Charges	Rates
Gas Used	\$0.123167/m^3
Gas Price Adjustment	\$0.016160/m^3
Transport to Union Gas	\$0.000000/m^3
Storage	\$0.0073310/m^3
Storage Price Adjustment	\$0.000039/m^3
Delivery	First 100 m^3: \$0.050591/m^3 Next 150 m^3: \$0.048051/m^3 Over 250 m^3: \$0.041228/m^3
Delivery Price Adjustment	\$0.000825/m^3
Cap-and-Trade	\$0.033421/m^3
HST	13%

The cost decreases as the homeowner uses more natural gas. For this simulation, the price of natural gas was taken as \$0.262/m^3 for the first 100 m^3, as shown in Table 2.9.

Table 2.9: Marginal Cost for natural gas

First 100 m^3	Next 150 m^3	Over 250 m^3
\$0.261746/m^3	\$0.258763/m^3	\$0.251053/m^3

In order to also estimate the GHG emissions the following conversion rates needed:

Equivalent electricity for natural gas: 10.395 kWh/m^3 [52].

GHG conversion for natural gas: 1.863 kg/m^3 [53].

GHG conversion for electricity: Since power generation in Ontario involves several different power plants, the GHG emission from electricity generation will vary greatly depending on which powerplant was operating during the hour. The method highlighted by Gordon and Fung [54, 55] was used to estimate the hourly GHG emission. Brookson et al. [56] used this method to estimate the GHG emissions within the Ontario electrical grid. Data was taken from IESO for the energy generated by every type of power plant [57]. Using updated information from IESO, the hourly generation data and GHG emission factor for 2018 was calculated.

The combination of the ASHP with a natural gas furnace was not a new idea and is currently a commercialized system. The current system implemented by the manufacturer was a set-point temperature switching system. When the outdoor temperature was above the set-point temperature, the ASHP was used for space heating. Alternatively, when the outdoor temperature was below the set-point temperature, the natural gas furnace will be used. For this study, the ASHP used in the base-case NZEH has a set-point range from 10°C to -15°C configurable by the occupant. The efficiency or COP of the ASHP for this system was identical to Figure 2.5, and the efficiency of the furnace was 89%.

2.2.3 Sensitivity analysis parameters

Several sensitivity analyses scenarios were performed to determine the effects of changing specific parameters. The different scenario includes addition of carbon pricing, different cities, different houses, and a different electricity TOU pricing plan.

2.2.3.1 Breakdown of carbon pricing

A carbon pricing was currently being imposed by the Canadian federal government to disincentivize the use of fossil fuels such as natural gas. This added cost will affect the benefit or cost-effectiveness of the SDFSS significantly and will highlight the economic and environmental benefits. The carbon pricing proposed by the government starts at \$20/tonne of CO_2 in 2019, and the cost will increase by \$10/tonne per year reaching \$50/tonne in 2022. The cost breakdown was shown in Table 2.10.

Table 2.10: Canadian federal carbon pricing breakdown

	Year				
	2018	***2019***	***2020***	***2021***	***2022***
Carbon Pricing (\$/tonne)	0	20	30	40	50
Carbon Pricing (\$/m^3)	0	0.0391	0.0587	0.0783	0.0979

Since the carbon price was dependent on the amount of GHG emissions, the natural gas price was greatly affected. The carbon price per m^2 of natural gas was also provided by the Canadian Department of Finance to illustrate the added cost to natural gas [35].

2.2.3.2 Breakdown of parameters for different cities

Another sensitivity analysis was performed to determine the effects of operating different heating systems in different cities. One of the parameters that were changed was the outdoor temperature. The four other cities selected for this sensitivity analysis are located in different regions and also in different climates. This sensitivity analysis can be translated to investigate the effects of the different switching systems for different cities across the world in similar climates as the selected test cities.

Since the fuel price was different for a different region, a secondary analysis was performed using the marginal fuel cost for the different region. The fuel pricing will affect the effectiveness of the SDFSS and depending on the different cities, and the benefits could change drastically. The summary of the input parameters for different cities was illustrated in Table 2.11.

Table 2.11: Different utility cost for cities

	Cities														
	Strathroy			***Toronto***			***Windsor***			***Ottawa***			***Thunder Bay***		
HDD[1]	3810			3873			3409			4477			5683		
Marginal Electricity Pricing [2] ($/kWh)	**OP**	**MP**	**P**	**OP**	**MP**	**P**	**OP**	**MP**	**P**	**OP**	**MP**	**P**	**OP**	**MP**	**P**
	0.0922	0.1236	0.1625	0.1098	0.1413	0.1801	0.0972	0.1277	0.1676	0.0972	0.1277	0.1676	0.0931	0.1236	0.1635
Marginal Natural Gas Pricing ($/m^3)	0.2617			0.3225			0.2617			0.3225			0.3428		

[1] HDD is normalized Heating Degree Days for 1981 to 2010 calculated with 18°C as reference base temperature. Calculated using data from climate normal stations from Environment Canada [58]
[2] OP – Off-peak hours, MP – Mid-peak hours, P – Peak hours

As seen in Table 2.11, Thunder Bay shows the highest heating degree days (HDD), and Windsor was found to have the lowest HDD. The fuel pricing was also presented for the different electrical TOU electricity schemes corresponding to different cities. The electricity price for Thunder Bay was relatively low when compared to Ottawa and Windsor even though the HDD was higher.

2.2.3.3 Mathematical models for different houses

The three different houses used for the sensitivity analysis are listed: (1) Strathroy NZEH, (2) Vaughan TRCA ASH, (3) Ottawa CCHT. The model for the Strathroy NZEH was collected from the calibrated TRNSYS model. A linear mathematical model for the heating load, as a function of outdoor temperature, was developed to better compare the different houses. The Vaughan TRCA ASH model was previously researched, and the mathematical model was developed from the results [50].

Similarly, Ottawa CCHT mathematical model was developed using prior research [45]. These parameters are used to compare the effects of the different houses. The results from this sensitivity analysis will display the benefits of the SDFSS for less efficient houses. Table 2.12 shows the mathematical model for the different house models, the peak demand and also the annual heating demand for the three houses.

Table 2.12: Annual and peak space heating demand for different houses using Strathroy weather data

	Strathroy NZEH	**Vaughan TRCA ASH**	**Ottawa CCHT**
Annual Heating Demand (kWh)	12090 kWh	14350 kWh	20550 kWh
Peak Demand	4.83 kW	7.25 kW	11.27 kW
Mathematical Model	y = -0.0822x+2.8125	y=-0.1582x+3.3586	y=-0.2625x+4.8161

Table 2.12 shows that the peak demands for the CCHT house are the highest, and the Strathroy NZEH has the lowest peak demand. This means that generally, the Ottawa CCHT consumes a larger amount of energy to heat the house. The results can be further translated to other houses with similar house performances.

2.2.3.4 The breakdown for the different electrical pricing scheme

In addition to the regular electricity TOU and natural gas pricing, a new pricing scheme was developed to incentivize the use of electrical heating during the off-peak periods (See Figure 2.7). This new pricing plan was referred to as the Advantage Power Pricing (APP). A sensitivity analysis was performed on the benchmark model to determine the effects and benefits of the APP. The pricing breakdown was similar to

the original pricing, but the commodity price portion was modified with the new pricing plan. The off-peak period was from 7 pm to midnight and resumed from 6 am to 7 am for just one hour. The new super off-peak hours were from midnight to 6 am. The mid-peak and on-peak hours remain the same 7 am to 11 am, from 11 am to 5 pm, 5 pm to 7 pm.

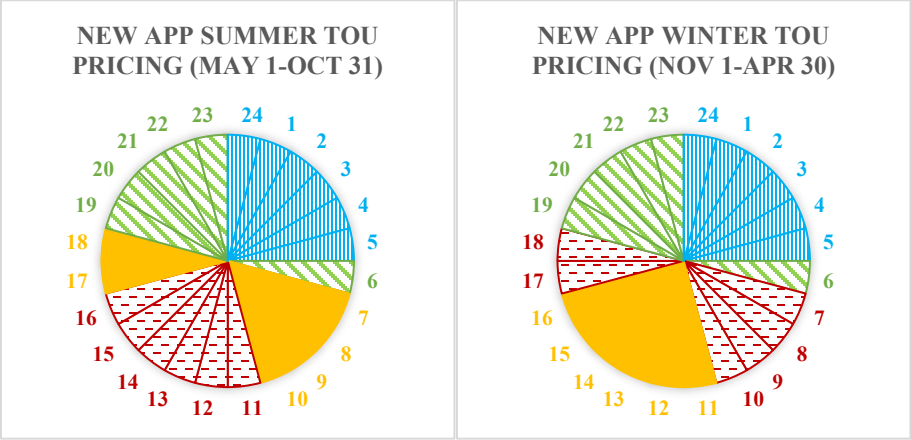

Figure 2.7: Proposed new Advantage Power Pricing (APP)

The result of this sensitivity analysis serves to investigate the benefits of upcoming new pricing policies. This APP pricing plan was reflecting the demand where the electricity pricing was highest during peak demand and lowest during low electricity demand. This analysis on the APP will also translate to a newer, more dynamic pricing plan. The dynamic pricing plan has an hourly changing electricity pricing depending on the demand of that hour.

Table 2.13 outlines both the wholesale electricity price not taking account of the extraneous prices also the higher marginal price when taking account of the additional surcharges. The wholesale price was the price of electricity, not accounting the additional cost previously illustrated in Table 2.6. The marginal price includes the other surcharges from Table 2.6, and the pricing was shown for each kWh electricity consumed for each tier. The weekend and holiday prices are considered off-peak tier similar to the first pricing tier.

Table 2.13: Wholesale and marginal TOU electricity prices for APP

Pricing Tier	Wholesale Price	Marginal Price
Off-Peak	6.5 ¢/kWh	9.22 ¢/kWh
Mid Peak	9.2 ¢/kWh	12.05 ¢/kWh
On-Peak	18.3 ¢/kWh	21.61 ¢/kWh
Super Off-Peak	2.0 ¢/kWh	4.49 ¢/kWh

2.3 Results

2.3.1 TRNSYS simulation results and calibration

The space heating demand of the benchmark NZEH was first simulated using TRNSYS. The model was first created using the information collected from the energy audit. In order to fully calibrate the model, experimental data from the sensors during daily operations were collected. Calibrating the model will help fine-tune the model to take into account unforeseen discrepancies.

A 3D model was first created using SketchUp with TRNSYS-SketchUp toolbar. Using the select TRNSYS plugin, the appropriate air nodes, windows and doors of the house were modelled in SketchUp.

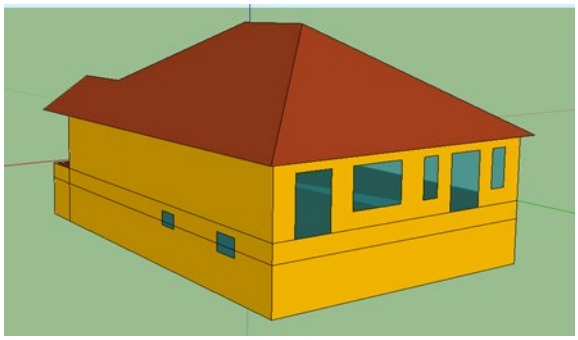

Figure 2.8: Eastside view of the NZEH

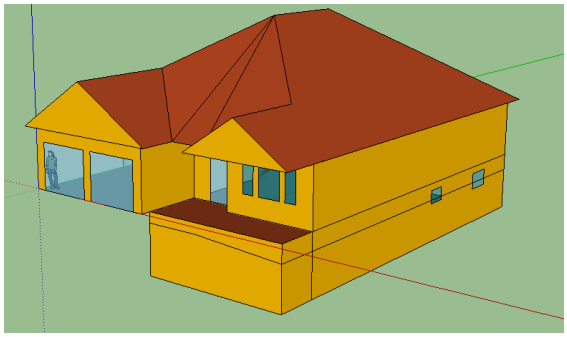

Figure 2.9: Westside view of the NZEH

The TRNSYS model was created with accurate windows and dimensions. The ground level was properly modelled for the basement. The house also sits on uneven ground where the basement windows are sitting halfway between the grade-line. Portions of the window and wall were configured with ground parameters while the other portion was designed to be exposed to ambient air. This unconditioned air was taken into account in the model with the calibration.

Real data was needed in order to calibrate the model accurately to account for the occupant behaviour and other unforeseen discrepancies. During the depressurization test, a damper in the basement allowed makeup air to flow into the house. This makeup air was brought into the house when ventilation in the natural gas cooktop range hood was activated. When the natural gas cooktop was used, a makeup air damper was activated to allow outdoor air in to avoid carbon monoxide poisoning. Because the makeup air was unconditioned, the results from the model must account for the fresh air intake.

To account for this discrepancy, the heating data collected from mid-February 2018 to November 2018 was used to estimate the space heating demand line. The period where the house only uses natural gas for heating was captured, and heating demand was calculated using natural gas's energy density along with the natural

gas consumption. The heating demand was paired with actual recorded outdoor temperature to generate a linear regression between the two variables. Similarly, the simulation data from TRNSYS was also used to generate a linear regression. The ventilation and infiltration rate in the TRNSYS model was modified and adjusted until the regression line for the simulation matches the experimental data, as shown in Figure 2.10.

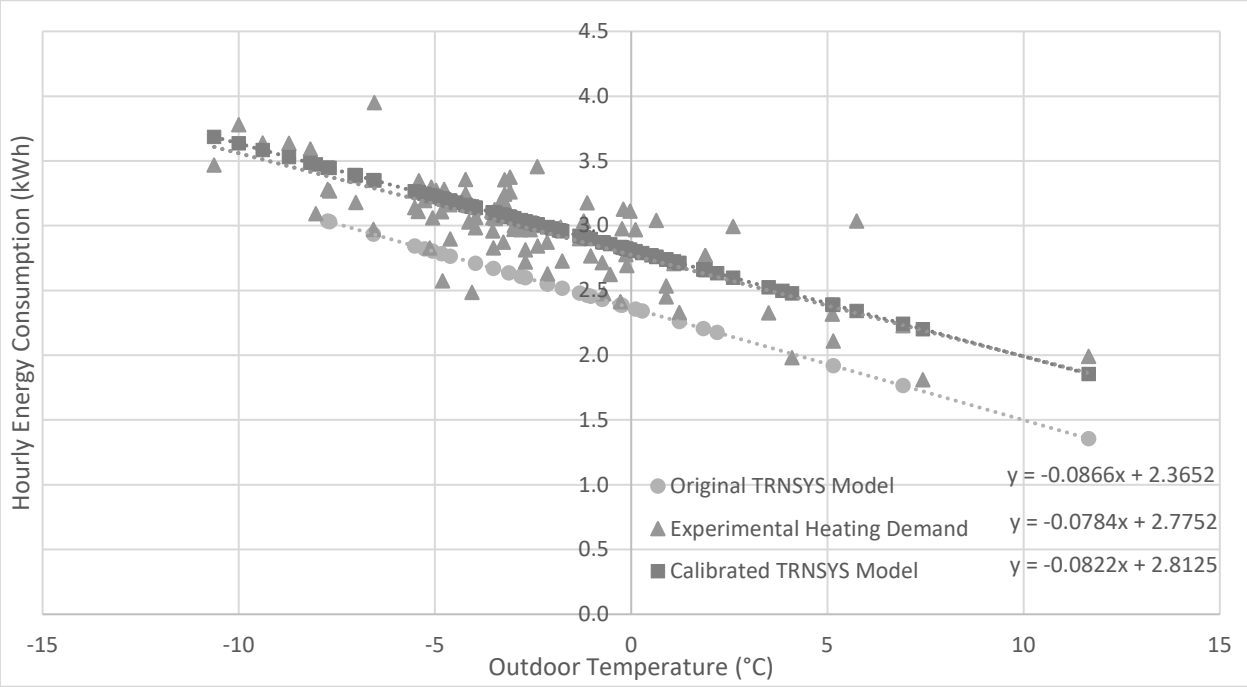

Figure 2.10: Comparison between experimental results and simulation results

The error was calculated between the experimental heating demand and the calibrated TRNSYS model regression using the root mean square error (RMSE) method. Using the regression model, hourly energy consumption was simulated for temperatures of -13℃ to 11.5℃ with 0.5℃ intervals. Using these values, the RMSE was found to be 0.05 kWh. This calibrated linear model was then used in the SCM.

The calibrated simulation model was simulated again with the Typical Meteorological Year for London, Ontario. The results of the simulation showed that the annual total heating demand was 12,090 kWh, and the peak heating load was found to be 4.83kW. The results were also compared with the TRCA ASH House A model developed by Safa et al. [43, 44, 50]. The simulation model of the TRCA ASH House A was found to have a peak heating demand of 6.76 kW.

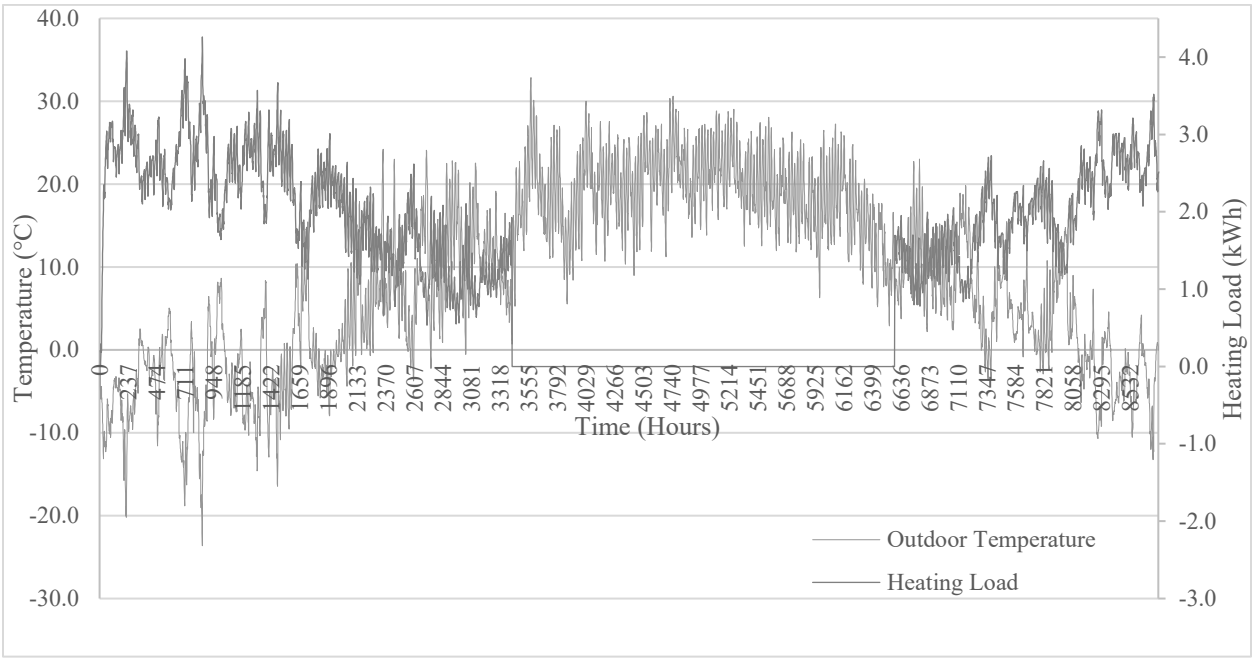

Figure 2.11: Hourly space heating load and outdoor temperature of the NZEH for London weather

The combination of the outdoor temperature and hourly space heating load graphs are overlaid in Figure 2.11. This shows the relationship between the outdoor temperature and the hourly heating demand. As the outdoor temperature increases, the heating demand decreases. The opposite can be seen when the outdoor temperature decreases.

2.3.2 Results of the switching control model

The SCM uses the hourly space heating demand simulated from the calibrated TRNSYS model to estimate the annual natural gas consumption, electricity consumption, GHG emission and operational cost.

The six main configurations simulated are the SDFSS, natural gas furnace only, manufacturer ASHP/furnace switching at -5°C and -15°C, manufacturer ASHP/electric base-board switching at -15°C and full 100% electric baseboard heating. The six different configurations were as described in Section 2.1.2. The natural gas furnace was assumed to consume a negligible amount of electricity for the electrical furnace board. The results simulated for the model only takes account the energy used for the heat generation. The simulation was to determine the amount of natural gas being offset by the ASHP.

Table 2.14 shows the results for the six different scenarios for electricity and natural gas cost for 2018. The results show that the total annual cost for the SDFSS was drastically lower when compared to the other five configurations. The SDFSS configuration has an annual operational cost of 3% lower and an annual GHG

emission 16% lower than the natural gas furnace only option. This cost and GHG emission reduction are due to the SDFSS's lower natural gas consumption in exchange for a more efficient electrical ASHP option.

Table 2.14: Summary of results of the benchmark building scenario

	SDFSS	Natural Gas Furnace Only	Manufacturer Switching at -5°C (Furnace)	Manufacturer Switching at -15°C (Furnace)	Manufacturer Switching at -15°C (100% Efficiency Baseboard)	100% Efficiency Baseboard Heating
Natural Gas Consumption (m^3)	1086.26	1306.77	374.31	24.06	0.00	0
Electricity Consumption (kWh)	491.00	0	2942.45	4498.86	4721.42	12089.679
Total Cost ($)	331.52	342.04	420.24	496.87	514.43	1321.52
GHG Emission (kg)	2039.46	2434.52	812.89	216.90	181.17	461.40

The manufacturer switching system switches from the air source heat pump to a natural gas furnace when the outdoor temperature drops below the set-point temperature. In this study, two different set-point temperatures were investigated: -5°C and -15°C. The results of the SCM show that the annual operating cost of the SDFSS was significantly lower than both the manufacturer switching option. SDFSS annual cost savings are over 21% and 33% compared to that of manufacturer switching system at set-point temperature of -5°C and -15°C, respectively. This cost difference was mainly due to the manufacturer switching system only using a simple switching parameter such as the outdoor temperature. The manufacturer switching system will continue to operate using the ASHP as the primary heat source even when the price of electricity was high or when the performance of the ASHP was poor. On the other hand, the SDFSS not only accounts for the outdoor temperature, it also takes account of temporal equipment efficiencies, capacities, and energy prices. This allows the SDFSS to provide the same amount of heat with the more economical fuel options.

However, due to the pollutive nature of natural gas, the GHG emission for the SDFSS was higher compared to the fixed set-point switching system that the manufacturers devised. This was because the GHG emission from consuming electricity was much lower than burning natural gas. Though the manufacturer switching systems have a higher annual operating cost than the natural gas furnace only configuration, and the SDFSS configuration, the GHG emissions are significantly lower due to the higher usage of electricity. However, since the SDFSS was a flexible system, the inclusion of a carbon tax will further increase the cost difference between the SDFSS and the other configurations. A carbon tax inclusion will not only lower the annual operating cost for the SDFSS; it also lowers the GHG emission.

To better describe the effects of the SDFSS, a heat map shown in Figure 2.12 was developed to illustrate the distribution of the heat pump operating status. The data was organized with columns listing the heating months. Each hour of the day was listed as rows. The sum of all days within the month and hour that the ASHP was on. For example, for February at 4 am, there are only two days within the month that the ASHP was in operation. Figure 2.12 shows that in April, the ASHP was operated more frequently with (414 hours or 57%) whereas, in January, the ASHP was rarely used (12 hours or 2%) due to the higher cost for the ASHP to operate in colder outdoor temperature.

	1	*2*	*3*	*4*	*11*	*12*	
Hour	January	February	March	April	November	December	
0	1 dy 3.2%	3 dy 10.7%	6 dy 19.4%	17 dy 56.7%	16 dy 53.3%	1 dy 3.2%	44 hr 1.0%
1	1 dy 3.2%	4 dy 14.3%	5 dy 16.1%	17 dy 56.7%	14 dy 46.7%	1 dy 3.2%	42 hr 1.0%
2	1 dy 3.2%	3 dy 10.7%	4 dy 12.9%	15 dy 50.0%	12 dy 40.0%	2 dy 6.5%	37 hr 0.9%
3	1 dy 3.2%	3 dy 10.7%	4 dy 12.9%	16 dy 53.3%	11 dy 36.7%	1 dy 3.2%	36 hr 0.8%
4	1 dy 3.2%	2 dy 7.1%	4 dy 12.9%	14 dy 46.7%	11 dy 36.7%	1 dy 3.2%	33 hr 0.8%
5	1 dy 3.2%	2 dy 7.1%	4 dy 12.9%	14 dy 46.7%	11 dy 36.7%	1 dy 3.2%	33 hr 0.8%
6	1 dy 3.2%	2 dy 7.1%	5 dy 16.1%	14 dy 46.7%	12 dy 40.0%	1 dy 3.2%	35 hr 0.8%
7	0 dy 0.0%	1 dy 3.6%	2 dy 6.5%	6 dy 20.0%	2 dy 6.7%	0 dy 0.0%	11 hr 0.3%
8	0 dy 0.0%	1 dy 3.6%	3 dy 9.7%	10 dy 33.3%	2 dy 6.7%	0 dy 0.0%	16 hr 0.4%
9	0 dy 0.0%	1 dy 3.6%	3 dy 9.7%	11 dy 36.7%	2 dy 6.7%	0 dy 0.0%	17 hr 0.4%
10	0 dy 0.0%	2 dy 7.1%	2 dy 6.5%	12 dy 40.0%	5 dy 16.7%	2 dy 6.5%	23 hr 0.5%
11	0 dy 0.0%	2 dy 7.1%	6 dy 19.4%	22 dy 73.3%	13 dy 43.3%	2 dy 6.5%	45 hr 1.0%
12	0 dy 0.0%	2 dy 7.1%	6 dy 19.4%	22 dy 73.3%	13 dy 43.3%	3 dy 9.7%	46 hr 1.1%
13	0 dy 0.0%	2 dy 7.1%	7 dy 22.6%	21 dy 70.0%	15 dy 50.0%	3 dy 9.7%	48 hr 1.1%
14	0 dy 0.0%	2 dy 7.1%	9 dy 29.0%	22 dy 73.3%	16 dy 53.3%	3 dy 9.7%	52 hr 1.2%
15	0 dy 0.0%	2 dy 7.1%	10 dy 32.3%	22 dy 73.3%	15 dy 50.0%	2 dy 6.5%	51 hr 1.2%
16	0 dy 0.0%	2 dy 7.1%	9 dy 29.0%	22 dy 73.3%	14 dy 46.7%	2 dy 6.5%	49 hr 1.1%
17	0 dy 0.0%	2 dy 7.1%	5 dy 16.1%	11 dy 36.7%	4 dy 13.3%	2 dy 6.5%	24 hr 0.6%
18	0 dy 0.0%	2 dy 7.1%	4 dy 12.9%	10 dy 33.3%	4 dy 13.3%	2 dy 6.5%	22 hr 0.5%
19	1 dy 3.2%	3 dy 10.7%	9 dy 29.0%	26 dy 86.7%	17 dy 56.7%	2 dy 6.5%	58 hr 1.3%
20	1 dy 3.2%	3 dy 10.7%	8 dy 25.8%	25 dy 83.3%	14 dy 46.7%	2 dy 6.5%	53 hr 1.2%
21	1 dy 3.2%	3 dy 10.7%	8 dy 25.8%	23 dy 76.7%	14 dy 46.7%	2 dy 6.5%	51 hr 1.2%
22	1 dy 3.2%	3 dy 10.7%	6 dy 19.4%	21 dy 70.0%	15 dy 50.0%	1 dy 3.2%	47 hr 1.1%
23	1 dy 3.2%	3 dy 10.7%	6 dy 19.4%	21 dy 70.0%	14 dy 46.7%	1 dy 3.2%	46 hr 1.1%
Monthly Total	12 hr 1.6%	55 hr 8.2%	135 hr 18.1%	414 hr 57.5%	266 hr 36.9%	37 hr 5.0%	919 hr 21.3%
							4321 hr

Figure 2.12: Heat map for ASHP operation in the heating season

To further analyze the SDFSS, the weekend data was separated from the weekday data in the heat map. As mentioned in Section 2.2.3.4, the cost of electricity in the weekend was considered the off-peak tier. Figure 2.13 shows the heat map when only the weekday was considered. It can be observed that during the colder winter months (January, February, and December), the ASHP was not cost-effective to operate during the peak and mid-peak hours (from 7 am to 7 pm). This was due to the higher electricity cost and low outdoor temperature. The ASHP was not efficient enough during the cold weather to be cost-effective when

compared with the natural gas furnace. During months with milder outdoor temperature, the ASHP was efficient enough to be cost-effective compared to the natural gas furnace. Compare to the previous combination heat map, the weekday-only heat map did not show any consumption during the peak and mid-peak period. This was because the ASHP was operating during the weekend when the time-of-use tier was considered off-peak.

	1		*2*		*3*		*4*		*11*		*12*			
Hour	January		February		March		April		November		December			
0	1 dy	4.5%	1 dy	5.3%	3 dy	14.3%	10 dy	47.6%	13 dy	59.1%	0 dy	0.0%	28 hr	22.8%
1	1 dy	4.5%	3 dy	15.8%	3 dy	14.3%	11 dy	52.4%	12 dy	54.5%	1 dy	5.3%	31 hr	25.2%
2	1 dy	4.5%	2 dy	10.5%	2 dy	9.5%	10 dy	47.6%	10 dy	45.5%	1 dy	5.3%	26 hr	21.1%
3	1 dy	4.5%	2 dy	10.5%	2 dy	9.5%	11 dy	52.4%	10 dy	45.5%	1 dy	5.3%	27 hr	22.0%
4	1 dy	4.5%	1 dy	5.3%	2 dy	9.5%	10 dy	47.6%	9 dy	40.9%	1 dy	5.3%	24 hr	19.5%
5	1 dy	4.5%	1 dy	5.3%	2 dy	9.5%	10 dy	47.6%	9 dy	40.9%	1 dy	5.3%	24 hr	19.5%
6	1 dy	4.5%	1 dy	5.3%	3 dy	14.3%	10 dy	47.6%	10 dy	45.5%	1 dy	5.3%	26 hr	21.1%
7	0 dy	0.0%	0 dy	0.0%	0 dy	0.0%	0 dy	0.0%	0 dy	0.0%	0 dy	0.0%	0 hr	0.0%
8	0 dy	0.0%	0 dy	0.0%	0 dy	0.0%	2 dy	9.5%	0 dy	0.0%	0 dy	0.0%	2 hr	1.6%
9	0 dy	0.0%	0 dy	0.0%	0 dy	0.0%	3 dy	14.3%	0 dy	0.0%	0 dy	0.0%	3 hr	2.4%
10	0 dy	0.0%	0 dy	0.0%	0 dy	0.0%	4 dy	19.0%	0 dy	0.0%	0 dy	0.0%	4 hr	3.3%
11	0 dy	0.0%	0 dy	0.0%	3 dy	14.3%	13 dy	61.9%	8 dy	36.4%	0 dy	0.0%	24 hr	19.5%
12	0 dy	0.0%	0 dy	0.0%	3 dy	14.3%	13 dy	61.9%	8 dy	36.4%	0 dy	0.0%	24 hr	19.5%
13	0 dy	0.0%	0 dy	0.0%	4 dy	19.0%	12 dy	57.1%	10 dy	45.5%	0 dy	0.0%	26 hr	21.1%
14	0 dy	0.0%	0 dy	0.0%	6 dy	28.6%	13 dy	61.9%	10 dy	45.5%	0 dy	0.0%	29 hr	23.6%
15	0 dy	0.0%	0 dy	0.0%	6 dy	28.6%	13 dy	61.9%	9 dy	40.9%	0 dy	0.0%	28 hr	22.8%
16	0 dy	0.0%	0 dy	0.0%	5 dy	23.8%	13 dy	61.9%	9 dy	40.9%	0 dy	0.0%	27 hr	22.0%
17	0 dy	0.0%	0 dy	0.0%	1 dy	4.8%	3 dy	14.3%	0 dy	0.0%	0 dy	0.0%	4 hr	3.3%
18	0 dy	0.0%	0 dy	0.0%	1 dy	4.8%	2 dy	9.5%	0 dy	0.0%	0 dy	0.0%	3 hr	2.4%
19	1 dy	4.5%	1 dy	5.3%	6 dy	28.6%	18 dy	85.7%	14 dy	63.6%	1 dy	5.3%	41 hr	33.3%
20	1 dy	4.5%	1 dy	5.3%	5 dy	23.8%	17 dy	81.0%	12 dy	54.5%	1 dy	5.3%	37 hr	30.1%
21	1 dy	4.5%	1 dy	5.3%	5 dy	23.8%	15 dy	71.4%	12 dy	54.5%	1 dy	5.3%	35 hr	28.5%
22	1 dy	4.5%	1 dy	5.3%	3 dy	14.3%	13 dy	61.9%	12 dy	54.5%	0 dy	0.0%	30 hr	24.4%
23	1 dy	4.5%	1 dy	5.3%	3 dy	14.3%	13 dy	61.9%	12 dy	54.5%	0 dy	0.0%	30 hr	24.4%
Monthly Total	12 hr	2.3%	16 hr	3.5%	68 hr	13.5%	239 hr	47.4%	189 hr	35.8%	9 hr	2.0%	533 hr	17.9%
														2976 hr

Figure 2.13: Heat map for weekdays during the heating season

Figure 2.14 shows the ASHP operation during the weekends. This shows that there are more periods where the ASHP was in operation compared to the weekday heat map. This was due to the aforementioned less costly off-peak price tier. During weekends and holidays, the utility charges the lowest pricing tier. During this time, the SDFSS will allow the heat pump to operate more frequently due to the more economical circumstances.

	1	*2*	*3*	*4*	*11*	*12*	
yr 2018	January	February	March	April	November	December	
0	0 dy 0.0%	2 dy 22.2%	3 dy 30.0%	7 dy 77.8%	3 dy 37.5%	1 dy 8.3%	16 hr 27.6%
1	0 dy 0.0%	1 dy 11.1%	2 dy 20.0%	6 dy 66.7%	2 dy 25.0%	0 dy 0.0%	11 hr 19.0%
2	0 dy 0.0%	1 dy 11.1%	2 dy 20.0%	5 dy 55.6%	2 dy 25.0%	1 dy 8.3%	11 hr 19.0%
3	0 dy 0.0%	1 dy 11.1%	2 dy 20.0%	5 dy 55.6%	1 dy 12.5%	0 dy 0.0%	9 hr 15.5%
4	0 dy 0.0%	1 dy 11.1%	2 dy 20.0%	4 dy 44.4%	2 dy 25.0%	0 dy 0.0%	9 hr 15.5%
5	0 dy 0.0%	1 dy 11.1%	2 dy 20.0%	4 dy 44.4%	2 dy 25.0%	0 dy 0.0%	9 hr 15.5%
6	0 dy 0.0%	1 dy 11.1%	2 dy 20.0%	4 dy 44.4%	2 dy 25.0%	0 dy 0.0%	9 hr 15.5%
7	0 dy 0.0%	1 dy 11.1%	2 dy 20.0%	6 dy 66.7%	2 dy 25.0%	0 dy 0.0%	11 hr 19.0%
8	0 dy 0.0%	1 dy 11.1%	3 dy 30.0%	8 dy 88.9%	2 dy 25.0%	0 dy 0.0%	14 hr 24.1%
9	0 dy 0.0%	1 dy 11.1%	3 dy 30.0%	8 dy 88.9%	2 dy 25.0%	0 dy 0.0%	14 hr 24.1%
10	0 dy 0.0%	2 dy 22.2%	2 dy 20.0%	8 dy 88.9%	5 dy 62.5%	2 dy 16.7%	19 hr 32.8%
11	0 dy 0.0%	2 dy 22.2%	3 dy 30.0%	9 dy 100.0%	5 dy 62.5%	2 dy 16.7%	21 hr 36.2%
12	0 dy 0.0%	2 dy 22.2%	3 dy 30.0%	9 dy 100.0%	5 dy 62.5%	3 dy 25.0%	22 hr 37.9%
13	0 dy 0.0%	2 dy 22.2%	3 dy 30.0%	9 dy 100.0%	5 dy 62.5%	3 dy 25.0%	22 hr 37.9%
14	0 dy 0.0%	2 dy 22.2%	3 dy 30.0%	9 dy 100.0%	6 dy 75.0%	3 dy 25.0%	23 hr 39.7%
15	0 dy 0.0%	2 dy 22.2%	4 dy 40.0%	9 dy 100.0%	6 dy 75.0%	2 dy 16.7%	23 hr 39.7%
16	0 dy 0.0%	2 dy 22.2%	4 dy 40.0%	9 dy 100.0%	5 dy 62.5%	2 dy 16.7%	22 hr 37.9%
17	0 dy 0.0%	2 dy 22.2%	4 dy 40.0%	8 dy 88.9%	4 dy 50.0%	2 dy 16.7%	20 hr 34.5%
18	0 dy 0.0%	2 dy 22.2%	3 dy 30.0%	8 dy 88.9%	4 dy 50.0%	2 dy 16.7%	19 hr 32.8%
19	0 dy 0.0%	2 dy 22.2%	3 dy 30.0%	8 dy 88.9%	3 dy 37.5%	1 dy 8.3%	17 hr 29.3%
20	0 dy 0.0%	2 dy 22.2%	3 dy 30.0%	8 dy 88.9%	2 dy 25.0%	1 dy 8.3%	16 hr 27.6%
21	0 dy 0.0%	2 dy 22.2%	3 dy 30.0%	8 dy 88.9%	2 dy 25.0%	1 dy 8.3%	16 hr 27.6%
22	0 dy 0.0%	2 dy 22.2%	3 dy 30.0%	8 dy 88.9%	3 dy 37.5%	1 dy 8.3%	17 hr 29.3%
23	0 dy 0.0%	2 dy 22.2%	3 dy 30.0%	8 dy 88.9%	2 dy 25.0%	1 dy 8.3%	16 hr 27.6%
Monthly Total	0 hr 0.0%	39 hr 18.1%	67 hr 27.9%	175 hr 81.0%	77 hr 40.1%	28 hr 9.7%	386 hr 28.2%
							1368 hr

Figure 2.14: Heat map for weekends during the heating season

2.3.3 Calculating the optimal switching temperature

The SDFSS was a flexible system that can take into account different temporal parameters to estimate fuel consumption. Though the system was flexible, the current base-case simulation model can be simplified to three fixed set-point temperatures. Using the mathematical model for the space heating demand and the ASHP specification curves, three different optimal switching temperatures were set, one for each electricity pricing tier. These switching temperature can be used to determine the optimal switching temperature for the given hour.

The idea of the SDFSS was to use the most cost-effective fuel source available. The NZEH for the base-case analysis used both ASHP and a natural gas furnace. Recap of *(Equation 5)*, as long as the equation holds, the ASHP was in use. If the equation shows false, the natural gas-fired furnace was used.

$$\frac{H}{COP} \times \mathrm{P}_e < \frac{H}{U_n} \times \frac{1}{\eta_n} \times \mathrm{P}_n \qquad \textit{(Equation 5)}$$

The space heating demand (H) can be replaced with the linear mathematical model of the calibrated TRNSYS model illustrated in Section 2.3.1.

$$H = -0.0822t + 2.8125 \quad \textit{(Equation 13)}$$

Where: t = Hourly temperature (°C)

From Section 2.2.2, additional parameters can be found to include in the calculation:

Natural gas furnace efficiency: 89%

Natural gas energy density: 10.395 kWh/m^3

Natural gas marginal price: \$0.3038/m^3

Electricity marginal price: On-Peak: \$0.163/kWh

Mid-Peak: \$0.124/kWh

Off-Peak: \$0.092/kWh

(Equation 5) can be simplified using the parameters.

$$\frac{P_e}{COP_{Actual}} < \frac{P_n}{0.89 \times 10.395} \quad \textit{(Equation 14)}$$

$$COP_{Actual} > \frac{P_e}{P_n} \times 9.25155 \quad \textit{(Equation 15)}$$

$$COP_{Actual} > P_e \times 30.4528 \quad \textit{(Equation 16)}$$

Using *(Equation 16)*, and the three electricity marginal price, three separate equations can be created for each of the three electricity pricing tiers.

On-Peak: $COP_{Actual} > 4.964$ *(Equation 17)*

Mid-Peak: $COP_{Actual} > 3.776$ *(Equation 18)*

Off-Peak: $COP_{Actual} > 2.802$ *(Equation 19)*

Using *(Equation 12)* for the actual COP, along with the mathematical model for the ASHP capacity and COP, the actual COP can be derived. From Section 2.2.2, the minimum and maximum COP and capacity mathematical model are revisited.

$$Cap_{Min} = 0.0009797t^2 + 0.045719t + 1.749 \quad \textit{(Equation 20)}$$

$$Cap_{Max} = 0.0009798t^2 + 0.21629t + 8.9439 \quad \textit{(Equation 21)}$$

$$COP_{Min} = 0.0059t^2 + 0.1344t + 2.7011 \quad \textit{(Equation 22)}$$

$$COP_{Max} = 0.0006t^2 + 0.0462t + 2.5313 \quad \textit{(Equation 23)}$$

Using *(Equation 13)* for the space heating demand, along with *(Equation 20)* to *(Equation 23)* for the ASHP specifications, the actual COP mathematical model can be simplified.

$$COP_{Actual} = \frac{5\times10^{-6}t^4+1.77\times10^{-3}t^3+7.1187\times10^{-2}t^2+1.355644t+17.628324}{1\times10^{-7}t^2+0.170571t+7.1949} \quad \textit{(Equation 24)}$$

Using *(Equation 24)*, along with *(Equation 17)* to *(Equation 19)* for the different electricity pricing. The equation was then solved for temperature.

On-Peak: $t > 11.5°C$ *(Equation 25)*

Mid-Peak: $t > 7.2°C$ *(Equation 26)*

Off-Peak: $t > 2.4°C$ *(Equation 27)*

The results illustrated in *(Equation 25)* to *(Equation 27)* show the three optimal switching temperature for on-peak, mid-peak and off-peak. The SDFSS can calculate these optimal switching temperature using the input parameters and effectively switch the fuel source.

2.4 Sensitivity analysis

The results showed that there was a potential operational cost saving using the SDFSS compared to the other scenarios. To further estimate the effects of varying parameters, several sensitivity analyses are performed. These sensitivity analysis scenarios are procured to predict the foreseeable changes due to climate change regulations.

2.4.1 Carbon price increase

The federal government is currently imposing a carbon pricing scheme on fossil fuel usage. This additional cost towards high carbon sources will drastically change the operating cost for heating. Since natural gas was a commonly used fuel for heating in Canada, the use of electricity for heating can potentially be a cost-

effective alternative if implemented appropriately. Table 2.15 shows the summary of the results for different carbon taxes and six configurations.

Table 2.15: Summary of results for different carbon taxes

Smart Switching (SDFSS) with ASHP Heating						
	No Carbon tax	*$10/tonne Carbon Tax*	*$20/tonne Carbon Tax*	*$30/tonne Carbon Tax*	*$40/tonne Carbon Tax*	*$50/tonne Carbon Tax*
Natural Gas Consumption (m^3)	1086.26	1030.63	950.01	874.74	789.16	689.87
Electricity Consumption (kWh)	491.00	647.69	893.44	1138.80	1433.62	1797.18
Total Cost ($)	331.52	353.89	374.83	394.14	411.56	427.09
GHG Emission (kg)	2039.46	1941.04	1799.71	1668.69	1519.60	1347.93
Natural Gas Furnace Only						
	No Carbon tax	*$10/tonne Carbon Tax*	*$20/tonne Carbon Tax*	*$30/tonne Carbon Tax*	*$40/tonne Carbon Tax*	*$50/tonne Carbon Tax*
Natural Gas Consumption (m^3)	1306.77	1306.77	1306.77	1306.77	1306.77	1306.77
Electricity Consumption (kWh)	0.00	0.00	0.00	0.00	0.00	0.00
Total Cost ($)	342.04	369.55	397.06	424.57	452.08	479.59
GHG Emission (kg)	2434.52	2434.52	2434.52	2434.52	2434.52	2434.52
Default Manufacturer Switching at -5 °C (NG furnace)						
	No Carbon tax	*$10/tonne Carbon Tax*	*$20/tonne Carbon Tax*	*$30/tonne Carbon Tax*	*$40/tonne Carbon Tax*	*$50/tonne Carbon Tax*
Natural Gas Consumption (m^3)	374.31	374.31	374.31	374.31	374.31	374.31
Electricity Consumption (kWh)	2942.45	2942.45	2942.45	2942.45	2942.45	2942.45
Total Cost ($)	420.24	428.12	436.00	443.88	451.76	459.64
GHG Emission (kg)	812.89	812.89	812.89	812.89	812.89	812.89
Default Manufacturer Switching at -15 °C (NG furnace)						
	No Carbon tax	*$10/tonne Carbon Tax*	*$20/tonne Carbon Tax*	*$30/tonne Carbon Tax*	*$40/tonne Carbon Tax*	*$50/tonne Carbon Tax*
Natural Gas Consumption (m^3)	24.06	24.06	24.06	24.06	24.06	24.06
Electricity Consumption (kWh)	4498.86	4498.86	4498.86	4498.86	4498.86	4498.86
Total Cost ($)	496.87	497.37	497.88	498.38	498.89	499.40
GHG Emission (kg)	216.90	216.90	216.90	216.90	216.90	216.90
Default Manufacturer Switching at -15 °C (100% Efficiency Electric Baseboard)						
	No Carbon tax	*$10/tonne Carbon Tax*	*$20/tonne Carbon Tax*	*$30/tonne Carbon Tax*	*$40/tonne Carbon Tax*	*$50/tonne Carbon Tax*
Natural Gas Consumption (m^3)	0.00	0.00	0.00	0.00	0.00	0.00
Electricity Consumption (kWh)	4721.42	4721.42	4721.42	4721.42	4721.42	4721.42
Total Cost ($)	514.43	514.43	514.43	514.43	514.43	514.43
GHG Emission (kg)	181.17	181.17	181.17	181.17	181.17	181.17
100% Efficiency Electric Baseboard Only						
	No Carbon tax	*$10/tonne Carbon Tax*	*$20/tonne Carbon Tax*	*$30/tonne Carbon Tax*	*$40/tonne Carbon Tax*	*$50/tonne Carbon Tax*
Natural Gas Consumption (m^3)	0.00	0.00	0.00	0.00	0.00	0.00
Electricity Consumption (kWh)	12089.68	12089.68	12089.68	12089.68	12089.68	12089.68
Total Cost ($)	1321.52	1321.52	1321.52	1321.52	1321.52	1321.52
GHG Emission (kg)	461.40	461.40	461.40	461.40	461.40	461.40

The results of the sensitivity analysis show that the SDFSS will continually be cost-effective compared to the other systems. The higher carbon pricing increases the price of natural gas furnace substantially when

compared to the electricity prices. This was evident when analyzing the difference between the operating cost of the SDFSS and the operating cost of the natural gas-only configuration. The SDFSS option shows that the operating cost was lower than the natural gas-only configuration. Additionally, the GHG emissions are significantly reduced as well. Both the manufacturer switching showed an increase similar to the natural gas-only system. This was because the manufacturer switching system does not take into account any cost parameters. The manufacturer switching system at -5°C was more cost-effective than the natural gas-only system with a $50/tonne carbon price increase. This shows that the SDFSS was compelling even with the newly imposed carbon pricing.

2.4.2 Different Canadian cities

The benchmark model of the switching system was created for the NZEH located in Strathroy. To demonstrate the effect of the SDFSS for different cities, several cities located in Ontario were selected for this sensitivity analysis. The selected cities are larger cities with different climates in order to investigate the impact of temperature changes.

Table 2.16 shows the results of the different scenarios when the temperature changes. It was evident from the results shown that the temperature dramatically affects the operational costs. However, when comparing the different switching systems, the savings are similar in proportion. This shows that the smart dual fuel switching system was valid regardless of the colder outdoor temperature.

Table 2.16: Summary of results for climactic differences with different cities

Smart Switching (SDFSS) with ASHP Heating					
	Strathroy	*Toronto*	*Windsor*	*Ottawa*	*Thunder Bay*
Natural Gas Consumption (m^3)	1086.26	1158.59	976.43	1280.43	1482.56
Electricity Consumption (kWh)	491.00	394.89	580.45	318.07	200.63
Total Cost ($)	331.52	341.25	311.27	365.81	407.13
GHG Emission (kg)	2031.86	2162.75	1831.16	2387.07	2757.85
Natural Gas Furnace Only					
	Strathroy	*Toronto*	*Windsor*	*Ottawa*	*Thunder Bay*
Natural Gas Consumption (m^3)	1306.77	1335.71	1238.49	1421.71	1565.02
Electricity Consumption (kWh)	0.00	0.00	0.00	0.00	0.00
Total Cost ($)	342.04	349.62	324.17	372.13	409.64
GHG Emission (kg)	2425.37	2479.07	2298.63	2638.69	2904.67
Default Manufacturer Switching at -5 °C (NG furnace)					
	Strathroy	*Toronto*	*Windsor*	*Ottawa*	*Thunder Bay*
Natural Gas Consumption (m^3)	374.31	428.12	230.62	678.64	948.39
Electricity Consumption (kWh)	2942.45	2897.93	3079.62	2389.78	2071.10
Total Cost ($)	420.24	430.66	396.08	441.81	474.42
GHG Emission (kg)	810.27	907.27	546.14	1348.17	1834.10
Default Manufacturer Switching at -15 °C (NG furnace)					
	Strathroy	*Toronto*	*Windsor*	*Ottawa*	*Thunder Bay*
Natural Gas Consumption (m^3)	24.06	36.27	5.82	145.62	354.23
Electricity Consumption (kWh)	4498.86	4643.83	4072.91	4788.08	4755.72
Total Cost ($)	496.87	514.90	444.48	558.81	614.75
GHG Emission (kg)	216.73	244.29	166.76	452.25	837.94
Default Manufacturer Switching at -15 °C (100% Efficiency Electric Baseboard)					
	Strathroy	*Toronto*	*Windsor*	*Ottawa*	*Thunder Bay*
Natural Gas Consumption (m^3)	0.00	0.00	0.00	0.00	0.00
Electricity Consumption (kWh)	6405.40	6858.69	5213.19	8668.26	10845.19
Total Cost ($)	696.46	742.40	566.63	939.22	1184.60
GHG Emission (kg)	242.10	256.75	199.06	335.20	427.80
100% Efficiency Electric Baseboard Only					
	Strathroy	*Toronto*	*Windsor*	*Ottawa*	*Thunder Bay*
Natural Gas Consumption (m^3)	0.00	0.00	0.00	0.00	0.00
Electricity Consumption (kWh)	12089.68	12357.36	11457.91	13153.02	14478.85
Total Cost ($)	1321.52	1349.67	1250.85	1436.11	1583.88
GHG Emission (kg)	461.40	468.74	435.94	501.04	556.74

Even though the commodity pricing of Ontario was consistent within the province, different regions in Ontario have different utility pricing due to its regulatory and transportation pricing. By including this cost, the operating cost of the selected cities will reflect better to the real cost, as shown in Table 2.17.

Table 2.17: Summary of results for different cities including both climatic differences and utility pricing

Smart Switching (SDFSS) with ASHP Heating					
	Strathroy	*Toronto*	*Windsor*	*Ottawa*	*Thunder Bay*
Natural Gas Consumption (m^3)	1086.26	1127.94	1016.02	1148.08	1302.26
Electricity Consumption (kWh)	491.00	476.84	474.50	712.68	769.49
Total Cost ($)	331.52	418.35	313.88	442.36	520.57
GHG Emission (kg)	2039.46	2116.68	1908.42	2161.84	2449.71
Natural Gas Furnace Only					
	Strathroy	*Toronto*	*Windsor*	*Ottawa*	*Thunder Bay*
Natural Gas Consumption (m^3)	1306.77	1335.71	1238.49	1421.71	1565.02
Electricity Consumption (kWh)	0.00	0.00	0.00	0.00	0.00
Total Cost ($)	342.04	430.78	324.17	458.52	536.44
GHG Emission (kg)	2434.52	2488.42	2307.30	2648.65	2915.63
Default Manufacturer Switching at -5 °C (NG furnace)					
	Strathroy	*Toronto*	*Windsor*	*Ottawa*	*Thunder Bay*
Natural Gas Consumption (m^3)	374.31	428.12	230.62	678.64	948.39
Electricity Consumption (kWh)	2942.45	2897.93	3079.62	2389.78	2071.10
Total Cost ($)	420.24	507.59	411.60	495.07	553.22
GHG Emission (kg)	812.89	910.27	547.76	1352.92	1840.74
Default Manufacturer Switching at -15 °C (NG furnace)					
	Strathroy	*Toronto*	*Windsor*	*Ottawa*	*Thunder Bay*
Natural Gas Consumption (m^3)	24.06	36.27	5.82	145.62	354.23
Electricity Consumption (kWh)	4498.86	4643.83	4072.91	4788.08	4755.72
Total Cost ($)	496.87	598.68	465.00	591.74	647.95
GHG Emission (kg)	216.90	244.55	166.80	453.27	840.42
Default Manufacturer Switching at -15 °C (100% Efficiency Electric Baseboard)					
	Strathroy	*Toronto*	*Windsor*	*Ottawa*	*Thunder Bay*
Natural Gas Consumption (m^3)	0.00	0.00	0.00	0.00	0.00
Electricity Consumption (kWh)	4721.42	4979.38	4126.78	6135.29	8032.94
Total Cost ($)	514.43	628.97	470.19	699.00	882.60
GHG Emission (kg)	181.17	187.66	157.63	236.87	316.65
100% Efficiency Electric Baseboard Only					
	Strathroy	*Toronto*	*Windsor*	*Ottawa*	*Thunder Bay*
Natural Gas Consumption (m^3)	0.00	0.00	0.00	0.00	0.00
Electricity Consumption (kWh)	12089.68	12357.36	11457.91	13153.02	14478.85
Total Cost ($)	1321.52	1566.74	1308.60	1502.27	1597.56
GHG Emission (kg)	461.40	468.74	435.94	501.04	556.74

With the inclusion of the utility cost, the SDFSS can still optimize the operating cost to provide the lowest cost compared to the other scenarios.

2.4.3 Different houses

To explore whether the SDFSS would be beneficial for different envelopes, two other house models are selected for this sensitivity analysis. The house located at the Toronto and Region Conservation Authority was relatively efficient. The mathematical model was taken from previous studies and was used for the heating demand. The most efficient envelope in this test was the NZEH where the CCHT was the least efficient.

The three different houses were simulated to estimate the effects of the SDFSS, natural gas furnace, default manufacturer switching at -5°C and default manufacturer switching at -15°C. The operational cost and GHG emissions were simulated with different houses and are summarized in Table 2.18.

Table 2.18: Summary of results for different houses

Smart Switching (SDFSS) with ASHP Heating			
	NZEH	*TRCA ASH*	*CCHT*
Natural Gas Consumption (m^3)	1086.26	1346.74	2002.26
Electricity Consumption (kWh)	491.00	472.35	500.43
Total Cost ($)	331.52	397.45	571.77
GHG Emission (kg)	2039.46	2524.22	3746.74
Natural Gas Furnace Only			
	NZEH	*TRCA ASH*	*CCHT*
Natural Gas Consumption (m^3)	1306.77	1551.07	2221.27
Electricity Consumption (kWh)	0.00	0.00	0.00
Total Cost ($)	342.04	405.99	581.41
GHG Emission (kg)	2434.52	2889.64	4138.22
Default Manufacturer Switching at -5 °C (NG furnace)			
	NZEH	*TRCA ASH*	*CCHT*
Natural Gas Consumption (m^3)	374.31	502.34	753.20
Electricity Consumption (kWh)	2942.45	3419.23	4880.60
Total Cost ($)	420.24	505.57	730.85
GHG Emission (kg)	812.89	1070.82	1596.25
Default Manufacturer Switching at -15 °C (NG furnace)			
	NZEH	*TRCA ASH*	*CCHT*
Natural Gas Consumption (m^3)	24.06	34.75	306.65
Electricity Consumption (kWh)	4498.86	5465.54	6742.78
Total Cost ($)	496.87	604.49	813.72
GHG Emission (kg)	216.90	274.11	829.67
Default Manufacturer Switching at -15 °C (100% Efficiency Electric Baseboard)			
	NZEH	*TRCA ASH*	*CCHT*
Natural Gas Consumption (m^3)	0.00	0.00	0.00
Electricity Consumption (kWh)	4721.42	5787.06	9579.73
Total Cost ($)	514.43	629.88	1043.38
GHG Emission (kg)	181.17	222.50	368.84
100% Efficiency Electric Baseboard Only			
	NZEH	*TRCA ASH*	*CCHT*
Natural Gas Consumption (m^3)	0.00	0.00	0.00
Electricity Consumption (kWh)	12089.68	14349.80	20550.18
Total Cost ($)	1321.52	1565.74	2240.81
GHG Emission (kg)	461.40	550.08	789.06

The results show that for all three scenarios, the SDFSS provides a cost and GHG reduction. When comparing the natural gas-only option with the SDFSS option, the less efficient envelope saw marginally

fewer cost savings in comparison to the more efficient envelope. However, when comparing the default manufacturer switching with the SDFSS, the cost savings are marginally higher for the TRCA ASH. Overall, the cost savings are relatively similar regardless of the building efficiency.

2.4.4 Different pricing profile

The last sensitivity analysis performed was to determine the impact of the new Advantage Power Pricing (APP). This new pricing plan aims to reduce the electricity cost during the overnight off-peak hours. Table 2.19 shows the four different costs associated with the new APP pricing plan.

Table 2.19: Different pricing tier and its marginal price

Pricing Tier	Pricing per kWh
Off-Peak	9.22 ¢
Mid Peak	12.05 ¢
On-Peak	21.61 ¢
Super Off-Peak	4.49 ¢

This new pricing was included in the simulation, and in addition to analyzing the price change to the benchmark scenario, the new pricing was also implemented to simulate the effect in combination with the upcoming carbon pricing. Table 2.20 shows a summary of the results due to the new APP and different carbon pricing.

Table 2.20: Summary of results with new APP also looking at the inclusion of carbon pricing

Smart Switching (SDFSS) with ASHP Heating						
	No Carbon tax	*$10/tonne Carbon Tax*	*$20/tonne Carbon Tax*	*$30/tonne Carbon Tax*	*$40/tonne Carbon Tax*	*$50/tonne Carbon Tax*
Natural Gas Consumption (m^3)	893.87	847.71	785.78	730.49	666.58	594.76
Electricity Consumption (kWh)	1251.24	1379.94	1565.82	1742.72	1958.71	2216.32
Total Cost ($)	310.68	329.10	346.35	362.38	377.00	390.25
GHG Emission (kg)	1702.35	1620.76	1512.50	1416.64	1305.69	1182.11
Natural Gas Furnace Only						
	No Carbon tax	*$10/tonne Carbon Tax*	*$20/tonne Carbon Tax*	*$30/tonne Carbon Tax*	*$40/tonne Carbon Tax*	*$50/tonne Carbon Tax*
Natural Gas Consumption (m^3)	1306.77	1306.77	1306.77	1306.77	1306.77	1306.77
Electricity Consumption (kWh)	0.00	0.00	0.00	0.00	0.00	0.00
Total Cost ($)	342.04	369.55	397.06	424.57	452.08	479.59
GHG Emission (kg)	2434.52	2434.52	2434.52	2434.52	2434.52	2434.52
Default Manufacturer Switching at -5 °C (NG furnace)						
	No Carbon tax	*$10/tonne Carbon Tax*	*$20/tonne Carbon Tax*	*$30/tonne Carbon Tax*	*$40/tonne Carbon Tax*	*$50/tonne Carbon Tax*
Natural Gas Consumption (m^3)	374.31	374.31	374.31	374.31	374.31	374.31
Electricity Consumption (kWh)	2942.45	2942.45	2942.45	2942.45	2942.45	2942.45
Total Cost ($)	396.32	404.20	412.08	419.96	427.84	435.72
GHG Emission (kg)	812.89	812.89	812.89	812.89	812.89	812.89
Default Manufacturer Switching at -15 °C (NG furnace)						
	No Carbon tax	*$10/tonne Carbon Tax*	*$20/tonne Carbon Tax*	*$30/tonne Carbon Tax*	*$40/tonne Carbon Tax*	*$50/tonne Carbon Tax*
Natural Gas Consumption (m^3)	24.06	24.06	24.06	24.06	24.06	24.06
Electricity Consumption (kWh)	4498.86	4498.86	4498.86	4498.86	4498.86	4498.86
Total Cost ($)	458.07	458.58	459.09	459.59	460.10	460.61
GHG Emission (kg)	216.90	216.90	216.90	216.90	216.90	216.90
Default Manufacturer Switching at -15 °C (100% Efficiency Electric Baseboard)						
	No Carbon tax	*$10/tonne Carbon Tax*	*$20/tonne Carbon Tax*	*$30/tonne Carbon Tax*	*$40/tonne Carbon Tax*	*$50/tonne Carbon Tax*
Natural Gas Consumption (m^3)	0.00	0.00	0.00	0.00	0.00	0.00
Electricity Consumption (kWh)	4721.42	4721.42	4721.42	4721.42	4721.42	4721.42
Total Cost ($)	472.17	472.17	472.17	472.17	472.17	472.17
GHG Emission (kg)	181.17	181.17	181.17	181.17	181.17	181.17
100% Efficiency Electric Baseboard Only						
	No Carbon tax	*$10/tonne Carbon Tax*	*$20/tonne Carbon Tax*	*$30/tonne Carbon Tax*	*$40/tonne Carbon Tax*	*$50/tonne Carbon Tax*
Natural Gas Consumption (m^3)	0.00	0.00	0.00	0.00	0.00	0.00
Electricity Consumption (kWh)	12089.68	12089.68	12089.68	12089.68	12089.68	12089.68
Total Cost ($)	1219.29	1219.29	1219.29	1219.29	1219.29	1219.29
GHG Emission (kg)	461.40	461.40	461.40	461.40	461.40	461.40

The results show that, with the SDFSS option, the new APP reduces the operational cost. The default manufacturer switching system set at -15°C did not benefit from this change as much as the SDFSS since

the system was operating the ASHP majority of the time and the lower cost during the night does offset the high cost during the day. The natural gas-only scenario was not affected since changing the cost of electricity does not impact a natural gas-fired furnace.

As expected from the previous analysis, as the carbon pricing increases, the operating cost for all the scenarios increases. However, with this added APP, the operating cost comparison between natural gas-only option and the SDFSS showed an increased cost reduction. This analysis fully shows the effects of the foreseeable changes in tax pricing and electricity pricing.

Chapter 3 – Heat Pump Water Heater Performance Testing and Assessment in Cold Climate

3.1 Methods

In this study, the team installed the air source heat pump water heater (ASHPWH) in the Toronto and Region Conservation Authority Archetype Sustainable House (TRCA ASH) located in Woodbridge, Ontario. The ASH was a semi-detached house, each unit fitted with different energy-efficient technology for real-life testing scenarios. The ASHPWH system was set up at "House A" which had R21 Roxul Batt Fibre Insulation with Styrofoam fitted outside totalling to R30 walls. The Archetype Sustainable House is an accessible location for many research projects and many performance tests. Since the house is located in Woodbridge, Ontario, the climate is an excellent representation of the Toronto climate.

3.1.1 The Location

The TRCA ASH is located in Woodbridge, a region in the north-west of Toronto, Ontario. The location is not obstructed and is in a conservation area. The weather at Woodbridge is relatively similar to that of the Toronto region. Since the location is relatively close to Toronto, the Toronto weather data is used in the TRNSYS simulation model. The TRCA ASH is roughly 17.5 km northeast from the Toronto Pearson Airport.

3.1.2 House Specifications

The ASHPWH for the study was installed in the TRCA ASH. The ASH is a relatively efficient house compared to the standard house built to the Ontario building code. This semi-detached house was separated into two separate houses, House A and House B. The study was performed on house A, and the ASHPWH was installed in the basement of the house. This house has several energy-efficient equipments installed [59].

Table 3.1 lists the HVAC equipment installed in House A. The flat plate solar collector was covered to ensure that the solar energy did not affect the overall results. The ASHP was initially designed and used for space heating. However, for the purpose of this study, the ASHP was used to heat the domestic hot water, and the space heating was replaced with another experimental hydronic system. In addition to all the efficient equipment, the ASH is well insulated. Table 3.2 summarizes the envelope features of the TRCA Archetype House A.

Table 3.1: HVAC and water heating equipment in House A [59]

Equipment
Heat Recovery Ventilator
Air Source Heat Pump
Air Handling Unit
Drain Water Heat Exchanger
*Flat Plate Solar Collector
Mini Boiler
Domestic Hot Water Tank

Table 3.2: Envelope features of the Archetype Sustainable House A [43]

House Features	Specification
Basement Walls	R-20 with Durisol Blocks
Walls	R-30
Wall Insulation	R-21 Roxul Batt Fibre w/ 3" Styrofoam
Windows	Double Paned, Low "E", Fibreglass framed
Roof	R-40 insulated with Styrofoam panels

3.1.3 Domestic Hot Water Heater

Figure 3.1 shows the schematic of the ASHPWH and all the components of the system. For the performance testing of the system, the existing setup was modified in the TRCA ASH House A to accommodate the ASHP system.

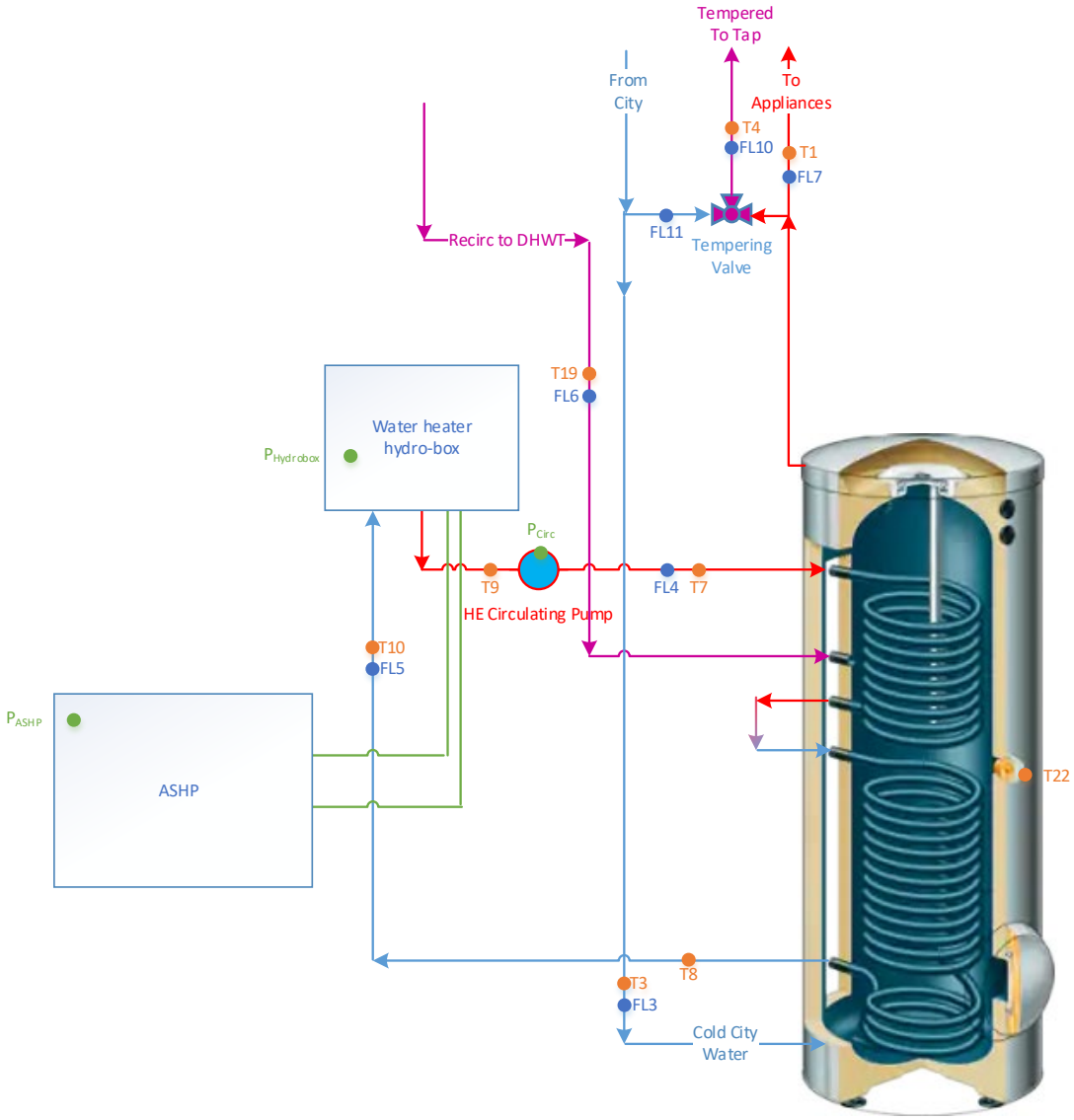

Figure 3.1: Schematic of the testing system

House A had a solar water heater and a greywater heat recovery system installed in the piping. In order to collect the most accurate performance data for the ASHPWH system, these auxiliary equipments were disconnected to prevent it from supplying heat and also avoid thermal siphoning. The tank used in this study has two heat exchanger coils, one for the ASHPWH and the other for the solar collectors. In typical installations, the heat pump and auxiliary heater fit into the smaller upper coil, and the solar collector connects to the bigger lower coil of the tank.

Since the study does not need the solar collector, the two coils in the tank were connected. The two connected coils will increase the contact surface of the heating fluid and the tank water, allowing the heating fluid to transfer the maximum amount of heat to the tank water.

Figure 3.1 shows the testing system where the hot fluid from the ASHPWH hydro-box directly passes through both tank coils in series. The water from the loop returns into the hydro-box to be heated. The heated tank water was mixed with the cold city water with the tempering valve to prevent scalding. The tank supplied the hot water directly to the appliances that require high-temperature hot water, such as the dishwasher and the clothes washer. Multiple sensors were installed into the system in order to collect all the required data for performance testing and evaluation. There were 24 sensors installed in this system where some of the sensors were redundant and were used to verify essential readings. There were temperature and flow sensors in all the piping to and from the DHW tank. Additionally, the power consumption of the ASHP and auxiliary heater device was measured. The outdoor temperature, outdoor humidity, basement temperature and basement humidity were also measured.

3.1.4 TRNSYS Model

A TRNSYS model was created in order to simulate the performance of the ASHPWH. The TRNSYS simulation model for the Toronto and Region Conservation Authority (TRCA) Archetype Sustainable House (ASH) was taken from the research performed by Safa et al. [60]. The TRNSYS model was modified to include the ASHPWH within the TRNSYS system. The manufacturer specifications were taken and programmed within the TRNSYS heat pump module. The hourly draw profile (explained in Section 3.2.1 was also programmed into the simulation.

The data collected from the sensors were analyzed to calculate the capacity and COP of the ASHPWH. The analysis was performed with the developed MATLAB code to determine the produced thermal energy and also the COP of the system. The data collected was used to calibrate the simulation model to ensure that the model was accurate so that the model could be used to predict system performance in other regions.

Figure 3.2 shows the TRNSYS model created by Safa et al. and several indoor and outdoor conditions from the model were used as input for the ASHPWH model [61]. The original model was created and was obtained through the thesis attachments.

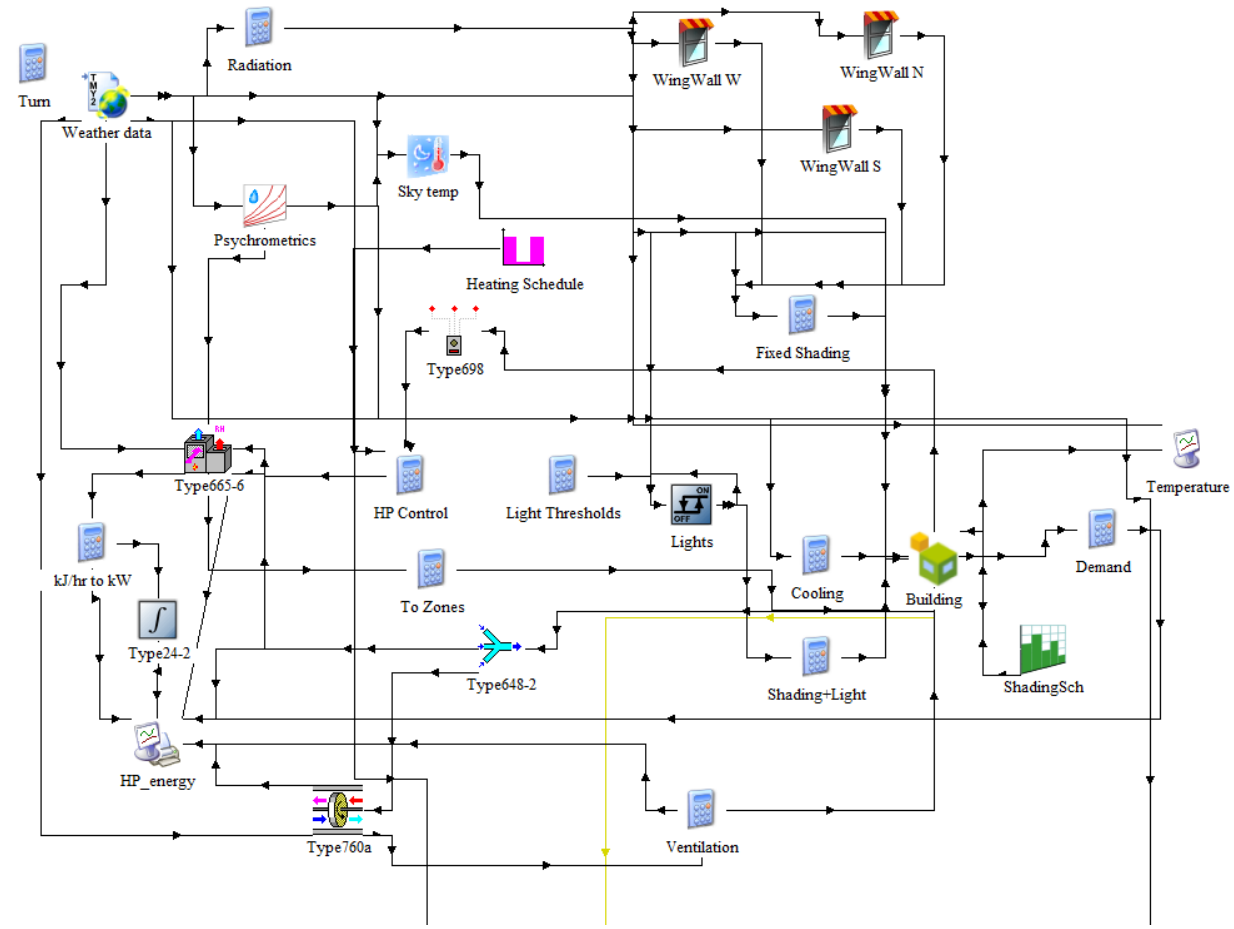

Figure 3.2: TRCA ASH TRNSYS model [61]

Figure 3.3 shows the ASHPWH simulation model. The input to the ASHPWH was collected from the TRCA ASH model. The module (Type938) simulates the ASHPWH and Type3d acts as the pump that moves the liquid around. Type1502 is the temperature control for both the heat pump and the electric resistance heating. Type2270 is the resistance heating module. When the ASHPWH was not efficient or cannot meet the hourly demand. Type14b is the flow controller for the hot water consumption using the draw profile discussed in Section 3.2.1. Type14e and Type649 are the city water and mixing plenum, respectively. All the modules are combined to simulate the ASHPWH system with the hot water storage tank.

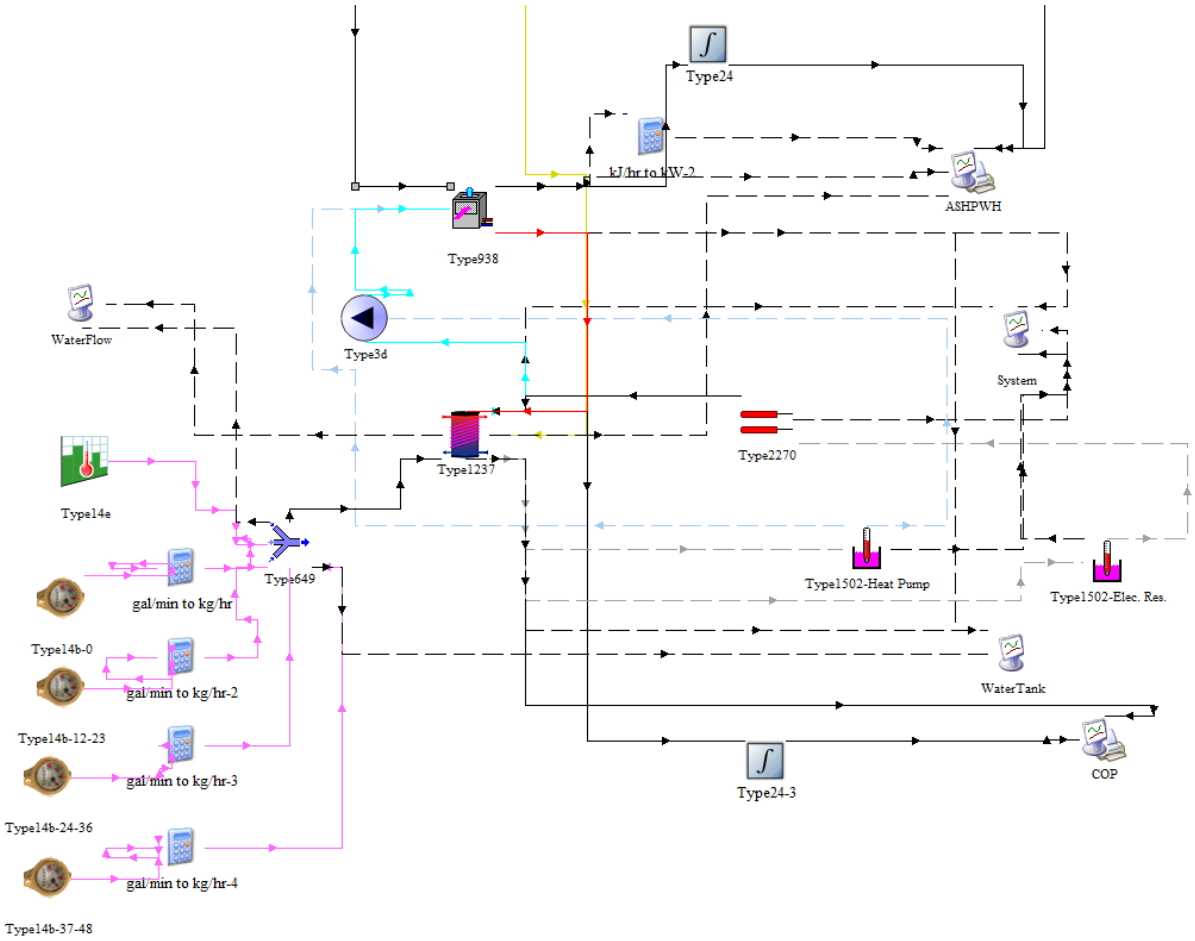

Figure 3.3: ASHPWH TRNSYS model schematic layout

3.1.5 Sensor Calibration

The sensors were implemented into the system to take specific readings for essential data for the performance analysis. The data for temperature and flow was captured and placed into a data acquisition system. Table 3.3 shows the sensors installed along with the identification tag used to name each specific sensor. The description of the sensor was also included to locate where the sensors are and what the sensor does.

Table 3.3: Sensor type information, identification and description

Tag	Sensor Type	Description	Temperature Range
T7	Temperature	Water temperature in the coil from the hydro-box into the tank	0°C - 160°C ±0.04°C
T8	Temperature	Water temperature in the coil from the tank back to the hydro-box	0°C - 160°C ±0.04°C
FL4	Water Flow	Water volumetric flow rate in coil from the hydro-box into the tank	1 to 25L/min ±3%
T10	Temperature	Water temperature in the coil from the tank back to the hydro-box	0°C - 160°C ±0.04°C
T9	Temperature	Water temperature in the coil from the hydro-box into the tank	0°C - 160°C ±0.04°C
FL5	Water Flow	Water volumetric flow rate in coil from the tank back to the hydro-box	1 to 25L/min ±3%
RH	Humidity	Outdoor Relative humidity	0-100% ±4%
AT	Temperature	Outdoor Ambient Air Temperature	-40 - 60°C ±0.2°C
T22	Temperature	Water Temperature in the middle of the tank	0°C - 160°C ±0.04°C
T1	Temperature	Potable water temperature in from the tank (1 ft down the pipe)	-50 to 250°C ±0.3°C
T3	Temperature	Cold city water temperature flowing into the tank	-50 to 250°C ±0.3°C
T4	Temperature	Tempered water temperature to the faucet	-50 to 250°C ±0.3°C
FL10	Water Flow	Tempered water flow rate to the faucet	1 to 25L/min ±3%
FL11	Water Flow	Cold city water flow rate to tempering valve	1 to 25L/min ±3%
FL3	Water Flow	Cold city water flow rate to tank	1 to 25L/min ±3%
FL6	Water Flow	The recirculation flow rate of domestic water into the tank	1 to 25L/min ±3%
FL7	Water Flow	Scalding water to appliances	1 to 25L/min ±3%
AT Basement	Temperature	Ambient air temperature for basement	-10°C to 60°C ±0.2°C
RH Basement	Humidity	Ambient air Relative Humidity	0-100% ±2%
P_{ASHP}	Power	Power of ASHP	120- 600VAC; 5 – 6000A ±0.5%
$P_{Hydrobox}$	Power	Power of hydro-box	120- 600VAC; 5 – 6000A ±0.5%
P_{Circ}	Power	Power of circulating pump	120- 600VAC; 5 – 6000A ±0.5%
P_{Load}	Power	Power of mini backup electric boiler	120- 600VAC; 5 – 6000A ±0.5%

Table 3.3 shows the sensor types and the location of the sensor for the system. There are numerous sensors that are installed to confirm and validate readings.

The temperature sensor probes were prepared with a calibrator, and the temperature was calibrated for 10°C, 20°C, 30°C, 40°C, 50°C, 60°C and 70°C. The calibrator used was the SiKa TPM 165S with ±0.01°C accuracy. The processes used to perform the calibration w referenced from Zhang [62].

The calibrator was set to the temperature, and the probes are left in the calibrator for an extended period of time until the calibrator reaches equilibrium. Since several mathematical models depend on the change in temperature, the pairs of temperature probe that are related to each other are calibrated together in the same calibrator well. The coil temperature probes are calibrated together, and two sets of probes are used to measure the coil temperatures and confirm the reading.

Figure 3.4 shows the calibration curves for the temperature probes used in the water tank coil. The calibration setting temperature was constant, and the sensor readings slowly increase until it reaches a steady

temperature. Every temperature for the calibrator was maintained for an extended period to ensure that the sensor was calibrated accurately. The calibration continued until the measurement shows a plateau to a constant temperature of 60°C.

The tank temperature probes are calibrated together to ensure that there are minimal errors between the readings.

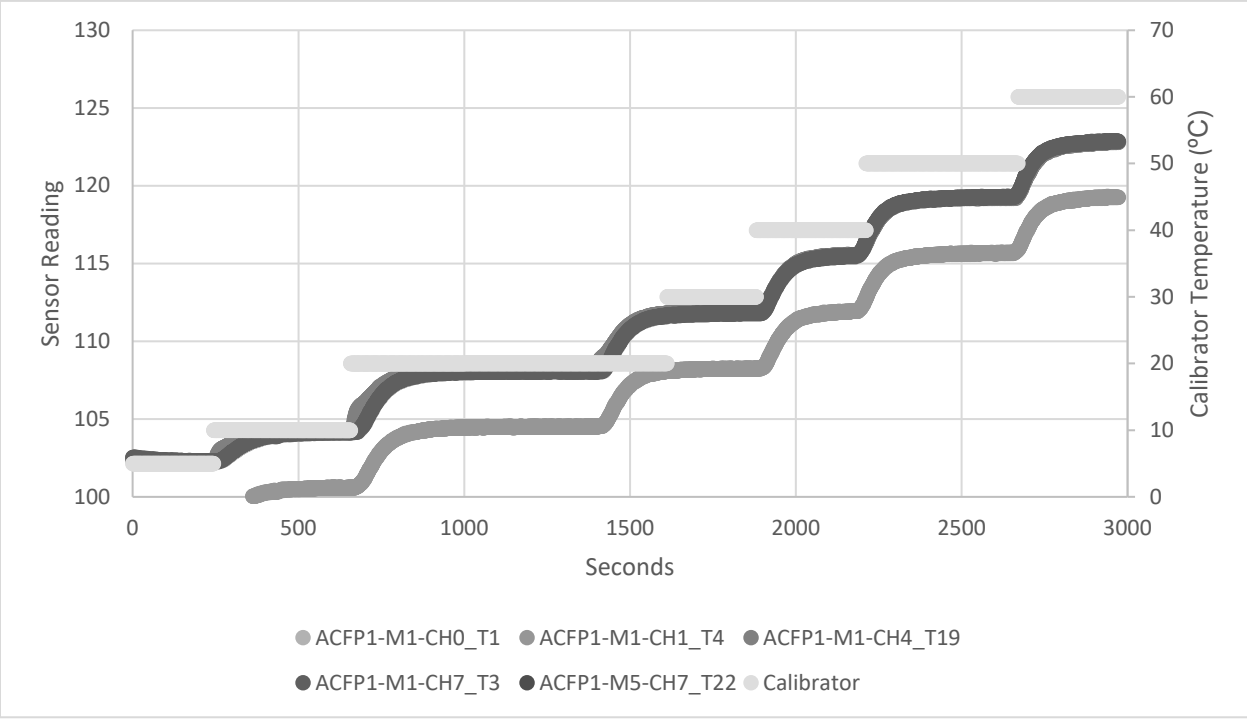

Figure 3.4: Sample of the temperature calibration curve

Similar to the temperature probes for the coils, the temperature for the tank was also calibrated with the same method. There was one temperature sensor located in the middle of the tank and a sensor located at the inlet pipe for city water. One temperature probe was located at the scalding water for appliances and another temperature probe for the tempered water. The indoor ambient air temperature, outdoor air temperature and the outdoor relative humidity are regularly maintained and calibrated by TRCA ASH. Figure 3.5 shows a sample of the temperature calibration.

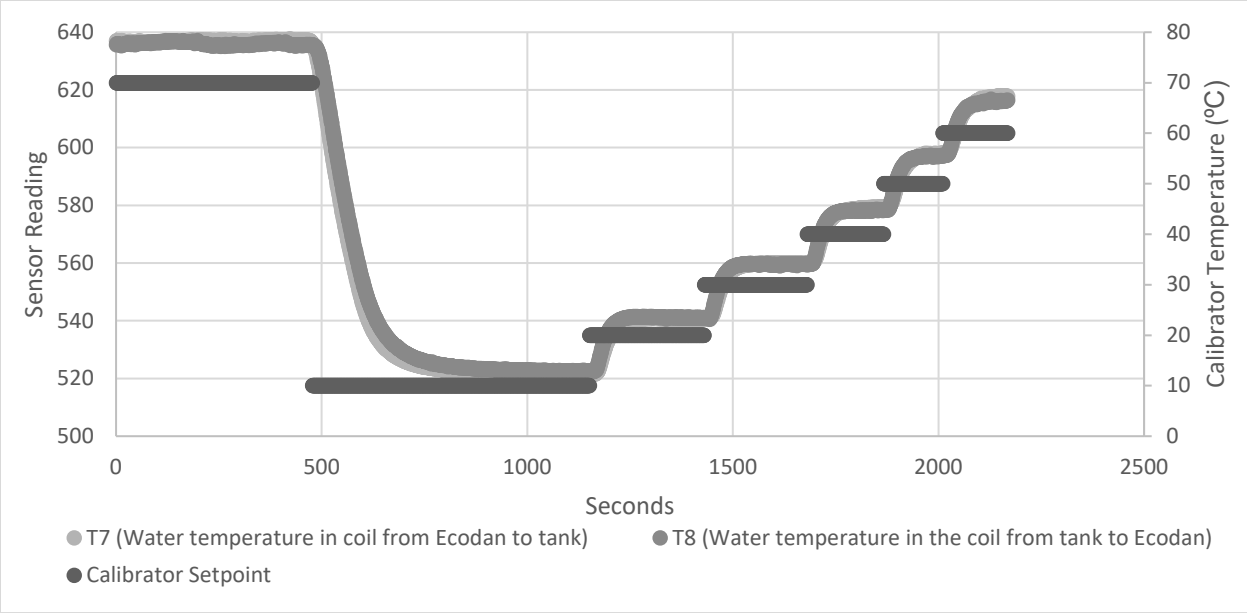

Figure 3.5: Sample of the temperature calibration curve

The flow meters are calibrated manually all at the same time. The flow meters are connected in series in a pipe where a pump forces water through the pipe. The flowing water was collected in a calibrated bucket. The duration and the quantity of water flowing into the bucket were recorded to calibrate the flow meters. A similar volume of water was tested multiple times for consistency, and different flow rates were tested. The volumetric flow rate can be calculated using the duration, and the volume measured. Figure 3.6 shows a sample of the calibrated curves for a flow sensor.

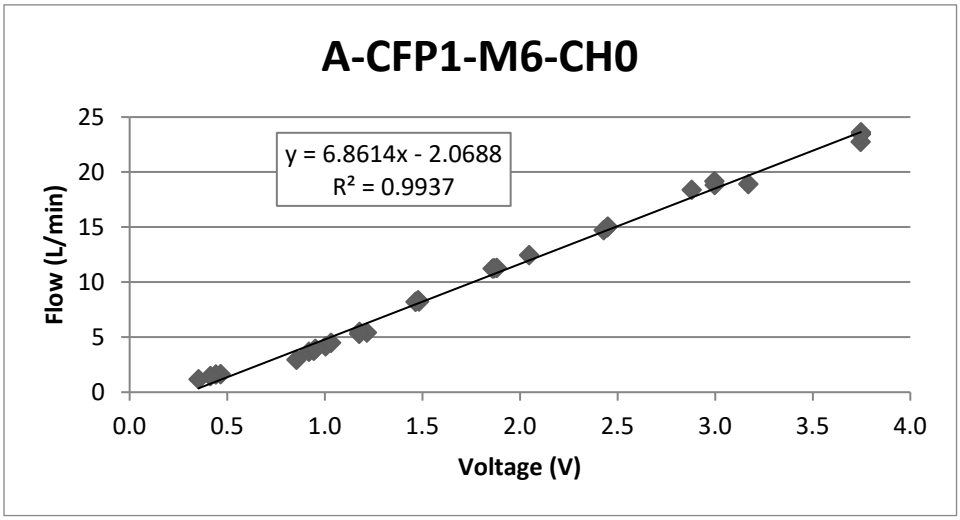

Figure 3.6: Sample of the calibration curve for flow sensors

3.1.6 Domestic Hot Water Draw Profile

The hot water draw profile was created using the guidelines from IEA Annex 42 [63]. The annual hot water consumption was made with 200L/day on average in mind. Since there are hardware restrictions within the testing setup, there can only be three flow rates that can be used. A calibration test was performed on the domestic hot water valves to measure the maximum and minimum flow rate of each of the valves. The three different flow rates were selected to represent different water usage. The three main usages selected for the flow rate are for short duration hand-washing, more prolonged duration hot water usage and lastly, showers.

Jordan and Vajen performed a study in domestic hot water consumption profile [64]. The study performed a realistic domestic hot water usage profile for different hours of the day. The study used 1L/min as the lowest flow rate and 6L/min for medium load and 8L/min for showers. Initially, the three actuators were calibrated to these flows, but it was found that the 1L/min flow rate was too low for the sensors to measure the flow rate accurately. The minimum flow rate was calibrated to 1.5L/min instead of 1L/min in order to have a more accurate reading.

3.1.7 MATLAB Analysis Program

MATLAB was used to analyze the data collected from the data acquisition system (DAQ). The data was collected at every second and each file from the DAQ system was saved daily. The MATLAB program was able to aggregate the data to minutely, hourly and daily averages. The program first imports every file for a range of dates. The imported data was expressed in three different matrices representing every minute, hour and day.

During the data importing, the importing subroutine averages or integrates the per second data and combines it to a per-minute format. The temperatures are averaged, and flow rates are integrated for one value to represent every minute. The heat produced for every minute was calculated using Equation 28.

$$\boldsymbol{Q = \dot{m} C p \Delta T} \qquad \textit{(Equation 28)}$$

Where: $\Delta T = Temperature$ (°C)

$Q = Heat\ supplied\ by\ ASHPWH\ (kWh)$

$\dot{m} = mass\ flowrate\ of\ the\ fluid\ (kg/min)$

$C_p = Specific\ heat\ capacity\ of\ the\ fluid\ (kj/kg°C)$

Since the data collected are either temperature or volumetric flow rate, Equation 28 must be modified in order for the calculation to be performed.

$$\boldsymbol{Q = \rho \dot{V} C_p (T_{supply} - T_{return})} \quad \textit{(Equation 29)}$$

Where: $\rho = Density\ of\ the\ fluid\ (kg/m^3)$

$\dot{V} = Volumetric\ flow\ rate\ (L/min)$

Equation 29 replaces the mass flowrate with density and volumetric flow rate. The specific heat of the fluid and density of the fluid varied depending on the temperature and was also represented by an equation.

$$\boldsymbol{\rho = 1000\left[1 - \frac{(T-4)^2}{119000 + 1365T - 4T^2}\right]} \quad \textit{(Equation 30)}$$

Equation 30 was used to calculate the density of the fluid. The equation was referenced from Shaughnessy [65], which was derived by Kravchenko [66]. This equation provides a more accurate estimation for the density of the fluid.

4.18 kJ/kg°C was used to calculate the specific heat [65]. Equation 29, Equation 30 and the specific heat of water were combined, and the temperatures used would be the average return and supply temperature of the heat pump. There were also conversion values used to convert the values for minutely and hourly formats.

The COP of the heat pump was calculated by dividing the heat generated by the electricity consumed by the ASHPWH.

$$COP = \frac{Q}{E_{in}} \quad \textit{(Equation 31)}$$

Where: $E_{in} = Electricity\ Input\ (kWh)$

The data was organized into different scenarios presented in Section 3.1.8.

3.1.8 Scenarios

This study was broken down into different scenarios in order to highlight the overall effect of the ASHPWH. The study also highlights the difference between the different installation configurations.

3.1.8.1 Pre Coil Change Configurations

The initial configuration was referred to in this paper as a pre-coil change configuration where the ASHPWH was only connected to the upper coil (refer to Figure 3.1 for visual). This water tank was meant for solar collector heating, connected at the lower coil, coupled with a secondary heater for backup, connected at the

upper coil. In this study, the solar collector was still connected, but the solar collector was covered with a wooden box fixture for the majority of the study and the valve was later shut off to prevent thermal siphoning. The pre coil change configurations further consist of several cases which include, pre coil change configuration without special cases, with solar heating collector active, no hot water draw, consistent hot water draw, and a cold start test. The data for all these scenarios were analyzed and illustrated in this section.

3.1.8.2 Post-Coil Change Configurations

The post coil change in this study was the combination of the two coils in the tank. The two coils are connected in series in order to significantly increase the performance of the ASHPWH. The increase of coil length in-turn increases the active surface area for the heat transfer and also increases the COP of the ASHPWH. The post coil change contains two cases, including, post coil change configuration without special cases, and cold start test.

3.1.9 Sensitivity Analysis

In order to accurately determine if the heat pump water heater was useful in different cities and different scenarios, a simulation model was required to investigate the effect of the system in different climates. The climate data for five major Canadian cities were selected for the simulation of the heat pump water heater. They are:

1. Toronto
2. Montreal
3. Vancouver
4. Edmonton
5. Halifax

The simulation will show whether the ASHPWH would work in these cities. The simulation model was created using TRNSYS, and the weather data was inputted as TMY data. The results of the simulation show the amount of electricity it consumes and how much heat it outputs. The COP was calculated and using all the simulated data; the ASHPWH can be analyzed to see whether or not it was viable or not. The sensitivity analysis was performed to analyze the impact on operating cost and performance when different parameters are changed.

Using the TRNSYS simulation model, five different Canadian cities were selected to estimate the operating cost and GHG emission. The utility cost and electricity GHG emission factors were kept constant with Toronto. In this sensitivity analysis, the outdoor temperature was varied depending on the climatic condition

of the selected city. This will show the performance of the ASHPWH in a different climate. The results of this sensitivity analysis can be further translated to other cold climate regions.

3.2 Input Data

This section provides an overview of the input parameters for the simulation models. The domestic hot water draw profiles are explained and identified first, and the input data for the TRNSYS model and analysis was discussed subsequently.

3.2.1 Domestic Hot Water Draw Profile

The domestic hot water draw profile was significant in this study as it resembles the average hot water usage. Using the DHWcalc 2.02 designed by Jordan and Vajen [64], the program uses a probability distribution and a total mean daily draw volume to generate a flow profile of a typical day. The outcome from the program was modified to use the available flow rate of 1.5L/min, 6L/min and 8L/min in order to meet each hourly demand. The flow resolution was per minute, and the hourly consumption was spread out over the hour to simulate a more realistic consumption.

Figure 3.7 shows the typical draw profile for a test day. This draw profile was used for the experiment to represent a daily hot water consumption of a typical household. This draw profile was used as the base case for all the analyses.

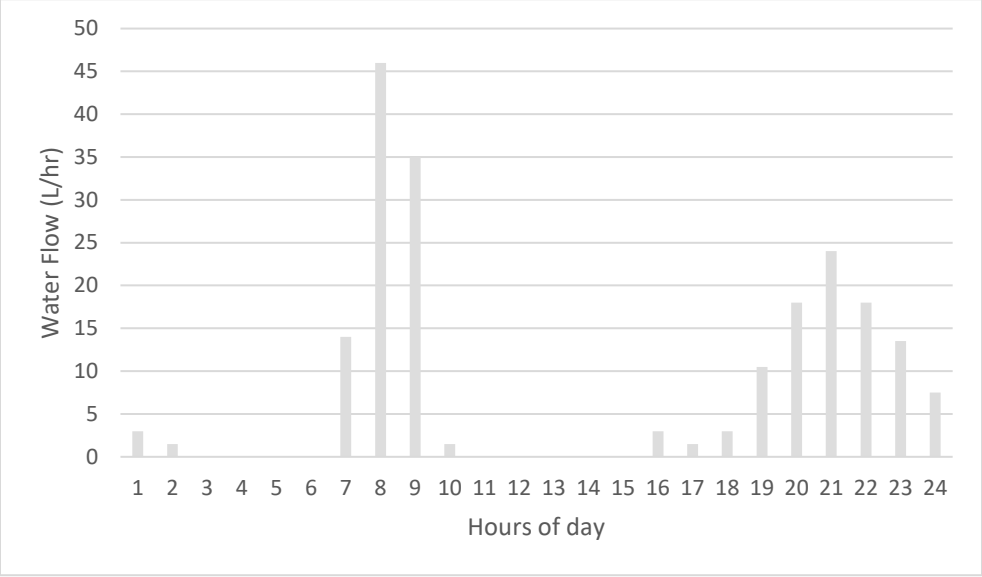

Figure 3.7: Typical draw profile for a day

A constant draw profile was also created to simulate a more significant instantaneous hot water consumption. This can be used to help to assess the performance of the ASHPWH by extending the operating time of the heat pump.

Figure 3.8 shows the draw profile for a consistent hot water draw test. The hot water draw was scheduled into four separate hours in order to allow the heat pump water heater to heat the water back up. This allows the ASHPWH to operate at a more prolonged duration rather than short cycles. Though this was not an excellent hourly representation of actual residential hot water consumption, the daily consumption volume was maintained consistently at 200L/day. The primary purpose of this process was to allow the ASHPWH to reach a steady-state operation by minimizing short cycling.

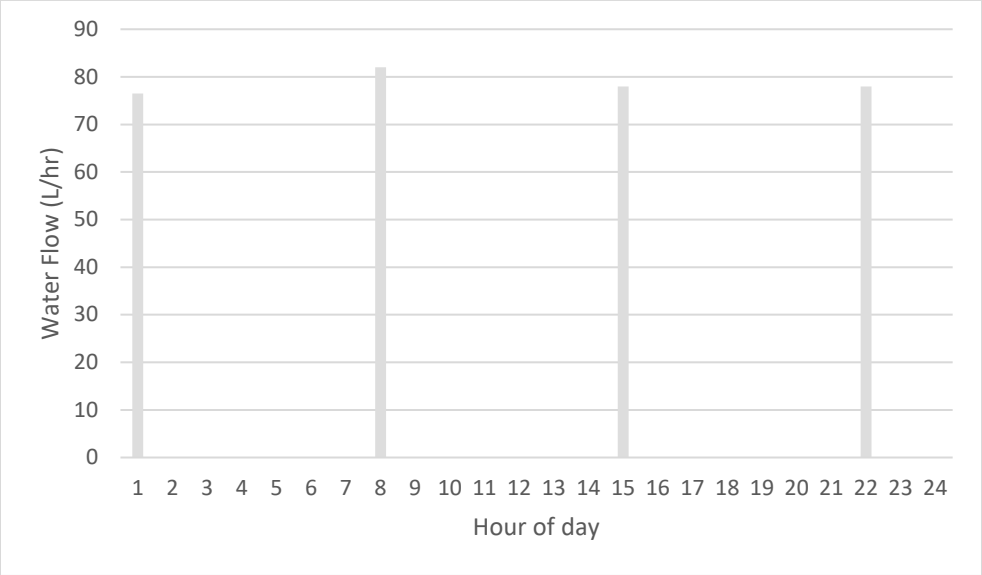

Figure 3.8: Consistent water draw profile for a day

3.2.2 TRNSYS Model Parameters

The TRNSYS simulation was modelled with the manufacturer specifications and also using the draw profile created. The ASHPWH manufacture performance was divided by outdoor temperature, supply water temperature and outdoor relative humidity. The performance profile was included in Appendix A. This file was used to map the performance in Type 938.

Similarly, Type 1237 represents the tank with the heat exchanger coils. The tank was modelled to match the manufacturer specification and the testing scenario. In this study, there are only three tank temperature nodes used, one at the top at the water outlet, one at the bottom at the city water inlet and one additional one at the center of the tank. The TRNSYS model was also configured similarly with only three tank nodes to simulate a stratified tank model.

Table 3.4 shows the tank specifications used for the TRNSYS model. The heat exchanger pipe dimensions are estimated using the manufacturer diagram. The tank wall thermal conductivity was estimated using the manufacturer's specified polyurethane foam.

Table 3.4: Tank specifications

Tank volume	0.3 m^3
Tank height	1.734 m
Tank wall thickness	6.35 cm
Tank wall thermal conductivity	0.126 kJ/hr-m-K
HX pipe inner diameter	0.01986 m
HX pipe outer diameter	0.0254 m
HX pipe length	19.23 m
Height of HX wrap	1.279 m
HX tube spacing	0.043 m

The water draw profile was set into Type 14b to operate using the set timings. The flowrate was configured for 1.5L/min, 6L/min and 8L/min. The plenum was used to consolidate the three flows, and the city water flows into the tank at the same rate of water draw from the tank by the draw profiles. A control was configured for the heat pump and electrical resistance heating. The control types will determine whether or not the heat pump will operate. If the heat pump does not operate, the electric resistance supplementary heater was used to meet the water demands.

3.2.3 Data Analysis

The purpose of this project was to analyze the performance of the heat pump water heater system. The data analysis portion of the project was one of the most crucial aspects of this project. The data was collected from the sensors, and a program written in MATLAB was used to organize the data. The system records data approximately every second; however, the MATLAB code organizes the data to average the results to every minute. Through the program, the data was used in the calculation to find the coefficient of performance, and the final results are displayed. Numerous mathematical models were created and used to calculate the final results. The performance was also analyzed to compare with natural gas boiler with a constant 80% efficiency (referenced from OBC SB-12 Compliance package M) [67].

3.2.3.1 Pricing and other parameters used

In Toronto, the electricity prices vary depending on the time of day. The time-of-use (TOU) pricing was split into two different seasons. The summer and winter seasons have different pricings where the mid-peak and high peak was switched around. Both seasons have the same time for off-peak hours. The electricity costs and the natural gas cost was taken from the Ontario Energy Board [46]. The tier schedule was presented previously in Figure 2.6.

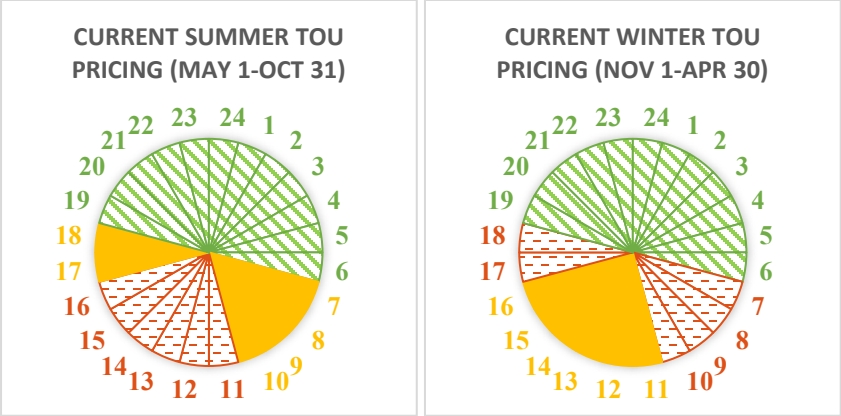

Figure 3.9: Time-of-use Schedules

Table 3.5 illustrates the different tier commodity pricing of the current electricity pricing. This pricing was the commodity price where the transportation charges and delivery charges were not included. The additional charges vary from distributors to distributors.

Table 3.5: Wholesale Ontario electricity time-of-use price for 2018

Price Tiers	Current Price
On-Peak	13.2 ¢/kWh
Mid-Peak	9.5 ¢/kWh
Off-Peak	6.5 ¢/kWh

Table 3.6 shows the additional charges that are included in the marginal cost calculations.

Table 3.6: Cost breakdown for April 2018 [68]

Charges	Rates
Distribution Charge	$0.01512/kWh
Retail Transmission Network Service Rate	$0.00763/kWh
Retail Transmission Connection Service Rate	$0.00567/kWh
Wholesale Market Service Rate	$0.0036/kWh
Global Adjustment Rate	$0.001721/kWh
Rural or Remote Electricity Rate Protection Charge	$0.0003/kWh
HST	13%
PST Rebate	-8%

The GHG emission from electricity varies depending on the time of day. Depending on the source of the generated electricity, the GHG impact fluctuated. Some of the power plans used for electricity generation are natural gas-powered and are mainly used to meet peak loads. Gordon et al. highlighted a method to estimate hourly GHG emissions[15, 16]. Brookson et al. also used this method to estimate the Ontario electrical grid [56]. Using this method, the hourly GHG emissions factor was calculated using the information from IESO [57].

After the surcharges were included in the commodity price, the marginal price was significantly increased. Table 3.7 shows the marginal price of electricity. It was also evident that the off-peak marginal price was significantly lower than the on-peak marginal price. The significant price difference was beneficial for electricity usage.

Table 3.7: Marginal TOU electricity prices for the Toronto

Off-Peak Marginal Price	Mid-Peak Marginal Price	On-Peak Marginal Price
$0.1098/kWh	$0.1413/kWh	$0.1801/kWh

The natural gas marginal price was calculated similarly to the marginal price of electricity. The price breakdown for natural gas was separated by the monthly natural gas consumption amount. Table 3.8 shows the pricing breakdown for natural gas.

Table 3.8: Price breakdown for Natural gas April 2018 [69]

Charges	Rates
Gas Used	$0.094452/$m^3$
Gas Price Adjustment	-$0.000885/$m^3$
Transport to Enbridge	$0.047525/$m^3$
Delivery	First 30 m^3: $0.110799/$m^3$ Next 55 m^3: $0.104625/$m^3$ Next 85 m^3: $0.0.099791/$m^3$ Over 170 m^3: $0.096188/$m^3$
Cap-and-Trade	$0.033518/$m^3$
HST	13%

In Table 3.9, the gas pricing was broken down into 4 different consumption tiers. For the purpose of this study, the pricing for the first 30 m^3 of natural gas was used for the analysis.

Table 3.9: Marginal Cost for natural gas

First 30 m^3	Next 55 m^3	Next 85 m^3	Over 170 m^3
$0.322512/$m^3$	$0.315536/$m^3$	0.310073m^3	$0.306002/$m^3$

For this study, natural gas was being compared with electricity, and the energy density for natural gas was needed. Union gas reported that the equivalent energy for natural gas was 10.395 kWh/m^3[70]. Similarly, the GHG emission intensity of natural gas was available from the Ontario government and 1.863 kg/m^3[53].

These pricing and information collected were used for the economic comparison between operating the ASHPWH and operating a typical 95% efficient natural gas furnace. The electricity and natural gas pricing remained constant for sensitivity analysis.

3.2.4 Sensitivity Analysis Parameters

Several scenarios of the sensitivity analysis were performed to determine the effects of changing specific parameters. Four other major Canadian cities located within different climates were used for the sensitivity analysis. The five cities include Toronto, Montreal, Vancouver, Edmonton, Halifax. The selected cities are

selected to represent different regions in Canada, including east and west coasts. The electricity and natural gas prices are kept constant. The main goal of this sensitivity analysis was to identify the performance of the ASHPWH in different climates. The variety of different climates tested can be extended to other cities in cold climate regions, and the impact of the change in outdoor temperature will yield a similar result as well. The TMY weather data was taken from TRYNSYS's database and was simulated for the annual results for each of the cities.

3.3 Results

The study results are separated into three main sections. The main findings are

1. TRNSYS simulation result
2. Heating characteristic curve
3. Related sensitivity analysis using the calibrated TRNSYS simulation model

3.3.1 TRNSYS Simulation

An energy model was created in TRNSYS to simulate the heat pump water heater electricity consumption. This TRNSYS model was created by modifying the house model created by Safa et al. [61] of the TRCA Archetype House A. The model was created using the heat pump manufacturer's specification and the tank manufacturer specifications. All the equipment specifications are added to the model to ensure that the model was as accurate as possible.

A full year simulation was performed to illustrate the hourly energy consumption profile for the year.

Figure 3.10 shows the hourly heat pump energy consumption for a typical year. The trend of the graph shows that the highest energy consumption was within the winter months. This was expected as the winter months have colder outdoor ambient temperatures, which cause the heat pump to consume more electricity to transfer the same amount of heat to the water.

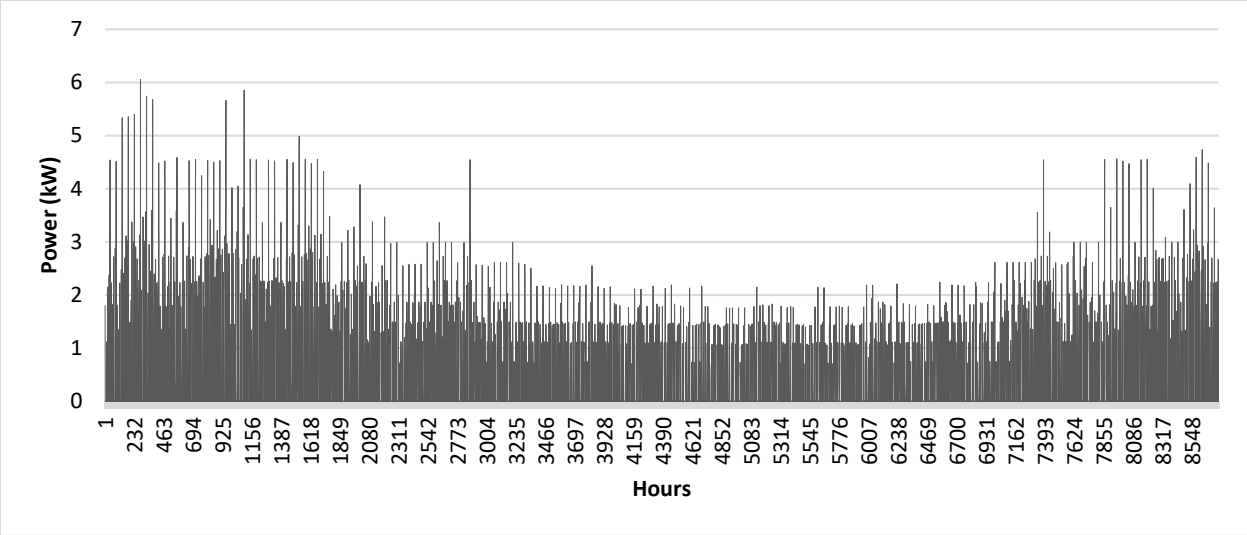

Figure 3.10: Average hourly heat pump power for a typical year

Similarly, the COP was also plotted against the outdoor ambient temperature to illustrate the COP, as shown in Figure 3.11. The trend for the COP graph was expected as the higher outdoor temperature will yield a higher COP, and the lower outdoor temperature will result in a lower COP. The TRNSYS simulation model used linear extrapolation to estimate the COP for temperatures lower than -15°C and temperatures above 20°C due to the lack of available data for these temperatures.

Figure 3.11 shows the COP compared with typical outdoor temperature for a year. Figure 3.11 shows the expected COP using the manufacturer's specification.

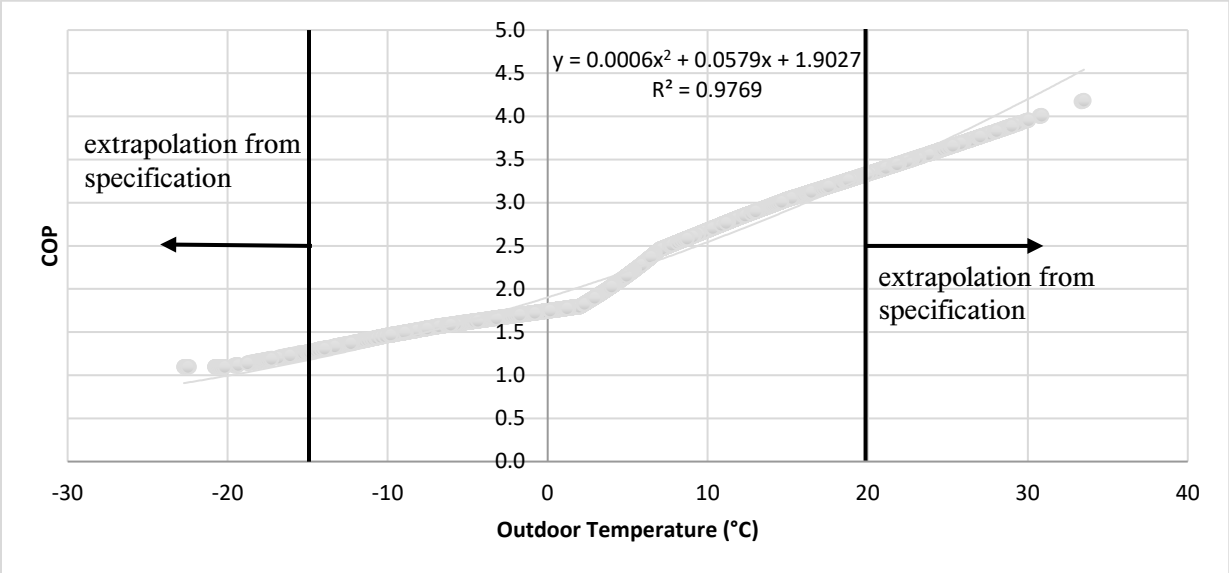

Figure 3.11: COP curve for corresponding outdoor air temperature

Table 3.10 shows the results of the annual energy consumption for the TRNSYS simulation. The annual operation cost and energy consumption are illustrated.

Table 3.10: Results of TRNSYS annual energy consumption simulation

Average Outdoor Temperature	Annual Energy Consumption	Peak Hourly Energy Consumption	Annual Electricity Cost	Seasonal COP
7.25°C	2075.85 kWh	6.06 kWh	$237.19	2.28

3.3.2 Performance of the ASHPWH

The ASHPWH was experimented using several different configurations. The different configurations were illustrated and explained in Section 3.1.8. The full-sized graphs are provided in Appendix B.

3.3.2.1 Pre-coil change – No special cases

This initial test was meant to investigate the performance of the ASHPWH during evening hours where the solar collector does not contribute to the heating. During this test period, the solar collector was physically covered but was still connected, and this was an attempt to simulate a cloudy or warm night where direct sunlight was not available.

The system and the sensors were fully operational at the end of August 2018. The data collection was officially started on September 1st, 2018, using the designed draw profile. During this time, the hot water tank was configured with only the upper coil connected to the ASHPWH, and the other larger lower coil was connected to the solar thermal collector. The solar thermal collector was covered initially but was still connected to the water tank. The system was modified to have both the lower and upper coil connected to the ASHPWH and data collection started on November 24, 2018.

The data collected was analyzed and organized into hourly data. The hourly data includes all temperatures, flow rates, and power readings. The hourly information was beneficial in illustrating the effect of the heat pump, the water draw, and the heat transfer of the heat pump. Since there are a few redundant sensors, the readings on the sensors are averaged together for the calculations.

The first interval analyzed was between September 1, 2018 to September 20, 2018. A graph of the full duration was created and was included in Appendix B. It shows that the daily consumption was consistent every day, and the flow rate follows the draw profile.

Figure B-1 (in Appendix B) shows the water temperature within the tank. The center tank temperature probe was shown in the graph to have fluctuate greatly depending on the water consumption pattern. The faucet flow rate was higher than the flow rate of city water flowing into the tank since the faucet flow rate includes the city water to temper the domestic hot water.

The temperature difference between the coil supply temperature and the coil return temperature was minimal. This shows that the heat supplied by the heat pump was low. The heat pump coil was on average at 52℃. The average supply temperature and return temperature of the coil are 52.2℃ and 52.0℃, respectively. The coil was maintained at the temperature for a long duration in order to heat the water.

Figure 3.12 compares daily average outdoor temperature and total daily energy consumption of the heat pump. As expected, the energy consumption increases as the outdoor temperature decreases.

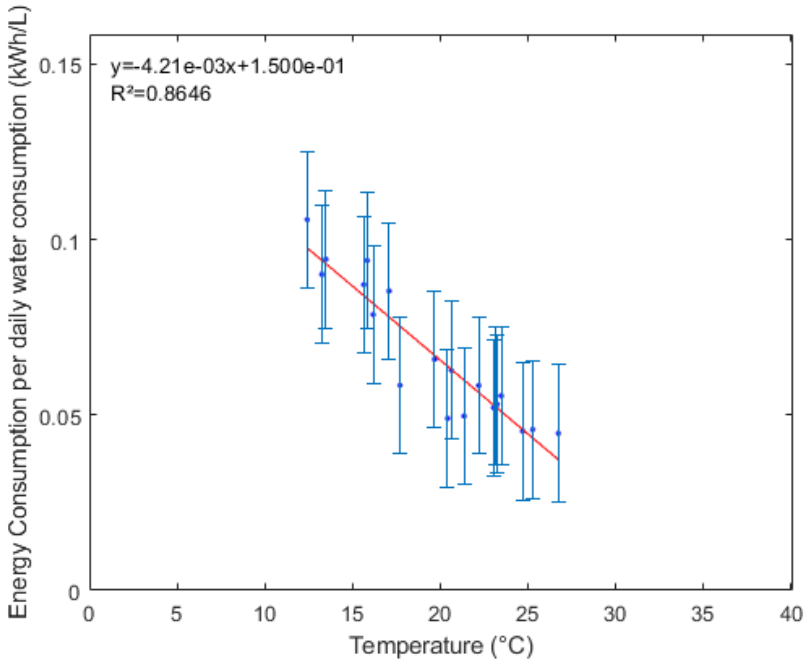

Figure 3.12: Daily energy consumption compared for daily average outdoor temperature (Sept 1 – Sept 20)

This graph was used as an initial benchmark where the heat pump was installed on the upper coil. The lower coil was connected to the solar collector; however, the collector was blocked off and was set not to provide heat to the tank. This initial interval consists of daily temperature between 12℃ and 25℃.

Figure 3.13 shows the COP compared to the daily outdoor temperature. Though the COP was extremely low, the trend shows the effect of colder temperature compared to the COP.

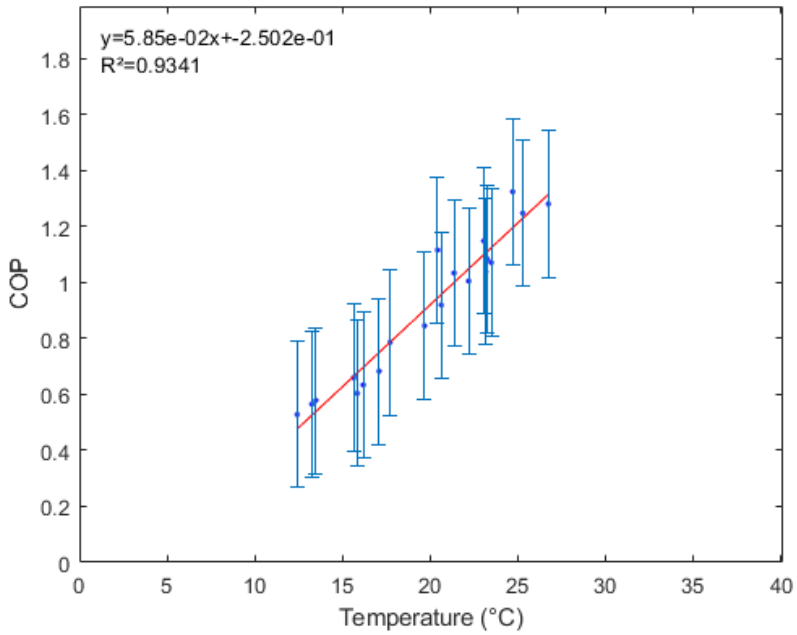

Figure 3.13: COP for average daily outdoor temperature (Sept 1 – Sept 20)

The pre-coil test without solar collector was continued from September 27, 2018, to October 4, 2018. The analysis was performed for data from September 27, 2018 to October 3, 2018 since the flow was interrupted from October 4. The data points are analyzed, and the results are graphed.

The line seen in Figure 3.14 does not have a good fit coefficient. It can be seen that there are several outliers on this graph. This was most likely because there are only seven data points for the line. Also, due to the colder outdoor temperature and the sub-par coil configuration, the system was short cycling.

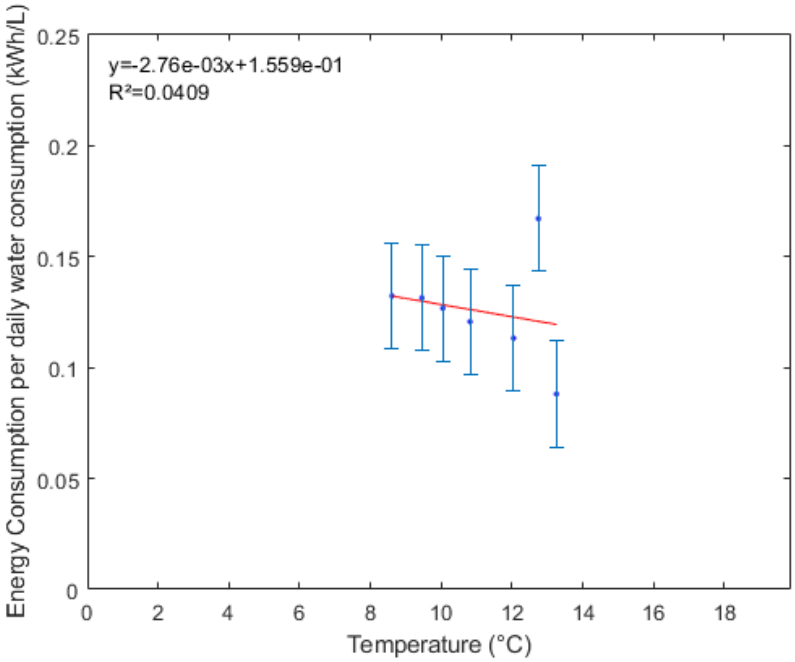

Figure 3.14: Pre-coil change daily energy consumption for outdoor temperature (Sept 27 – Oct 3)

The COP curve illustrated in Figure 3.15 was seen to have a poor regression fit. Similar to the problem of the daily energy consumption curve, the poor COP was a result of the small sample size and the problem with the coil configuration. To mitigate this error, all the data points from September 1, 2018 – September 20, 2018, was plotted along with the data points from September 27, 2018 – October 3, 2018.

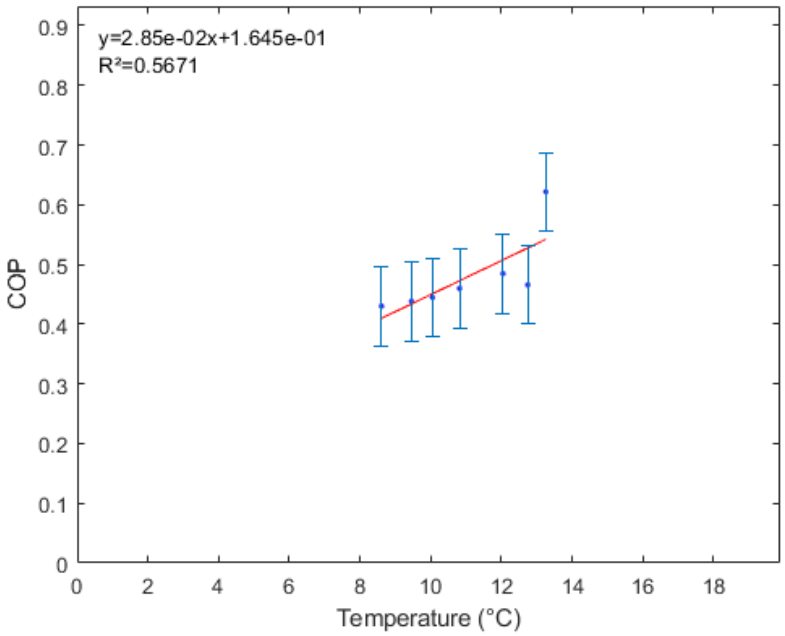

Figure 3.15: Pre-coil change COP for outdoor temperature (Sept 27 – Oct 3)

Figure 3.16 shows all the data points from September 1 to October 3 removing the data collected from the solar collector setup. The trend and R^2 value shown was the best fit. There are significantly more data points that range from 9°C to 25°C. There was an outliner that was seen outside the line of best fit.

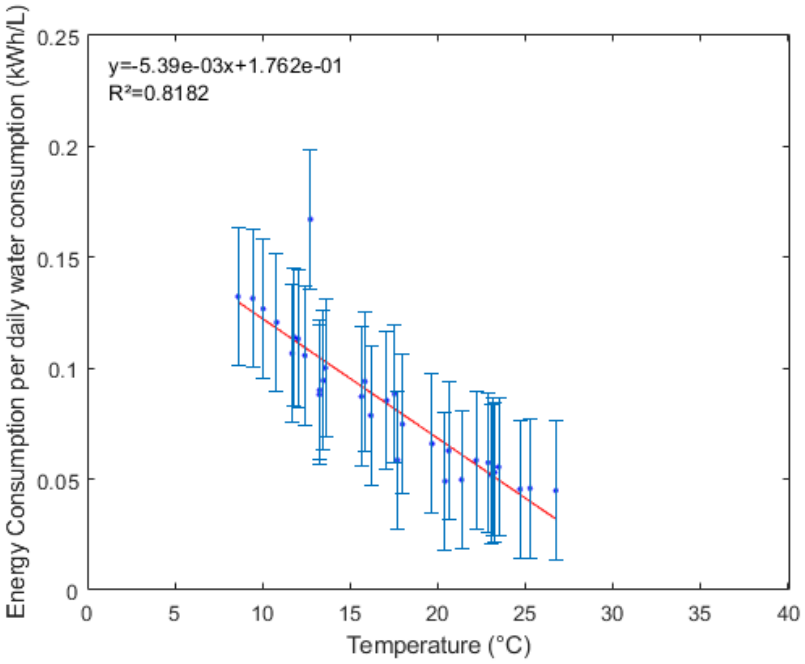

Figure 3.16: Pre-coil change energy consumption for outdoor temperature (Sept 1 - Oct 3)

The COP curve shown in Figure 3.17 consists of many data points and best reflects the performance of the system pre-coil change. Figure 3.17 shows the summary for the pre-coil change heat pump performance.

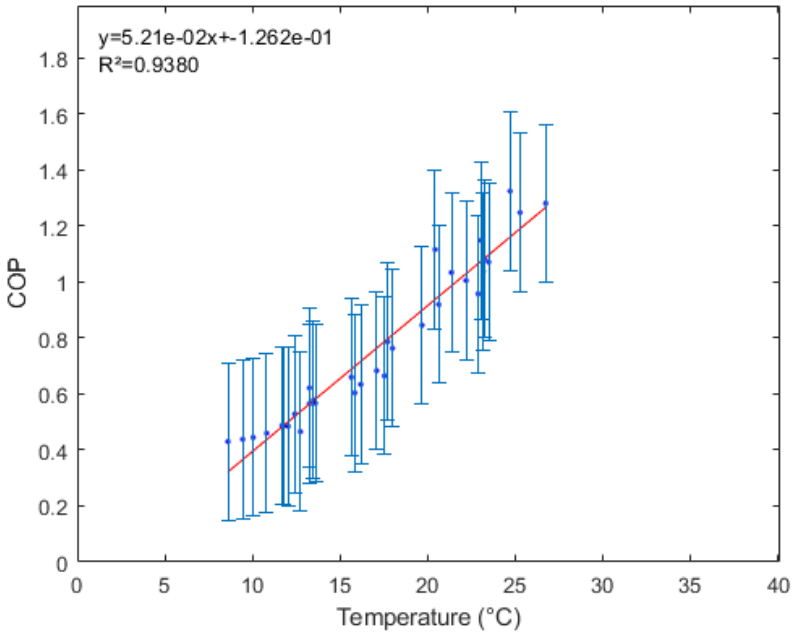

Figure 3.17: Pre-coil change COP for outdoor temperature (Sept 1 - Oct 3)

3.3.2.2 Pro coil change – Solar heating active

A solar heating collector was installed in the system and was usually covered to reduce the solar heat gain from the system. From September 21, 2018 to September 26, 2018, the cover for the solar collector was removed, and the solar heat collector was in operation. This data was analyzed to simulate a typical heating system with the solar collector connected.

A similar comparison was performed to compare the effects of the solar harvester. The solar harvester was connected to the lower coil, and the tank water preheats the city water flowing into the tank. The daily energy consumption was calculated and was illustrated in Figure 3.18. The energy consumption increases as the outdoor temperature decreases. This was expected tread, and it matches the trend of the previous heat pump scenario.

The energy consumption illustrated in Figure 3.18 was similar to the pre-coil set scenario without the solar harvester connected. The energy consumed by the heat pump also seems to be consistent with the previous curve. As mentioned previously, the trend was similar to that of the scenario without the solar collector connected. However, since there are limited data points, the effectiveness of the solar collecting heater cannot be definitively matched.

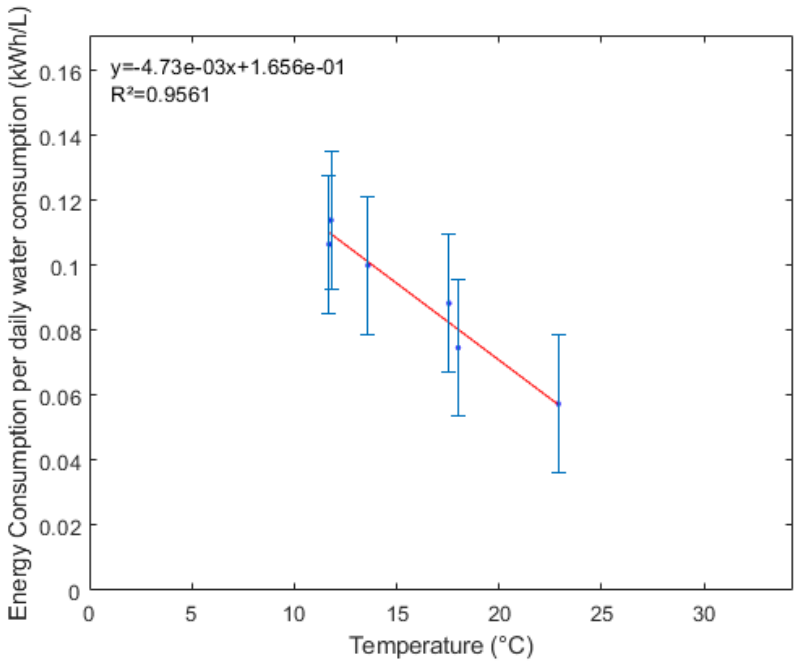

Figure 3.18: Daily energy consumption for solar harvesting option for outdoor temperature (Sept 21 – Sept 26)

Figure 3.19 shows the COP during the time the solar collector was active. The lower the outdoor temperature, the lower the COP will fall. The COP of the system seems to be very inefficient and was lower than 1. It was

also important to note that the overall COP decreased when the solar collector was connected compared to without the solar collector.

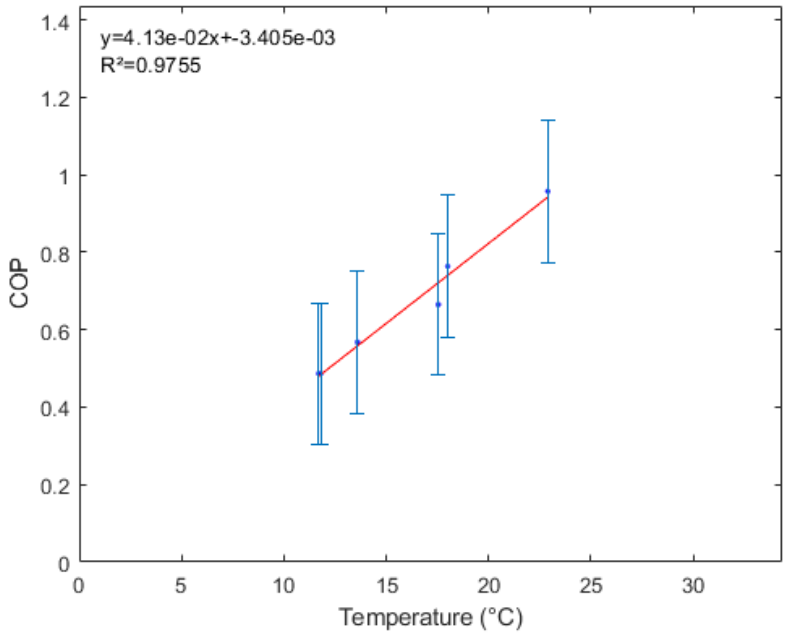

Figure 3.19: COP for solar harvesting option for outdoor temperature (Sept 21 – Sept 26)

With the limited data collected, it can be seen that the solar collector did not reduce the heat pump's energy consumption. It was suggested that the cause of this problem was due to the heat pump controls. It can be observed that the heat pump does not transfer its heat from the coil efficiently into the water tank. The data also showed that the heat pump coil was constantly maintaining a high temperature but the change in temperature between the supply and return ends of the coils was extremely low. This was further analysed with the no water draw test described in the next section, Section 3.3.2.3.

3.3.2.3 Pre coil change – No water draw

The system was configured to undergo a no water draw test. The purpose of this test was to analyze the energy consumption from the heat pump during a no water draw period. The results of the no water draw test showed that there was a constant daily energy consumption. Even during a no water draw period, the heat pump was still operating frequently. This energy consumption could likely be the tank energy losses.

Figure 3.20 shows the three days that the no water draw test was performed. The water temperature in the tank increased to a constant temperature, and the tank temperature was maintained by the heat pump coil. The observed energy consumption from the heat pump was still extremely high, considering that there was no hot water usage within this time interval. It can be concluded that the heat pump was currently consuming a consistent amount of energy regardless of the tank temperature.

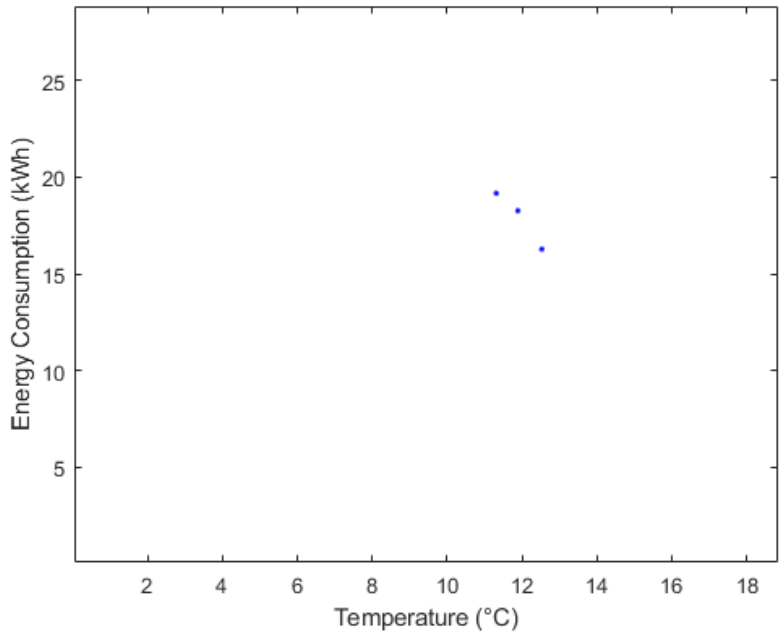

Figure 3.20: Daily Energy consumption for outdoor temperature (Oct 6 – Oct 9)

Figure 3.21 shows the COP of the system during the no water draw test. It was observed that the COP was extremely low as the heat pump was still operating even when heating was not required. The tank should only require minimum heating to maintain its temperature. This was the cause of such low COP.

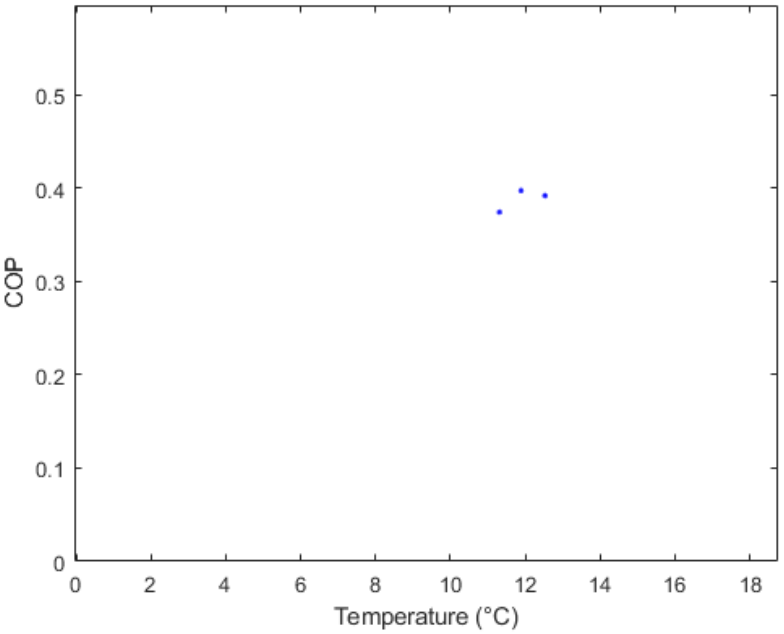

Figure 3.21: COP for outdoor temperature (Oct 6 – Oct 9)

3.3.2.4 Pre coil change – Consistent draw

Though the designed draw profile represents the average daily consumption, a consistent draw profile will allow the heat pump to reach a steady state. The consistent draw test was performed from October 20, 2018, to October 22, 2018. This test was to identify the performance of the system for a longer draw duration. The flow was modified to be using water for an extended time and paused to allow the tank to accumulate more hot water. During this testing period, the outdoor temperature was drastically lower compared to the other data points and testing intervals. The daily water consumption remains the same as the previously determined daily water consumption.

Figure 3.22 shows the energy consumption for the heat pump when the system was performing an extended water draw. The energy consumption was observed to be extremely high at this temperature. The daily water consumption was maintained a constant draw of up to 8 L/min for an extended time and was stopped. This allows the ASHP to operate at an extended time without emptying the tank. The energy consumption was still extremely high compared to the typical operation scenario.

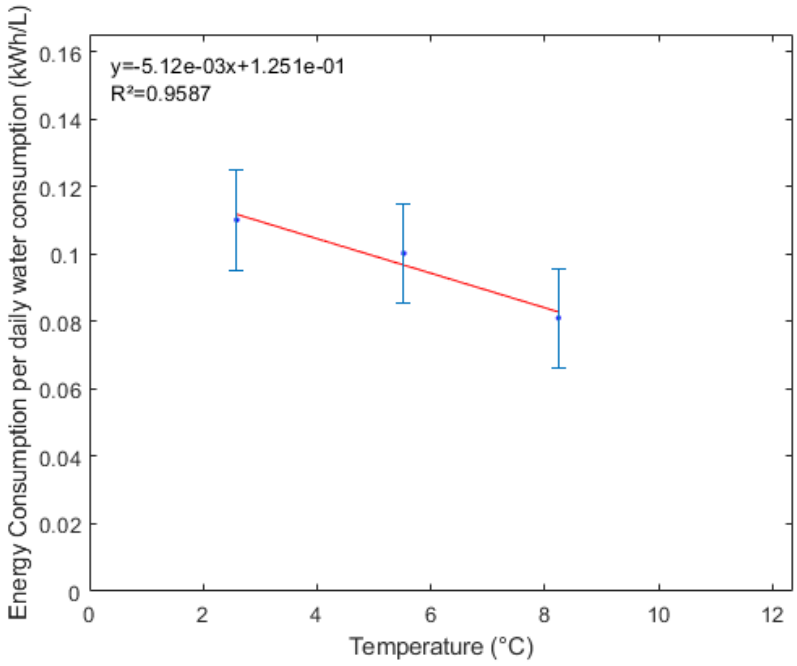

Figure 3.22: Constant water draw daily energy consumption for outdoor temperature (Oct 20 – Oct 22)

The COP shown in Figure 3.23 was extremely low. The COP would mean that the heat pump was relatively inefficient compared to even an electric resistance heating.

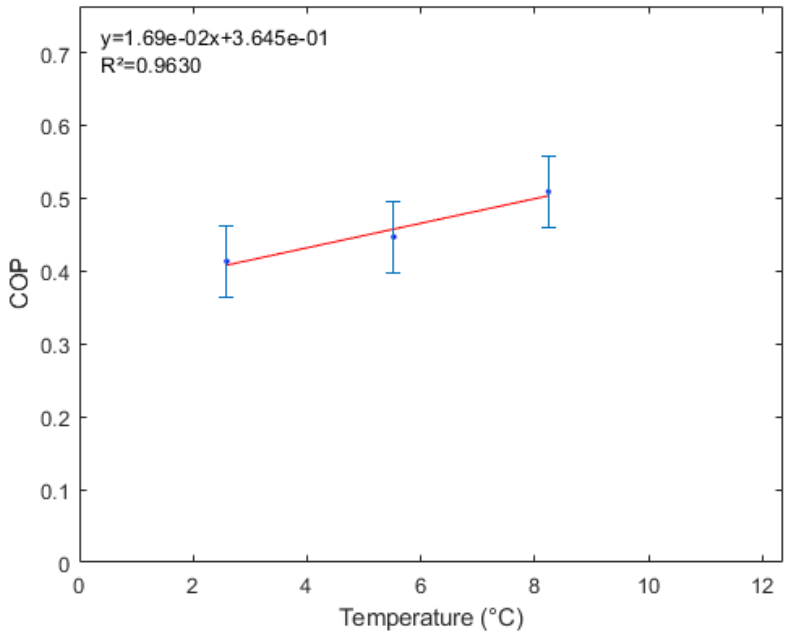

Figure 3.23: Constant water draw COP for outdoor temperature (Oct 20 – Oct 22)

3.3.2.5 Pre coil change – Cold start tests

A cold start test was performed from November 19, 2018, to November 20, 2018. Since the results of the data analysis did not meet the expected performance, a cold start test was performed in order to analyze the maximum performance.

Figure 3.24 shows the overall trend of the heat pump water heater configured for a cold start water heating. It was clear that the supply temperature and the return water temperature has a more significant temperature difference than the previous typical operational scenarios.

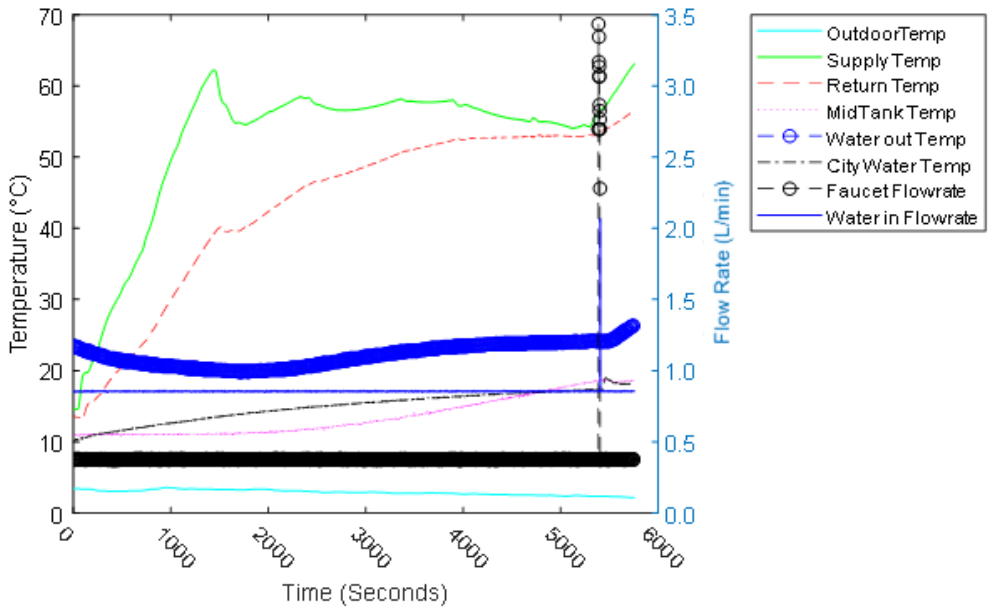

Figure 3.24: Cold start test using testing heat pump water heater

This also shows that the COP of the system was significantly higher. The COP over the course of this period was found to be 1.76, and the average outdoor temperature was 2.9°C. Using the COP model illustrated in Figure 3.11, the COP was expected to be 2.07 at 2.9°C. However, the testing duration for this COP was only 1 hour and 30 minutes and the mid tank temperature was heated from 11°C to 19°C. The supply temperature and return temperature slowly met the heating threshold of 55°C within 1 hour and 30 minutes.

Figure 3.25 shows the full tank heating from 11°C to 40°C. The time it took for the heat pump to heat the water to temperature was 14 hours in total. Because of this long duration, the COP was extremely low and was calculated to be 0.06. The total energy consumption was calculated to be 31 kWh, and the total heat transfer was only 1.76 kWh.

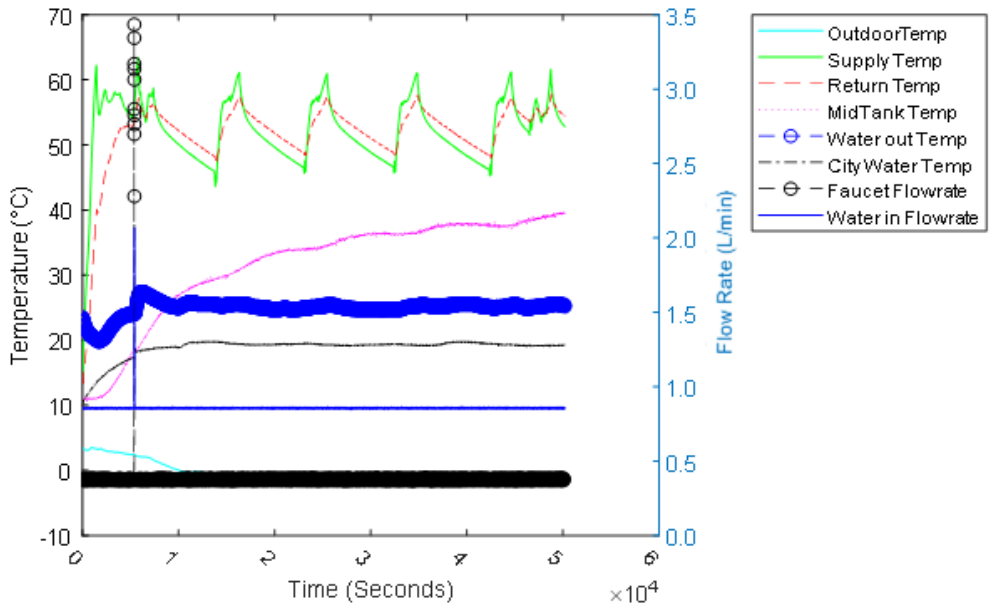

Figure 3.25: Cold start test full heating (11°C to 40°C)

Though the expected COP value was improved compared with the other scenarios, it was still lower than the expected manufacturer specifications. Due to this discrepancy, the system was assessed again, and a modification was done to the system to include the lower coil. The following data was analyzed again to determine the benefits of combining the two available heating coils inside the water tank.

3.3.2.6 Post coil change – No special cases

The domestic hot water tank was modified to connect both the upper and lower coils. The two coils were then connected to the ASHPWH to increase the heat transfer rate from the coil to the water. The system was modified, and the data collection started on November 24, 2018. The time intervals investigated after the coil change was listed as followed:

November 24, 2018 – November 28, 2018

December 7, 2018 – December 15, 2018

December 18, 2018 – December 31, 2018

Figure 3.26 shows the daily energy consumption from the duration from November 24th to November 28th. The daily energy consumption was lower compared to the trend of the pre-coil change scenarios. This was most likely due to the increased coil surface area in the tank. This means that the heat pump was able to reject more heat to the water more efficiently.

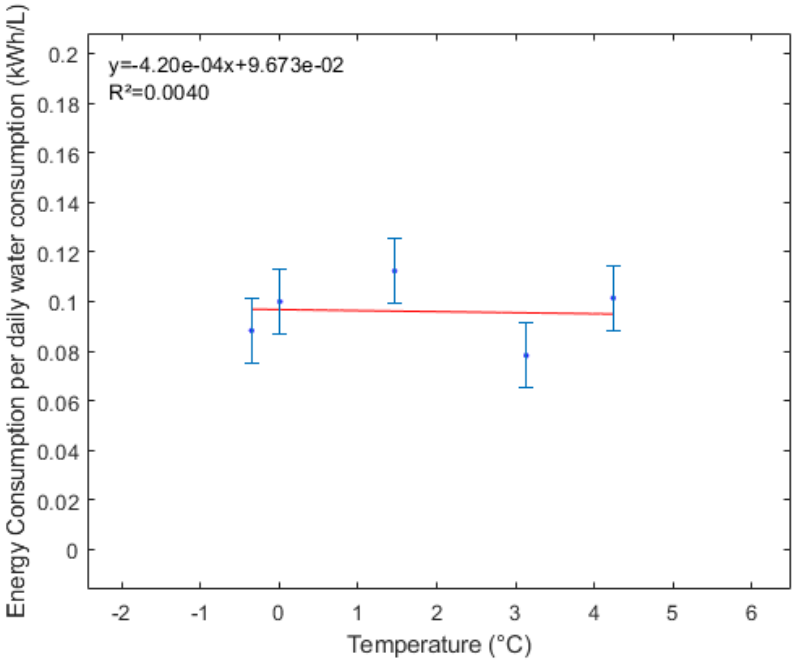

Figure 3.26: Post coil change daily energy consumption for outdoor temperature (Nov 24 – Nov 28)

The COP was illustrated in Figure 3.27. The COP was seen to be quite low, and this was resultant from the low outdoor temperature.

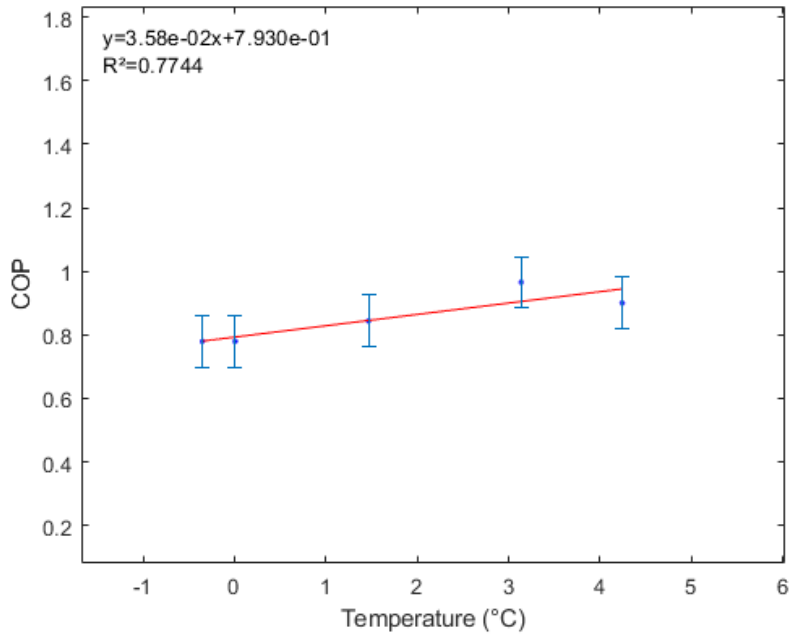

Figure 3.27: Post coil change COP for outdoor temperature (Nov 24 – Nov 28)

The energy consumption from December 7 to December 15 was illustrated in Figure 3.28. The average outdoor temperature within this interval was from -7.2℃ to 1.7℃, which shows a gradual increase in energy consumption as the temperature decreases.

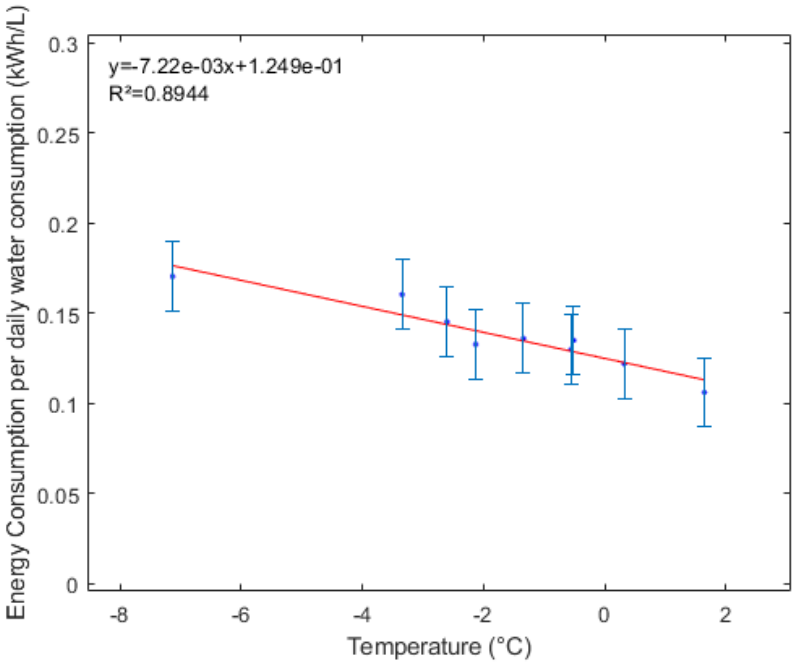

Figure 3.28: Post coil change daily energy consumption for outdoor temperature (Dec 07 – Dec 15)

The COP within the time interval, as illustrated in Figure 3.29. The COP slowly decreases as the temperature decreases.

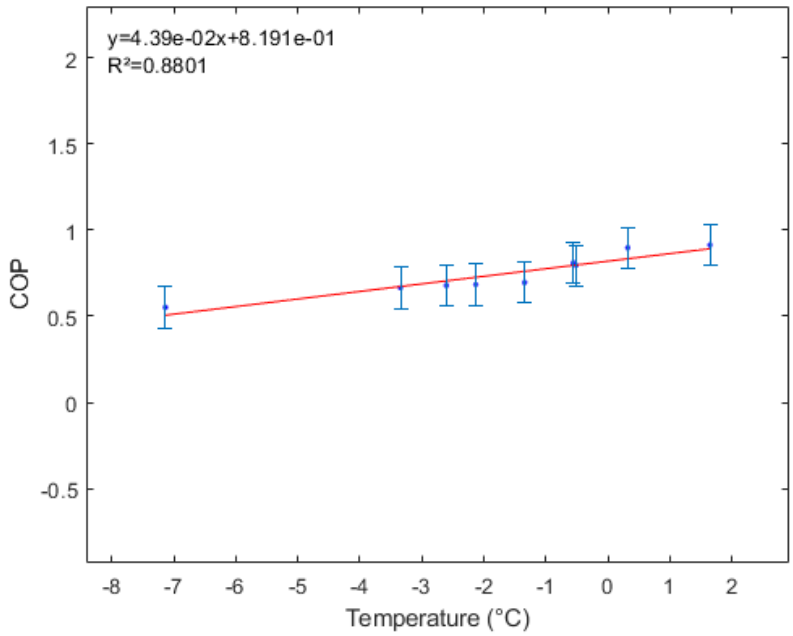

Figure 3.29: Post coil change COP for outdoor temperature (Dec 07 – Dec 15)

Figure 3.30 showed the daily energy consumption for the post coil change from December 18 to December 30. The post coil change had a different energy consumption pattern compared to that of the pre coil change testing. The energy consumption for the post coil change scenario showed that there was a lower energy consumption compared to the pre-coil change scenario.

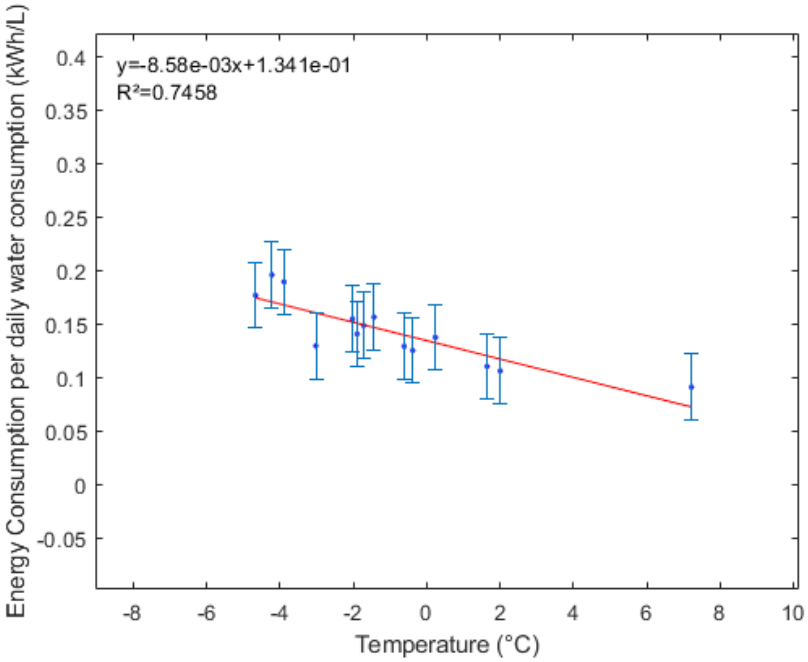

Figure 3.30: Post coil change daily energy consumption for outdoor temperature (Dec 18 – Dec 31)

Figure 3.31 showed the COP for the post coil change scenario for the time interval of December 18 to December 30. Similar to the capacity curve, the COP was improved after the coil change. The improvement was due to the increased surface area and increased heat transfer. Analyzing the COP graph shows that the system was improved compared to the pre-coil change, however, it was still lower performance than the expected manufacturer specifications.

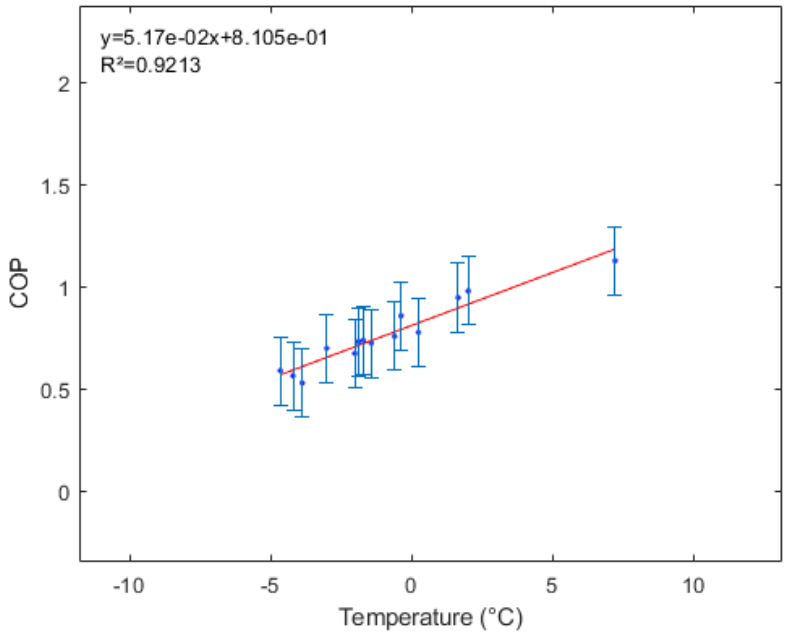

Figure 3.31: Post coil change COP for outdoor temperature (Dec 18 – Dec 31)

Figure 3.32 shows all the points for the post coil change daily energy consumption. This set of information shows all the data collected prior to the coil change. It can be concluded that during the low outdoor temperature, the energy consumption was higher when compared to the warmer temperature.

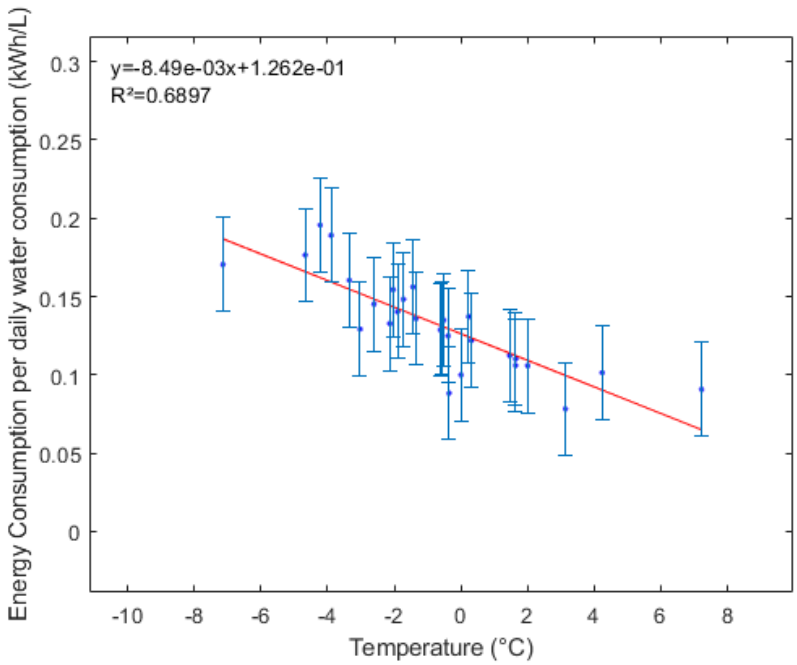

Figure 3.32: Post coil change daily energy consumption for outdoor temperature (Nov 24 – Dec 31)

Figure 3.33 shows the COP prior to the coil change of the water tank. The COP was seen to be higher at a higher temperature.

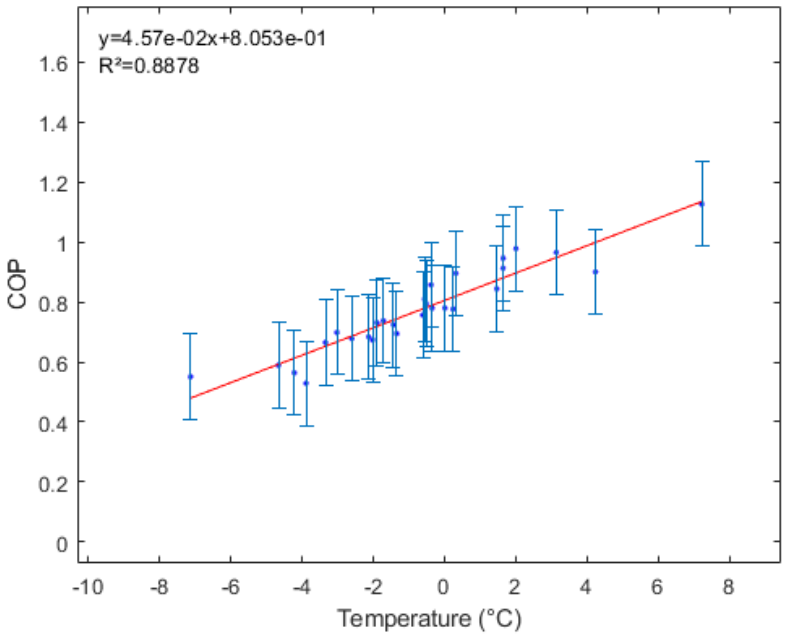

Figure 3.33: Post coil change COP for outdoor temperature (Nov 24 – Dec 31)

3.3.2.7 Post coil change – Cold start tests

Cold start tests were performed with the new configuration to analyze the performance increase from connecting both the upper and lower coil. The test was performed on December 6, 2018, and also from January 14, 2019, to January 15, 2019.

A cold start test was performed after changing the coils, and the COP was found to be 1.12 at an average outdoor temperature of 0.54°C. The took the heat pump 1 hour and 30 minutes to raise the temperature from 24°C to 55°C. This was significantly faster than the previous test. This was due to the additional coil and the increase in the coil surface area. This also shows the importance of the tank in the heat pump water heater system. Figure 3.34 shows the cold start test results for the post coil change configuration.

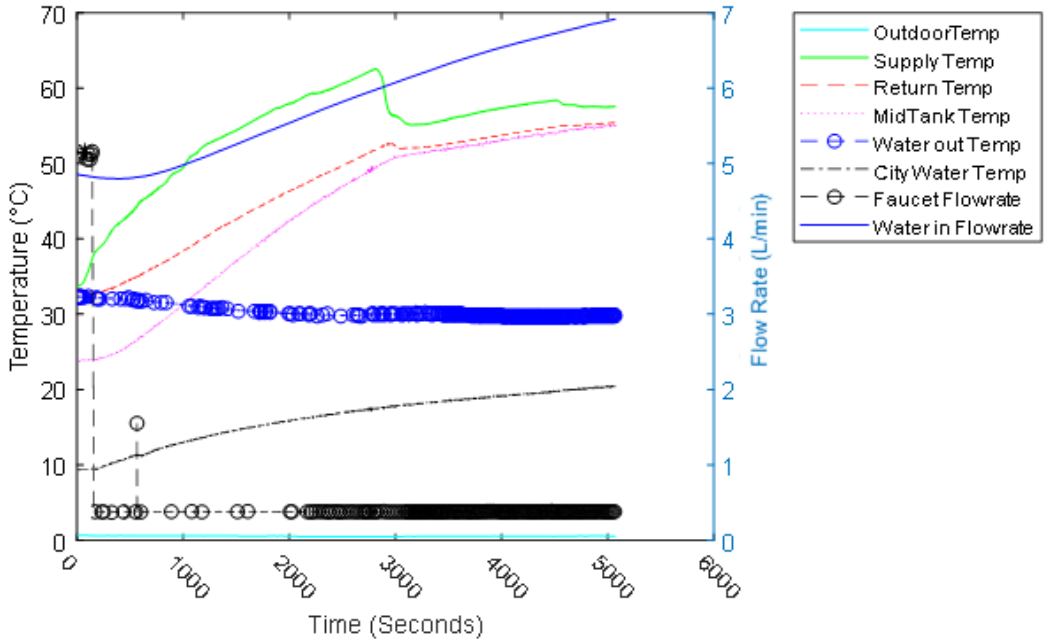

Figure 3.34: Post coil change cold start test (Dec 6)

Figure 3.35 shows the result of the first cold start test performed on January 14. It took slightly over 2 hours and 30 minutes to heat the water from 7°C to 55°C during an average outdoor temperature of -1.9°C. Though this took a longer time than the previous test performed during December, it was essential to note that the starting tank temperature during this first test was significantly lower than the previous test. The overall COP during the time of operation was calculated to be 0.89.

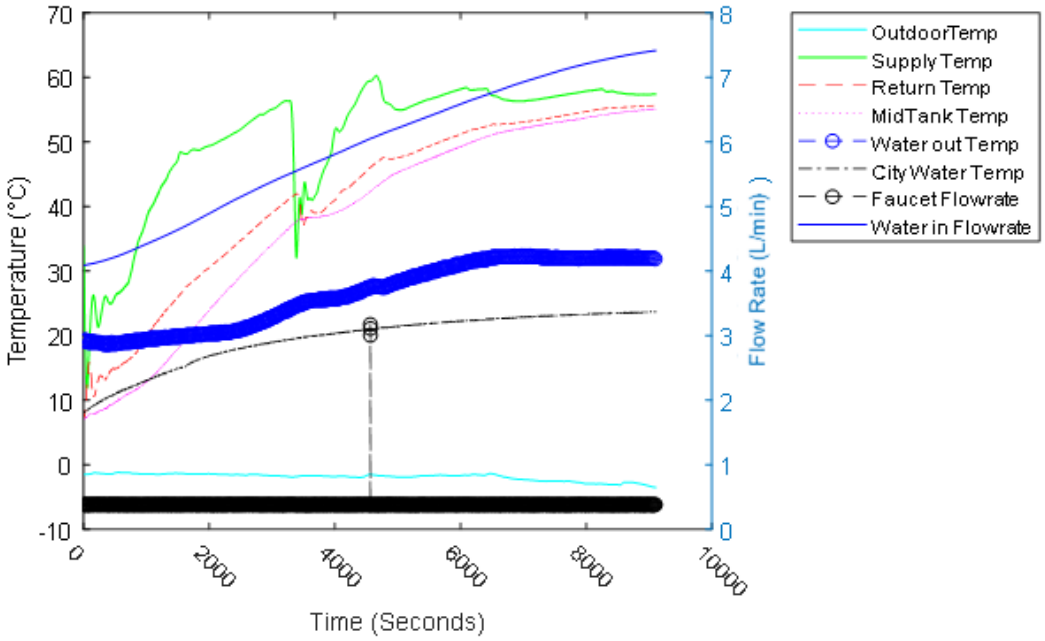

Figure 3.35: Post coil cold start test 1 (Jan 14)

Figure 3.36 was the second cold start test performed in January. In this test, the average outdoor temperature was found to be -0.4°C. The tank water was heated from 7.5°C to 55°C and took just under 2 hours and 30 minutes. The time it took the water to reach temperature was slightly lower than the first test, and the COP was calculated to be 0.97.

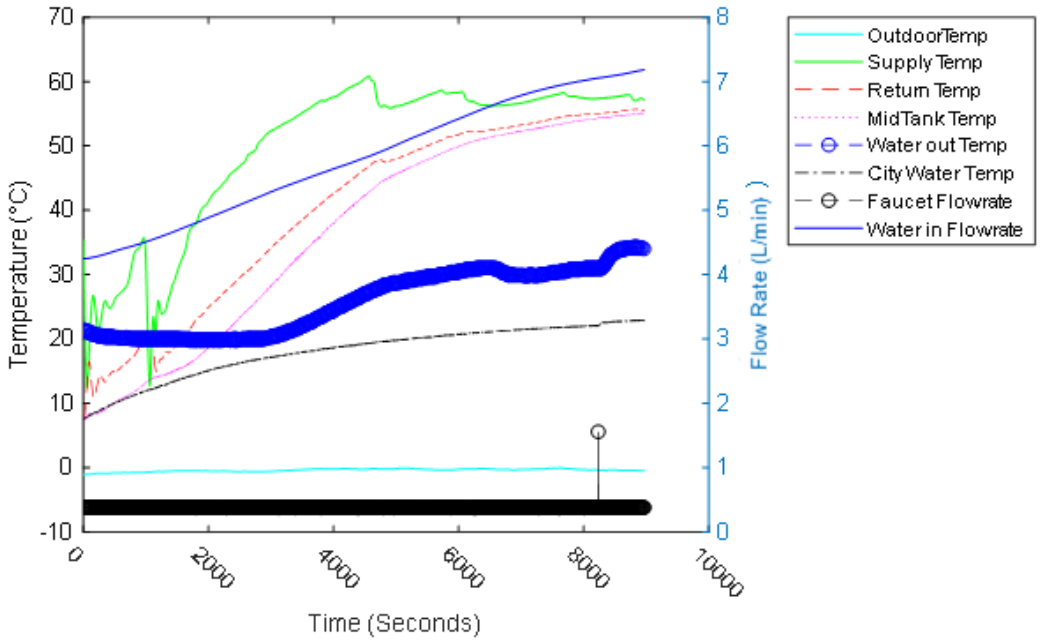

Figure 3.36: Post coil cold start test 2 (Jan 15)

Figure 3.37 illustrates the results of the third and final cold start tests performed in January. The test was performed with the tank water temperature starting at 7.8°C and heated to 55.1°C. The average outdoor temperature was -1.4°C, and the COP was 0.9. The heat pump was operating over 2 hours and 30 minutes, similar to the first test.

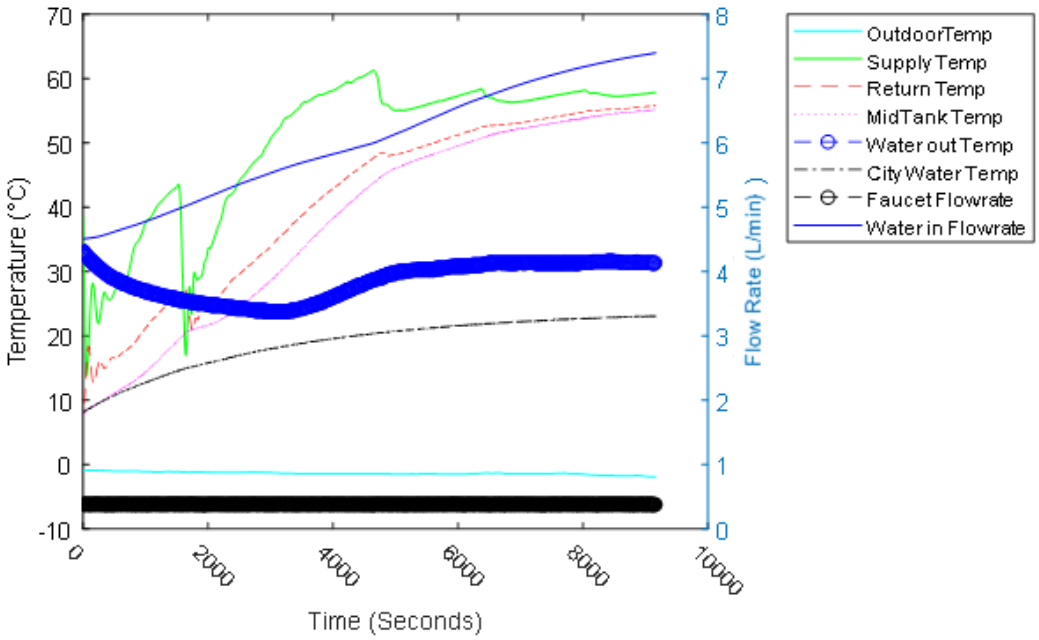

Figure 3.37: Post coil cold start test 3 (Jan 15)

3.3.3 Related Sensitivity Analysis

The electricity consumption, natural gas consumption, operating cost, and GHG emissions were simulated with the TRNSYS model and the mathematical calculation. Three scenarios using different heating modes were used for the analysis: ASHPWH, 80% efficiency natural gas boiler, 100% efficient electric resistance DHW heater.

3.3.3.1 Performance of the ASHPWH in Major Canadian Cities

The TRNSYS simulation was used to determine the annual energy consumption for five major Canadian cities. This sensitivity analysis was intended to analyze the effect of a change in outdoor air temperature. The simulation was performed using weather data from these five cities:

1. Toronto
2. Montreal

3. Vancouver
4. Edmonton
5. Halifax

Three different DHW heating systems were analysed, where the cost and energy consumption was simulated.

Table 3.11 summarizes the operation cost for three different types of DHW heating system. The operation cost for the ASHPWH was lower than the electrical resistance heating option. However, the cost when using natural gas was half the operational cost of the ASHPWH. The TOU prices for electricity costs for all five cities are kept consistent. The marginal cost used was taken from the Toronto residential price. It can be seen that the ASHPWH was not as cost-efficient as a natural gas boiler. This was due to the low natural gas cost in Toronto. The highest seasonal COP was in Vancouver. This was expected as the average outdoor temperature was the highest out of the five cities.

Table 3.11: Sensitivity analysis for different cities cost comparison

		Air Source Heat Pump Water Heater			80% Efficiency Natural Gas Heating		100% Electric Resistance Heating	
Cities	Average Outdoor Temperature	Annual Electricity Consumption	Annual Electricity Cost	Seasonal COP	Annual Natural Gas Consumption	Annual Natural Gas Cost	Annual Electricity Consumption	Annual Electricity Cost
Toronto	7.25°C	2075.85 kWh	$237.19	2.29	571.61 m^3	$184.35	4753.54 kWh	$548.53
Montreal	6.54°C	2174.49 kWh	$248.48	2.19	573.33 m^3	$184.90	4767.82 kWh	$550.33
Vancouver	9.84°C	1852.43 kWh	$212.85	2.58	575.24 m^3	$185.51	4783.66 kWh	$553.23
Edmonton	3.31°C	2343.69 kWh	$267.39	2.03	572.19 m^3	$184.53	4758.32 kWh	$548.40
Halifax	6.46°C	2089.28 kWh	$238.13	2.28	573.79 m^3	$185.05	4771.66 kWh	$550.53

Table 3.11 showed that the cost comparison between different DHW heating systems and different Canadian cities. The cost-saving switching from the natural gas boiler to an ASHPWH was -29% which means that the cost was increased when implementing ASHPWH. It can be seen that the ASHPWH was costly compared to a natural gas boiler in all the selected cities. However, when switching from an electric resistance heating system to ASHPWH, the cost savings are substantial.

Table 3.12: Percentage savings comparisons

Cities	Air Source Heat Pump Water Heater	80% Efficiency Natural Gas Heating		100% Electric Resistance Heating	
	Annual Electricity Cost	Annual Natural Gas Cost	Percent Saving	Annual Electricity Cost	Percent Saving
Toronto	$237.19	$184.35	-28.67%	$548.53	56.76%
Montreal	$248.48	$184.90	-34.39%	$550.33	54.85%
Vancouver	$212.85	$185.51	-14.74%	$553.23	61.53%
Edmonton	$267.39	$184.53	-44.90%	$548.40	51.24%
Halifax	$238.13	$185.05	-28.69%	$550.53	56.75%

The results of the simulation show that the ASHPWH that was being tested was not as effective in Canada when comparing the operating cost. An 80% efficient natural gas boiler was more cost-effective. In a climate with a higher average temperature with mild winter will improve the efficiency of the heat pump. Due to the combination of the cold winter climate and the high electricity cost in Toronto, the ASHPWP was not as feasible cost-wise in Toronto compared to a typical natural gas system. However, greenhouse gas (GHG) emission was currently an essential factor in the community.

Table 3.13 shows the difference in GHG emissions for different DHW heating systems and different cities. The GHG emission was extremely low for the ASHPWH option as it effectively uses electricity to heat the DHW. It can be observed that the natural gas boiler emits a high concentration of GHG due to the fuel's high GHG density. It was evident that implementing the ASHPWH was beneficial to the environment due to the substantial GHG reduction. The recent Canadian Federal carbon tax implemented would eventually affect the operating cost.

Table 3.13: Sensitivity analysis for different cities GHG emission comparison

		Air Source Heat Pump Water Heater		80% Efficiency Natural Gas Heating		100% Electric Resistance Heating	
Cities	Average Outdoor Temperature	Annual Electricity Consumption	GHG Emission	Annual Natural Gas Consumption	GHG Emission	Annual Electricity Consumption	GHG Emission
Toronto	7.25°C	2075.85 kWh	88.4 kg	571.61 m^3	1063.2 kg	4753.54 kWh	210.3 kg
Montreal	6.54°C	2174.49 kWh	93.3 kg	573.33 m^3	1066.4 kg	4767.82 kWh	212.2 kg
Vancouver	9.84°C	1852.43 kWh	80.3 kg	575.24 m^3	1069.9 kg	4783.66 kWh	212.9 kg
Edmonton	3.31°C	2343.69 kWh	100.7 kg	572.19 m^3	1064.3 kg	4758.32 kWh	212.4 kg
Halifax	6.46°C	2089.28 kWh	89.4 kg	573.79 m^3	1067.3 kg	4771.66 kWh	212.0 kg

Table 3.14 shows the comparison between the three analyzed systems and five different Canadian cities. The highest GHG emission reduction occurs in Vancouver, at 92.5% reduction, when switching a natural gas heater to the ASHPWH. This was a substantial improvement in terms of environmentally friendly alternatives. However, the low cost of natural gas currently deters the implementation of an electric system.

Table 3.14: GHG emission for different systems and cities

Cities	Air Source Heat Pump Water Heater	80% Efficiency Natural Gas Boiler		100% Electricity Resistance	
	Annual GHG Emission	Annual GHG Emission	Percent Reduction	Annual GHG Emission	Percent Reduction
Toronto	88.4 kg	1063.2 kg	91.69%	210.3 kg	57.96%
Montreal	93.3 kg	1066.4 kg	91.25%	212.2 kg	56.03%
Vancouver	80.3 kg	1069.9 kg	92.49%	212.9 kg	62.28%
Edmonton	100.7 kg	1064.3 kg	90.54%	212.4 kg	52.59%
Halifax	89.4 kg	1067.3 kg	91.62%	212.0 kg	56.42%

Chapter 4 – Discussion and Conclusion

This final chapter of the thesis discusses the findings and contributions of the research. This thesis also aims to explore the environmental benefits of implementing ASHP systems when compared to the typical system. The thesis also answers the following questions:

1. What can be done to lower the GHG emissions without overloading the electrical grid?
2. What is its role in the path of sustainability?
3. What are the environmental benefits?
4. What are the economic benefits?

The key findings from each case study are summarized below.

Chapter 2 – Residential Smart Dual Fuel Switching System (SDFSS) for Simultaneous Reduction of Energy Cost and GHG Emission

The purpose of this portion of the study was to investigate the SDFSS, simulate energy consumption, GHG emission, and operational costs. A sensitivity analysis was performed to see the effects of changing the outdoor temperature, changing the house envelope, adding the carbon pricing and implementing the new Advantage Pricing Plan. The results showed a small operational cost saving for the base-case scenario and up to a 19% cost saving for other scenarios. The GHG emission was substantially reduced when implementing the SDFSS. Up to 51% GHG emission reduction can be seen from the implementation of the system.

i. This system can be implemented in residential houses with two fuel sources. Since there are two fuel sources available, the system can control the electricity consumption during peak hours in order to reduce the impact on the electricity consumption peaks.
ii. This system can be seen as a transitional system in between the current natural gas dominant space heating to a cleaner electrically powered ASHP heating system. This technology can be used with other sustainable technologies to significantly reduce GHG emissions.

4.1 Discussion

4.1.1 Smart switching approach

Using electricity as the primary fuel source to replace natural gas will significantly reduce GHG emission from the residential space heating sector. There are no major transitional technologies in the literature to help encourage the current trend towards electricity heavy HVAC systems. The current pricing model and available switching control do not justify the increased cost of implementing an electrical heat pump. Using

the simulation highlighted in this paper, the model reports that the operating cost of using the manufacturer switching, in general, was costlier compared to the natural gas-only option. Moreover, the impact of several factors in the foreseeable future shows the disadvantage of the higher operating cost of the manufacturer switching system. Though the operating cost of the manufacturer switching was significantly higher than the natural gas-fired furnace option, the GHG emission was greatly reduced when the switching system was implemented.

A moral and economic dilemma exists between the reduction of GHG emissions and the lowering of operational cost. Residential homeowners are less likely to increase their operational costs for the sole purpose to reduce GHG emissions. Because of this, there was a lack of urgency to convert the natural gas furnace dominated heating system to a more environmentally friendly option of the electric heat pump. The SDFSS incentivizes the inclusion of heat pumps by theoretically lowering the operating cost while reducing GHG emissions. Though the GHG emission reduction was not as high as the result of operating the system under the manufacturer switching system, the GHG emission was still significantly lower than that of a natural gas-only system. The simulated results show that the SDFSS potentially provide up to 19% cost saving and GHG emission reduction of 51% when a $50/tonne carbon pricing and APP are implemented compared to a natural gas-only system. Part of the appeal of this smart system was the fact that it acts as a transitional technology between a full natural gas furnace and a full electricity heating system. This switching system was the start of new flexible control systems that can use numerous factors that can be implemented in the future.

The SDFSS was the most beneficial when an old central air conditioner system needs to be replaced. Though the cost of ASHP compared to a typical air conditioner was higher, the initial investment for the ASHP was not significantly higher than an air source heat pump. According to Q. Zhang et al. [71], the total initial investment when compared to an air conditioner was 50% higher for an ordinary residence. If a typical air conditioner was due for a replacement, the homeowner can pay a higher initial cost for an upgraded ASHP system and the SDFSS was able to reduce the operating cost and ensure that the new system will not cost more to operate than the natural gas furnace. With this dual-fuel system, an additional redundancy was added, which makes the system more reliable. In addition to that, GHG emission was greatly reduced with the addition of the ASHP.

Replacing the air conditioner means that the original furnace and the original air conditioner was sized to provide heating and cooling for the full house. A smaller sized heat pump to replace the air conditioner could potentially reduce the overall cost. Since there was a level of redundancy added to the heating system, a full-sized ASHP for the heating load was not necessary. The original natural gas furnace heating system was able to meet heating demands during extremely cold weather. Since the SDFSS will most likely switch to

using the natural gas furnace, as the performance of the ASHP was not cost-effective in cold outdoor air temperatures, this would not affect the overall performance of the system.

4.1.2 Potential improvements to the model

There are currently other sources of energy that potentially could be handled by a smart switching system such as the smart dual fuel switching system. Additional parameters from solar radiation for the solar panel to electric utility demand. These examples can extend the SDFSS to incorporate the extra electricity generated to reduce the overall operational cost. Incorporating this SDFSS will also allow utility companies for demand-side fuel switching to help manage the peak electricity demands.

The system can be further improved by allowing more flexible customer settings. Currently, the system only optimizes the system to lower the operational cost. An alternative was to have the system, including a customer-set price ceiling while lowering GHG emissions. Alternatively, this control can also be open for the utility company or the government to set a GHG emission cap to provide a demand-side management portal [72]. This cap can be used to manage GHG emission to eventually minimize it.

Additionally, since the switching parameters in this benchmark model are cost, occasionally the cost of operation for natural gas furnace was marginally lower than the cost of operating the heat pump. In the current configuration, the system will select natural gas as the fuel source. However, the system can include a cost dead-band that would allow the system to be lenient on the cost comparison. This will also potentially reduce GHG emissions while having a minimal impact on operational costs. Similarly, a load shifting configuration can be integrated as well to preheat/precool the house during off-peak hours [73]. Such load shifting technique was found to reduce the heating cost as much as 6% - 13% in France [74]. This technology was currently available; however, it does not take into account the other parameters that can be provided by the SDFSS, which potentially can provide an even more significant saving.

Another significant improvement for the system that could improve the flexibility of the system was to allow the user to input more parameters for the system to optimize the operation. These parameters can include future renewable technologies such as building integrated photovoltaic thermal systems, heat pump water heater systems, greywater heat recovery systems, electricity storage, and sewage heat recovery system [75–78]. In order to reduce GHG emissions, future renewable technologies should be interconnected in a system that can optimize the operation as one system. This can allow overall a more flexible system that can automatically adapt to parameter changes.

4.1.3 Representativeness of study results

This study was based on Strathroy, Ontario, Canada, but the general trends can be seen in different cities in Ontario and can further applied to other cold climactic cities too. After all, most cities in North America are actively trying to reduce GHG emissions through different initiatives such as the UNFCCC and North America 2050 [79, 80]. Moreover, even though the source of electricity could be generated using different fuels, the SDFSS could still account for the different GHG emissions and costs given the parameters.

In this benchmark model, the four main factors are 1) utility costs, 2) equipment performance, 3) temperature and 4) GHG density for the fuel. These parameters may change for different cities, and the system will still operate as intended. Firstly, the utility cost was different for different locations and cities. This factor was of the utmost importance when dealing with costs. Since the cost of the utility will affect the overall operating cost the most. Secondly, the equipment performance of the system affects the total hourly cost. Depending on how well the equipment performs, the hourly cost for fuel when being compared will change drastically. Though natural gas was more cost-effective per unit energy, if the furnace efficiency was extremely low, a newer air source heat pump could be more cost-effective during normal operations. In this paper, the performance of the air source heat pump was directly related to the third factor, temperature. In different locations, the temperature was different depending on the climate zone. The result of this study compared several different cities with slightly varying climates. All of which showed the potential of the SDFSS was consistent in all the different cities. Lastly, GHG density of fuel for natural gas and electricity impacts the GHG emission reduction potential calculation for different locations. Locations with fossil fuel-fired power plants will have higher GHG emissions compared to Ontario's cleaner electrical power generation methods. Since one of the main focus of the SDFSS was to reduce the GHG emission, the GHG density for the electricity and natural gas was a crucial factor.

The results of this project show that the potential cost savings when compared between the natural gas-only scenario and the SDFSS was not substantial. However, when comparing the results of the SDFSS and the manufacturer switching system showed that there was considerably lower cost. Additionally, the SDFSS has a substantially lower annual GHG emission when compared to the natural gas furnace. Since the primary goal of this study was to investigate the system from an economic point of view, at a glance, the results do not show a high potential in terms of cost savings. Since SDFSS was considered a transitional technology that was meant to complement environmentally friendly systems, the main comparison should not be between SDFSS and natural gas furnace. Without the SDFSS, the manufacturer switching was used as default, and the operating cost can increase by over 23%.

Chapter 3 – Heat Pump Water Heater Performance Testing and Assessment in Cold Climate

The purpose of this portion of the study was to analyze an ASHPWH and to simulate its performance for cold climate. The energy consumption, GHG emission, and operational cost were simulated using TRNSYS. A sensitivity analysis was performed on the system to analyze its performance in different major Canadian cities and its climate. The overall operational cost was unfortunately increased, but the GHG emission reduction can be seen to be up to 92.5%. With this ASHPWH system, the unit was able to reduce most of the GHG emissions.

i. This system can be implemented with the SDFSS or other linked control system. The ASHPWH can be controlled to operate during lower peak hours which will help limit the strain on the electricity grid.
ii. The system was an electric-only system which makes the system closer to the full electric goal. This was one step towards improvement, in terms of environmental impact, from a transitional system such as the SDFSS. It was expected that ASHPWH was frequently used in the future to eventually phase out from natural gas.

4.2 The Benefits of ASHPWH

Using the ASHPWH to replace the natural gas water heater will significantly reduce the GHG emission if the electricity used were generated from clean sources. Currently, there are several other research performed on ASHPWH. Wang et al. performed a study on a frost-free ASHPWH that would operate in a colder climate that was slightly below freezing. This technology was hugely beneficial as it improves the efficiency at near-freezing temperature and helps reduce frost [81].

Similarly, a study performed by Xu et al. investigated the performance of an ASHPWH in Northern China where the outdoor temperature falls to -21°C. The study shows promising results even during colder climate [82]. Such results from other studies show that performance can potentially follow the same trend in the Canadian climate.

Looking at the cold start test, the heat pump water heater during the first 1 hour and 30 minutes had a COP of 1.76. This was because the change in temperature from the supply and return was extremely high compared to when the tank water meets the required set-point temperature. During this period, the heat pump water heater was operating as intended with the average outdoor temperature of 2.9°C. The heat pump was shut off early as the ASHPWH met the required set point temperature relatively quickly. It took an additional 12 hours to reach the required tank temperature of 55°C. This long duration was due to the small surface area of the heating coils and also the reliance on natural convection for tank water mixing. This lead to an overall

COP of 0.06 due to wasted energy. The smaller coil was not able to provide as much heat as required to heat the hot water. Due to the low surface area with a high heating capacity from the ASHPWH, the COP was lower than expected. With the first configuration, it can be concluded that the heat pump water heater studied was oversized for the small top coil in the tank. The ASHPWH was not suitable to be used in tandem with the solar water heater system.

A second configuration with the ASHPWH connected to both tank coils was also tested. The tank coil was changed in late November, and the results reflected the change. Since the heat transfer was improved, the COP was also improved even during normal operations. The COP curve and the energy consumption curve showed that for a given average outdoor temperature, the COP was higher for the post-change scenario. Using the results from the cold start test, the system can be described with the results. The duration of the heating cycle from 7.5°C to 55 °C was found to be around 2 hours 30 minutes. The overall COP for the full duration was ranged from 0.97 to 0.89. There were three tests that was performed in January with similar temperatures. It can be seen that the ASHPWH system shuts off before the tank reaches the setpoint temperature. This could be due to a control issue or modulating issue.

The analysis was performed with the Toronto time of use electricity cost. The marginal cost was calculated to include other charges on the commodity prices. Using the TRNSYS simulation model of the ASHPWH, the annual electricity cost was found to be $237, and the annual energy consumption was found to be 2075 kWh. An electrical resistance water boiler with 100% efficiency will cost $548 to operate. This shows the high-cost saving when compared with an electrical heater. However, a 95% efficiency natural gas-fired boiler has an annual operating cost of $152, which has a significantly lower operating cost when compared to the ASHPWH.

Chapter 5 – Conclusion

The SDFSS case study and also illustrate its most important parameters. These parameters can be changed to simulate the operating cost and GHG emission of 4 switching systems for different locations, HVAC systems, or utility prices.

The simulation results show that the SDFSS may become significantly more beneficial in the coming decades: even when there are additional carbon pricing and new electricity pricing tiers. The simulation also shows that not only does SDFSS reduces cost, it also reduces GHG emission compared to a natural gas system.

The benchmark simulation scenario shows the SDFSS resulted in a 3% cost reduction and an 18% GHG emission reduction compared to the natural gas furnace. When compared to the manufacturer switching, the SDFSS resulted in a 21% saving and 33% saving when the set-point switching temperature was set to -5°C and -15°C respectively. However, when comparing GHG emissions, the SDFSS has a higher GHG emission of 150% higher and 840% higher than the manufacturer switching system with a set-point temperature of -5°C and -15°C respectively.

Still, the cost-saving presented was mainly the parameter that would incentivize users to switch from a typical natural gas heating system to an ASHP and natural gas hybrid system. Due to this, the SDFSS can be considered a transitional technology that would incentivize users to transition from natural gas furnace dependant heating to an electrically powered ASHP.

As a result, future ASHP systems can replace old or obsolete air conditioner systems that could run in heating mode to provide a low emission heating alternative. If the SDFSS can be implemented, the ASPH hybrid system will not only be more cost-effective than the manufacturer switching system and natural gas furnace, and it will also reduce the GHG emission compared to a full natural gas furnace system.

Lastly, due to the connectivity and flexibility of the SDFSS, many additional improvements can continually be implemented into the system. Additional control parameters such as utility demand response, PV systems, ASHP water heaters, temperature prediction, and house heating demand predictions can be added into the SDFSS cloud system. The integration of these systems can allow the SDFSS to assess all the parameters clearly to provide the most optimal switching criteria and potentially control other heating systems in the future.

The ASHPWH cast study was completed with small issues. During the course of this project, numerous testing strategies were applied in order to identify the efficiency of the system and to develop a computer

simulation model. The air source heat pump water heater was installed with the indoor Hydrobox unit and a DHW tank. The temperature and flow sensors were installed into the piping and tank. The sensors were calibrated carefully, and the calibration was performed multiple times to ensure the sensors were accurate.

The sensors were installed strategically to ensure that the data collected was accurate. There are several redundant sensors to verify essential readings. The data collected for the same reading was averaged together. Since there were limited available channels for the data acquisition system, there are only three sensors dedicated to measuring the tank temperature. The sensors are located in the middle of the tank, top of the tank (hot water outlet pipe), and the bottom of the tank (city water inlet pipe). Due to the hot water storage stratification, the mid tank water temperature was mainly used to identify the overall water temperature in the DHW tank. By taking the average with the output temperature, inlet water temperature, and the mid tank water temperature, the average tank temperature was calculated.

A custom draw profile was created for this project to simulate typical household hot water consumption of a typical day in a residential house. The profile used information from previous studies to create a realistic consumption profile. Additionally, due to the testing system, the water flow rate cannot be variable in value and was restricted to three different flow rates: 1.5 L/min, 6 L/min and 8 L/min for low flow, medium flow, and shower consumption rates. Using these three flow rate, a water draw profile was created around these three values. Most of the tests performed used this created draw profile. Additional tests performed on the system included a consistent water draw profile and a cold start test. These tests were performed to collect additional data about the system.

The collected data was analyzed and two major hardware configuration compared in this project was the pre-coil tank change and the post-coil tank change information. Due to the design of the DHW tank, there are two separate heat exchanger coils within the tank. The pre-coil change configuration only had the upper smaller coil connected to the heat pump water heater while the post-coil change configuration had both the top and bottom coils connected. Through the analysis, it was clear that the pre-coil change configuration was not performing as expected. The cold start test showed that it took over 14 hours to heat the tank water from 11°C to 40°C. This was concluded to be caused due to the low heat transfer rate and the fact that natural convection in the water tank does not sufficiently mix the tank water enough to heat the water efficiently in this configuration. The tank was initially designed for a solar hot water collector where stratification in the tank was sufficient. The larger lower coil was initially being designed for the solar hot water collector to slowly heat the colder city water. The smaller upper coil was designed for a supplementary heater to reach setpoint temperature. Due to this, the increased supply heat from the ASHPWH in the heating loop was not efficiently transferred to the water within the tank.

The post-coil change tank configuration showed improved efficiency and performance due to the increased surface area for heat transfer. The new change allows the water in the tank to heat up more efficiently and faster. Though the heat pump water heater did not cycle as much as the pre-coil change configuration, cycling can still be seen. To improve this, the tank should have a possible mixing apparatus that would efficiently move the water around, allowing the colder water to contact the heating coils more often. Another proposed improvement was to have the ASHPWH to draw potable water directly from the tank and directly supply the hot water into the tank. Doing so will allow the ASHPWH to more effectively heat the water. Since the ASHPWH has a Hydrobox system that splits the refrigerant from the potable water loop, this configuration was a possible solution. As seen in the results, the ASHPWH was capable of heating the loop water very efficiently and relatively quickly. By removing the heating coil, the extra heat transfer process was removed, and the tank water will also circulate more due to the flow of the ASHPWH.

Another main concern was the control system for the ASHPWH. It was seen in the first tank coil configuration that the ASHPWH kept periodically operate even when the tank temperature meets set-point temperature. This result was investigated during the no-water draw test. There was still high energy consumption when there was no water draw. The energy consumed was found to be on the same scale as regular operation. The controlling system can possibly be modified to include a more optimal system to control the flow rate, temperature, and capacity of the heat pump coil.

Overall, this case study showed that there was an excellent potential for reducing GHG emission compared to the current natural gas water heater. However, the operational costs are higher compared to the natural gas water heater.

5.1 The flexibility of the systems

This work has investigated the performance of two different residential applications of an ASHP with a focus on reducing the overall operational cost and GHG emissions when compared with a natural gas furnace. The SDFSS was a simplistic design that can be easily implemented without proprietary software or complex equations. The study intention was to use easily accessible software such as Microsoft Excel Spreadsheet to calculate the optimal economic switching point for the dual-fuel space heating system. The design of the SDFSS was also to have the required calculations performed off-site on a cloud-based server while connected to the local residential thermostat. This creates a dynamic system that could implement new changes to the environment and also allow updates to be quickly relayed to the residential thermostat. The connectivity of the system makes this system flexible and can include additional new parameters such as carbon pricing or changes in the electricity and natural gas marginal prices.

This study shows the flexibility of the SDFSS compared to the manufacturer switching system. Though the manufacturer switching system can be configured using an outdoor set-point temperature, it was still far less flexible compared to the SDFSS, which considers cost, temperature, and equipment performance. The system can consider many different changes and prediction values to optimize the operation of the system.

The literature review indicates that fuel switching can encompass more than just natural gas and electricity. The manufacturer switching system was often not too flexible and can only accommodate two different fuel types. However, there are locations where there are multiple different fuels and different costs [83]. The different fuel sources can be implemented as part of the switching parameters. This paper shows the possibility of controlling all the different fuel sources to optimize the operation for costs.

An additional benefit of having a cloud-based switching system was the ability to share local data within the system to provide a more accurate local reading. One example of that was with local temperature. Temperature sensors from the ASHP system can be affected by many surrounding effects such as wind, shading or just hardware malfunction. To potentially limit such issues, local data from surrounding houses could anonymously provide temperature reading for an overall average of a region. This can be compared with the individual sensor allowing an overall reading.

Additionally, the SDFSS was able to instantaneously adapt to virtually any changes. Since the SDFSS was a cloud-based system, system-wide updates can be done to push commands to a large area or on the other hand, execute smaller regional-based commands. With the cloud SDFSS, utility side demand response was also possible. With the help of SDFSS, utility companies will be able to actively switch the fuel preference and release strain on the utility grid allowing utility companies to slowly adapt to the added energy demand. Not only does this system benefit the end-user, but it also benefits the utility companies in the transitional stage from natural gas to electricity.

The ASHPWH study that was performed was to test the performance of a cold climate ASHP implemented to supply DHW. The product was originally intended to be able to supply both space heating and to cool through a hydronic system along with meeting domestic hot water supply. In this study, the ASHPWH was the only mode of heating tested. The ASHPWH was meant to provide a flexible solution to meet both the space heating and cooling demands and the DHW demands. Though the flexibility of the ASHPWH alone was not as impactful as the SDFSS, with a combination of the two systems, a natural gas boiler/ASHP hybrid system (with space heating hydronic system) could potentially take advantage of the switching capabilities of the SDFSS to economically switch between fuels and between space heating and DHW heating. This combination was a flexible solution to economically meet the two types of heating demands.

5.2 Can we reach the Paris Agreement goals?

One of the main drivers of the study was to investigate whether or not the 2030 Paris agreement goal of reducing 30% of the GHG emission and year 2050 goal of reducing 80% of the GHG emission was achievable. The goal of reducing 30% of the GHG emission was possible with the SDFSS if the carbon pricing reaches its peak in 2022 and the APP in implemented. The total estimated GHG emission using this method was expected to be over 50%. This was comfortably over the expected 30% before reaching 2030. However, when analyzing the system to see if the 2050 goal of 80% reduction can be met, the SDFSS would need additional support in order to incentivize a higher electricity consumption compared to natural gas consumption. At the moment, the SDFSS would not be able to meet the set 2050 goal without an additional increase to the federal carbon pricing.

In order to meet the Paris Agreement target, the GHG emission must be reduced by 30% from 2005 levels by 2030 and reduce the GHG emission levels by 80% by 2050. Using the results from this study, the SDFSS reduces the GHG emission by 16% when compared to the natural gas-only option. The baseline analysis did not account for any additional pricing charges, and the emission reduction will not meet the 30% GHG reduction target.

However, if the carbon tax and the new APP scheme was included, it can be seen that the GHG emission levels can be reduced by 51% using the SDFSS when compared to the natural gas only. This shows that the SDFSS potentially reduces 50% of the current GHG emission by 2022, when the carbon pricing meets \$50/tonne of CO_2. This will potentially allow Canadian's residential sector to meet the Paris Agreement target for 2030 but will not meet the target for 2050. The carbon pricing will need to increase consistently to meet the 80% GHG emission reduction target. The results of the manufacturer switching system with -15°C set-point temperature shows that 80% GHG emission reduction was possible. With the carbon pricing increasing, the SDFSS will use the ASHP more frequently compared to the natural gas furnace, eventually reaching an electric ASHP dominant space heating society.

Similarly, using an ASHPWH reduces over 90% of the GHG emission as it was primarily using electricity as its primary source of energy. Though the operating cost of this system was higher, it dramatically impacts the GHG emission reduction. This type of DHW system was able to exceed the 2030 goal of 30% reduction and also meet the 2050% goal of 80% reduction.

Though the SDFSS does not meet the 2050 Paris Agreement goals, it was able to meet the 2030 goal. This was a useful transitional system that would eventually sprout other GHG reduction technologies. A system such as the SDFSS could allow the electricity grid to adapt to the growing demand and also provide additional time for the shift from power plants which still uses fossil fuel.

5.3 Limitations and future research

This research was conducted over two years and has been a time demanding process. If given a chance to repeat the study, a few changes would have been made, which are mentioned here to illustrate the lessons learned and the limitations of the study. The research results for the SDFSS have shown great potential; however, the data collected from the experimental result could have provided an insight into net-zero energy houses.

The case study performed during the SDFSS research prompted the collection of important natural gas and electricity consumption data, and additionally, the electricity produced by the solar panels was also measured. To calculate whether this house was considered net-zero, both the electricity consumption and the natural gas consumption was compared with the electricity generated by the solar panels. A brief calculation showed that due to occupant behavior, the house was no longer an NZEH and the associated GHG emission was higher than anticipated due to this. This showed that even though the SDFSS can potentially provide operational cost savings, the GHG emission reduction could potentially be lessened due to the occupants. An interview with the occupants confirmed that this reckless behavior was stemmed from the solar panel net metering program. The occupants have a “use it or lose it” mindset and are continually being wasteful. Even though the base electricity consumption was similar in value to the electricity generated by the solar panel, the house was not considered net-zero as there was not enough production to off-set the equivalent electricity consumption of natural gas usage. The data collected from this case study will be further analyzed and investigated in the future for potential journal publication.

The case study performed for the ASHPWH similarly prompted a few crucial concerns and questions. As mentioned in Chapter 3, the domestic hot water tank was designed with two closed-loop coils, one for the solar heat collector for water heating and the other for a mechanical heating system. The tank design indicated that the more significant and longer coil was intended for the solar collector, most likely due to the low-grade heat from the collector. During the study, a problem arose where the ASHPWH was oversized for the coil it was connected to. This yields poor heating performance, short operating cycles and extended time to meet water set-point temperature. Though the impact of this issue was reduced by connecting the two loops in series, if this issue were known before the experimental testing, the tank would have been modified to be an open loop. The open-loop will have potable water flowing directly to the refrigerant to water heat exchanger and back into the tank for consumption. The water to refrigerant heat exchanger was designed with food-safe materials on the DHW side and was suitable for potable water. This would most likely improve the performance of the system. Another after-thought of this study was to implement the carbon pricing for the analysis of the ASHPWH. Though the added carbon pricing would not impact the GHG emission

reduction as it would affect the SDFSS, this added pricing will significantly improve the operational cost comparison between it and the natural gas water heater.

A. Appendix A

Appendix A shows the additional analysis performed for the net-zero energy house case study.

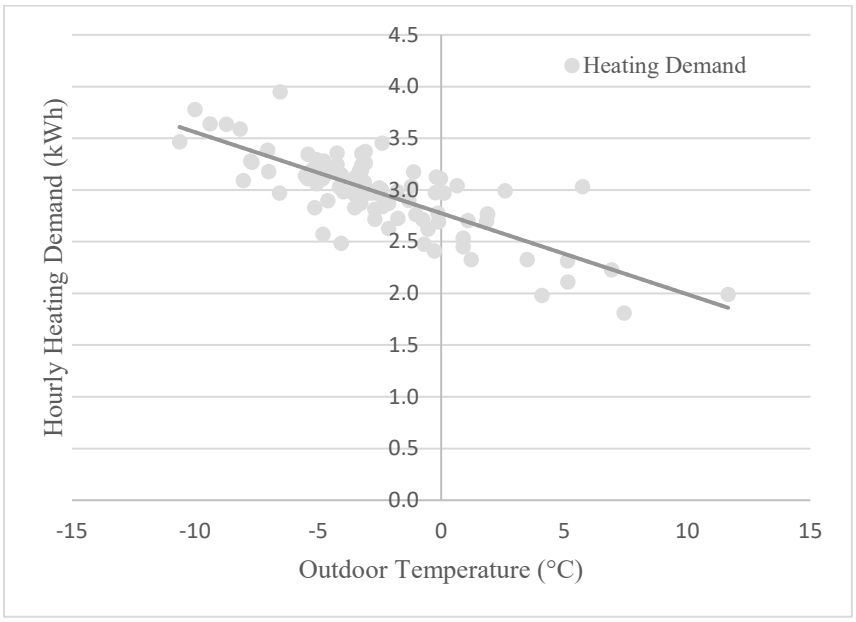

Figure A-1: Experimental space heating demand using furnace natural gas consumption data

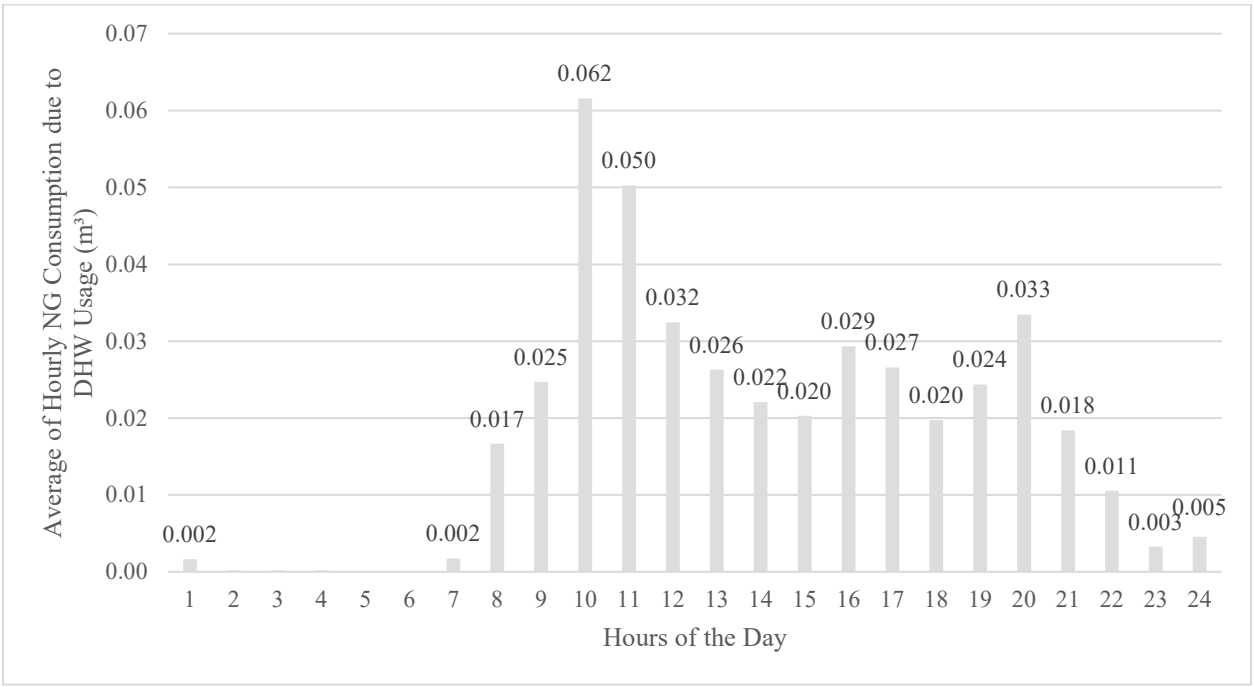

Figure A-2: Average daily natural gas consumption profile for DHW usage

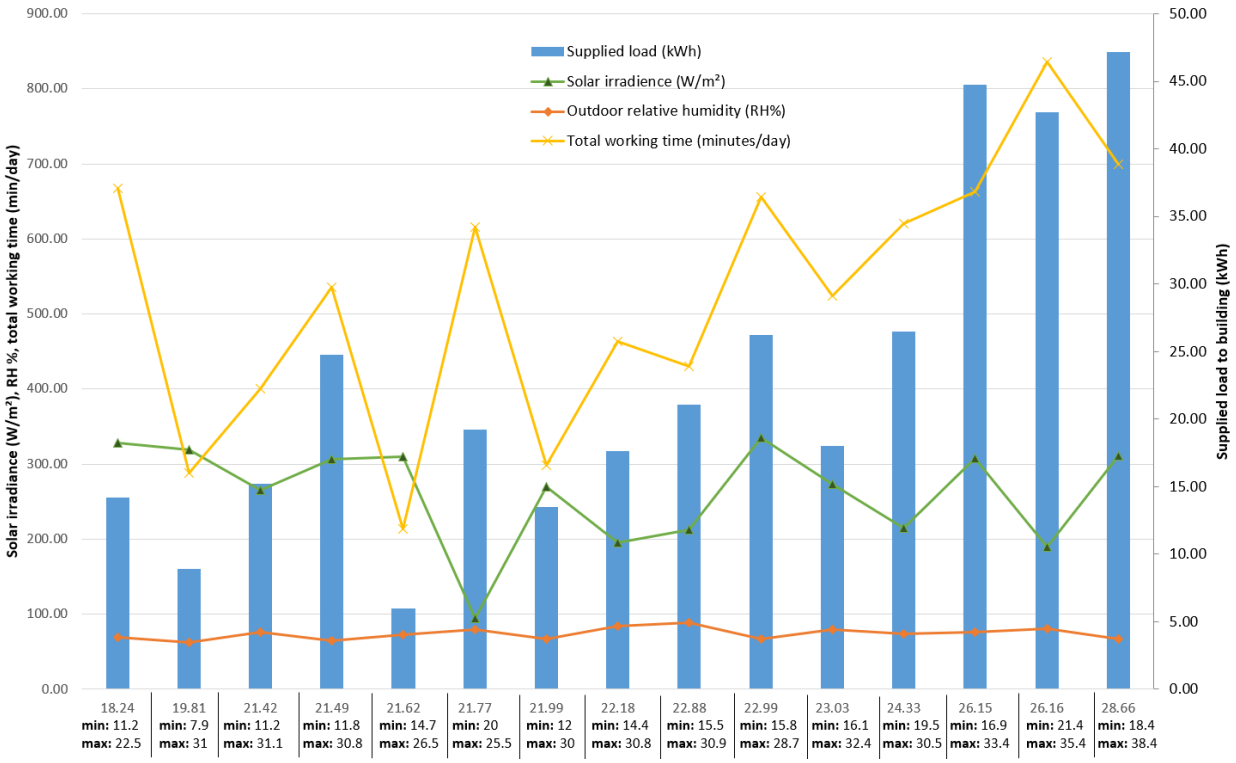

Figure A-3: Cooling load supplied compared to outdoor temperature including solar irradiance and operating duration

B. Appendix B

Appendix B shows the additional analysis performed for the ASHPWH.

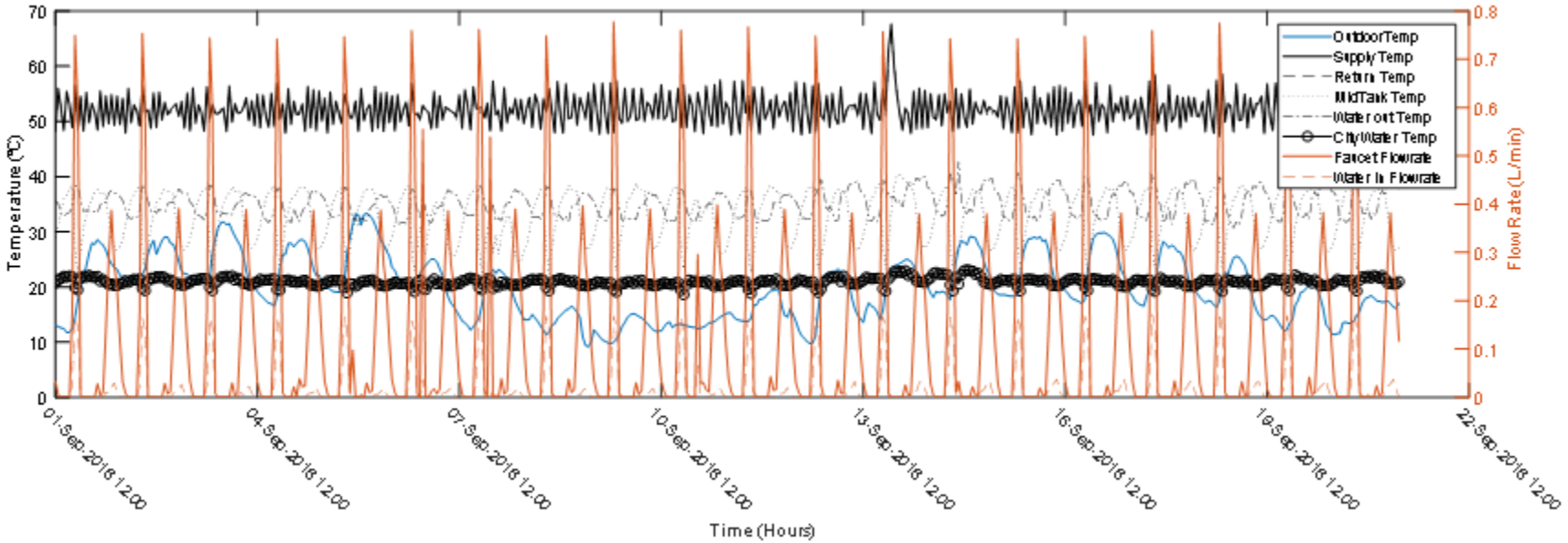

Figure B-B.1: Pre-coil change (Hourly Average) (Sept 1, 2018 – Sept 20, 2018)

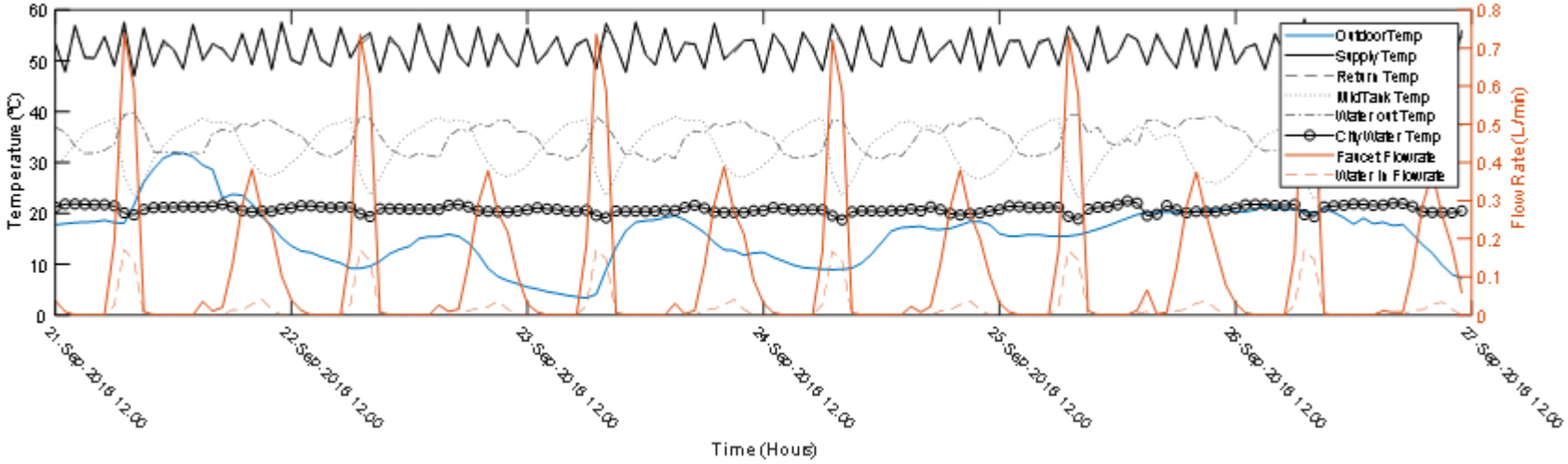

Figure B-B.2: Pre-coil change with active solar harvesting (Hourly Intervals) (Sept 21, 2018 - Sept 26, 2018)

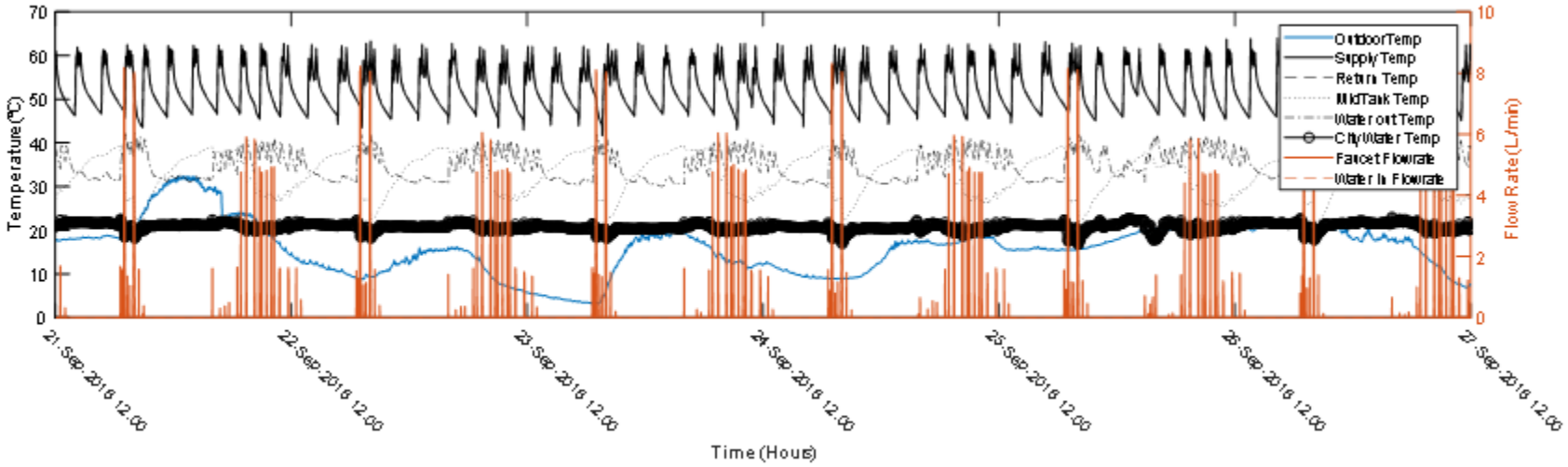

Figure B-B.3: Pre-coil change with active solar harvesting (Minutely Intervals) (Sept 21, 2018 – Sept 26, 2018)

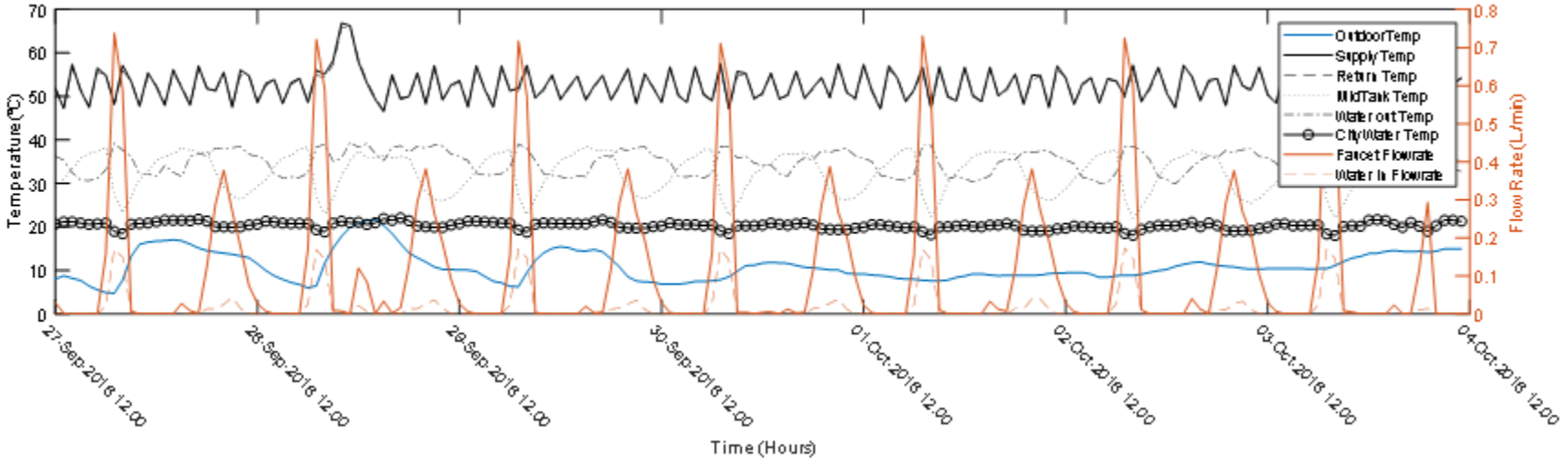

Figure B-4: Pre-coil change (Hourly Interval) (Sept 27, 2018 - Oct 3, 2018)

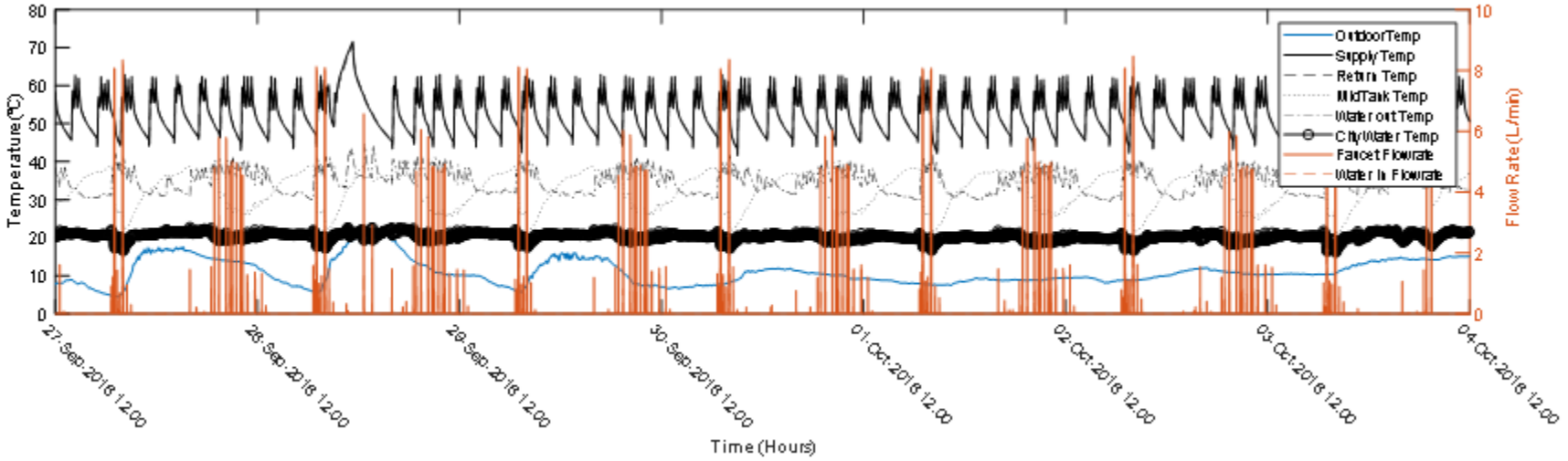

Figure B-5: Pre-coil change (Minutely Interval) (Sept 27, 2018 - Oct 3, 2018)

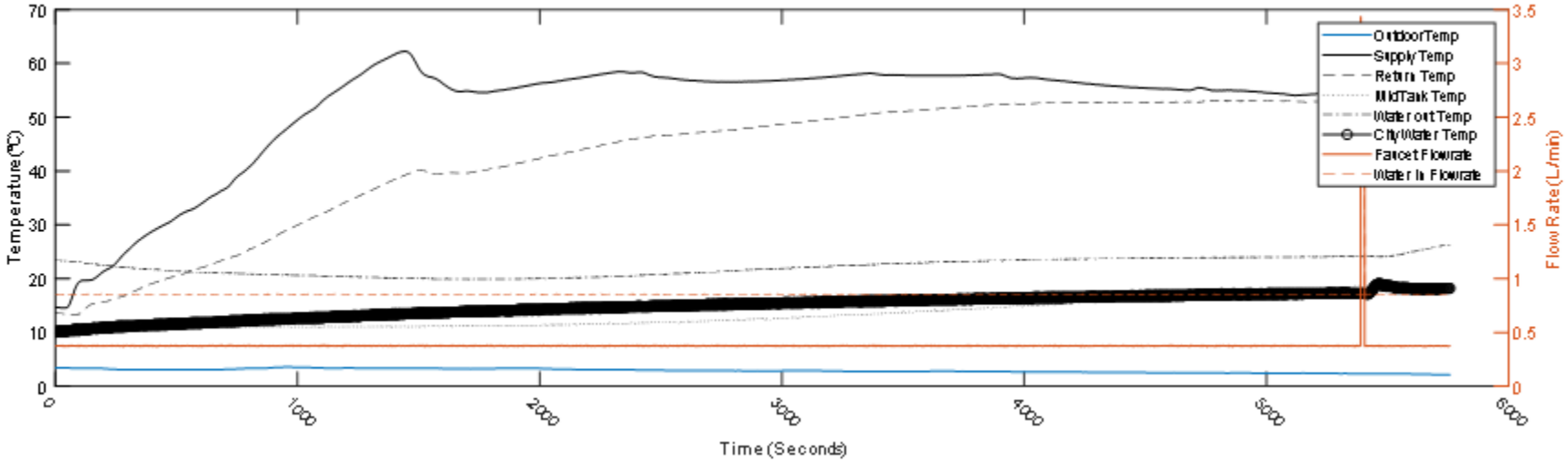

Figure B-6: Cold start heat pump performance test (11℃ to 19℃)

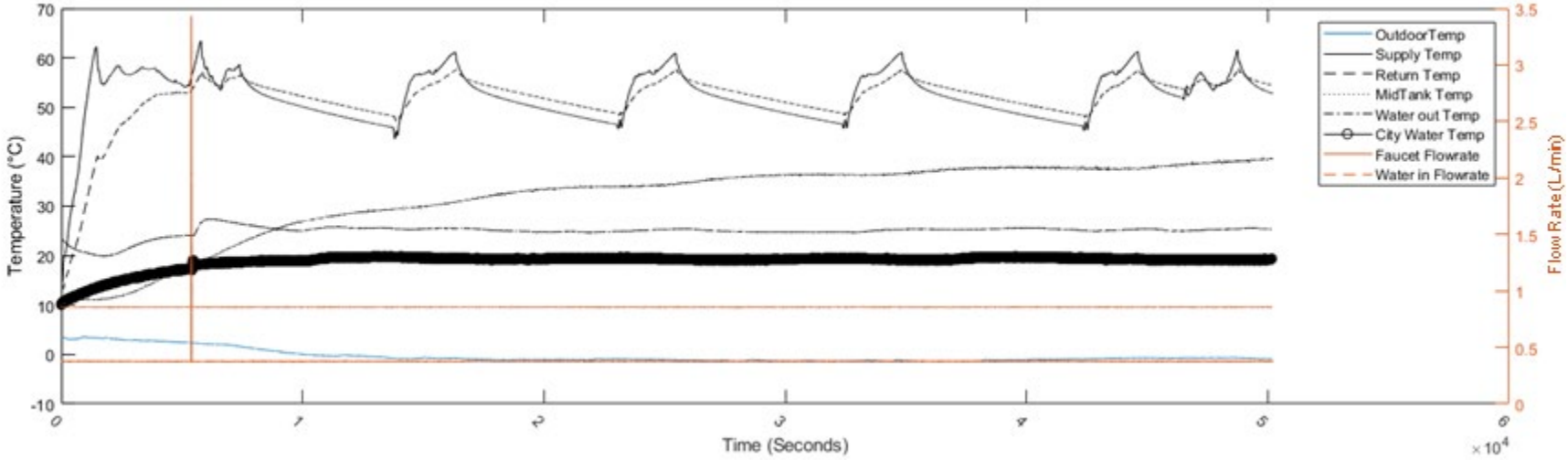

Figure B-7: Cold start heat pump performance test (11℃ to 40℃)

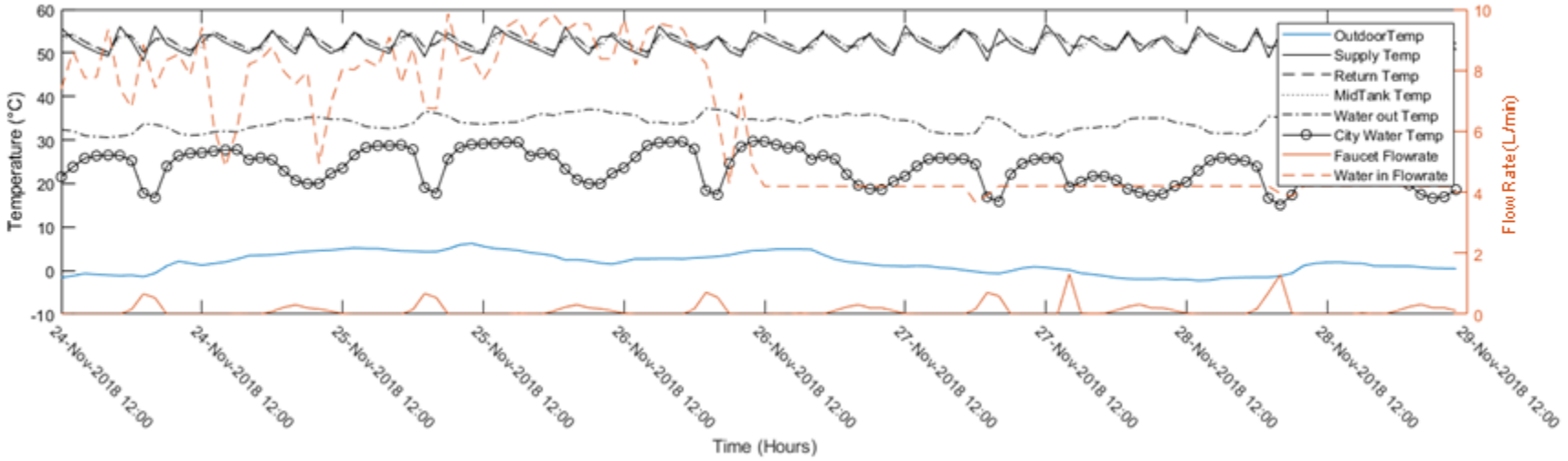

Figure B-8: Post-coil change first interval (Hourly Interval) (Nov 24, 2018 – Nov 28, 2018)

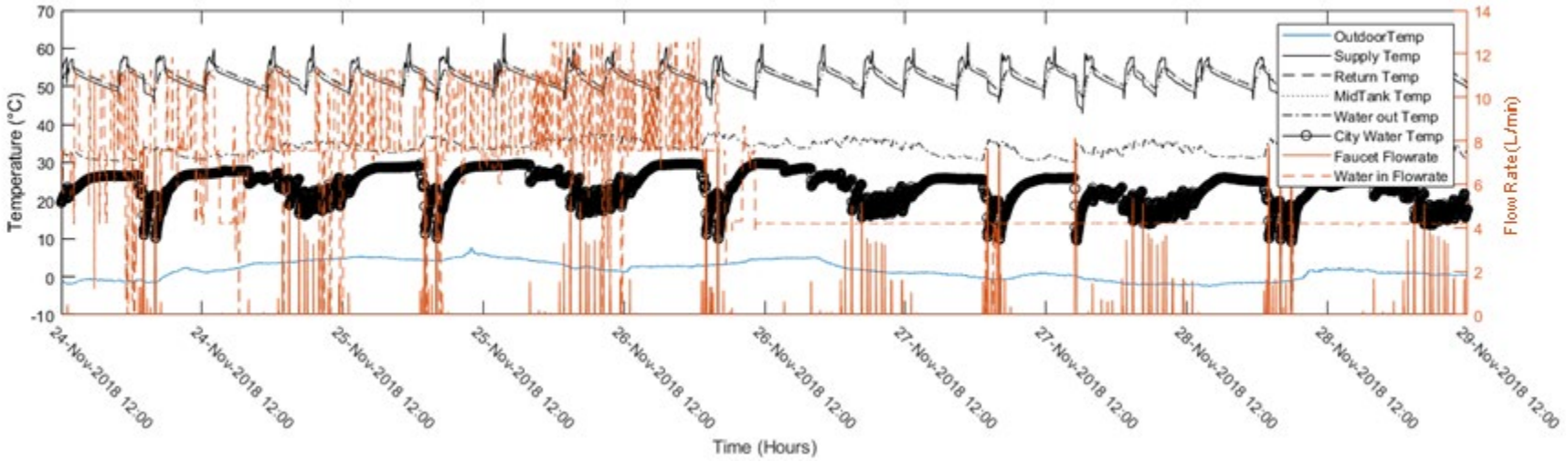

Figure B-9: Post-coil change first interval (Minutely Interval) (Nov 24, 2018 – Nov 28, 2018)

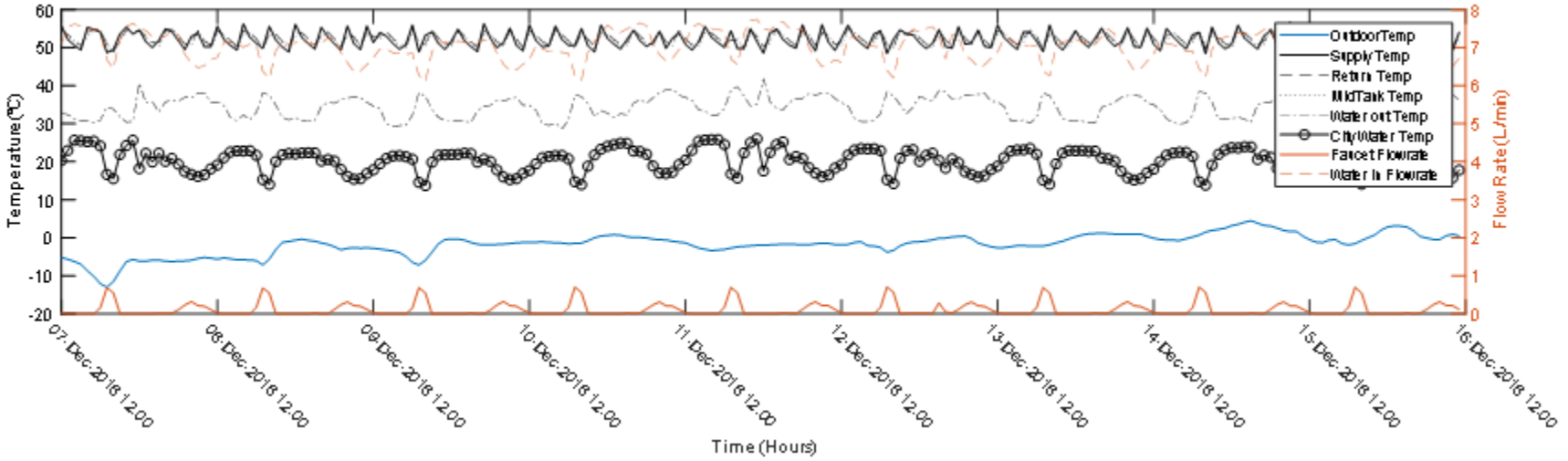

Figure B-10: Post-coil change first interval (Hourly Interval) (Dec 07, 2018 – Dec 15, 2018)

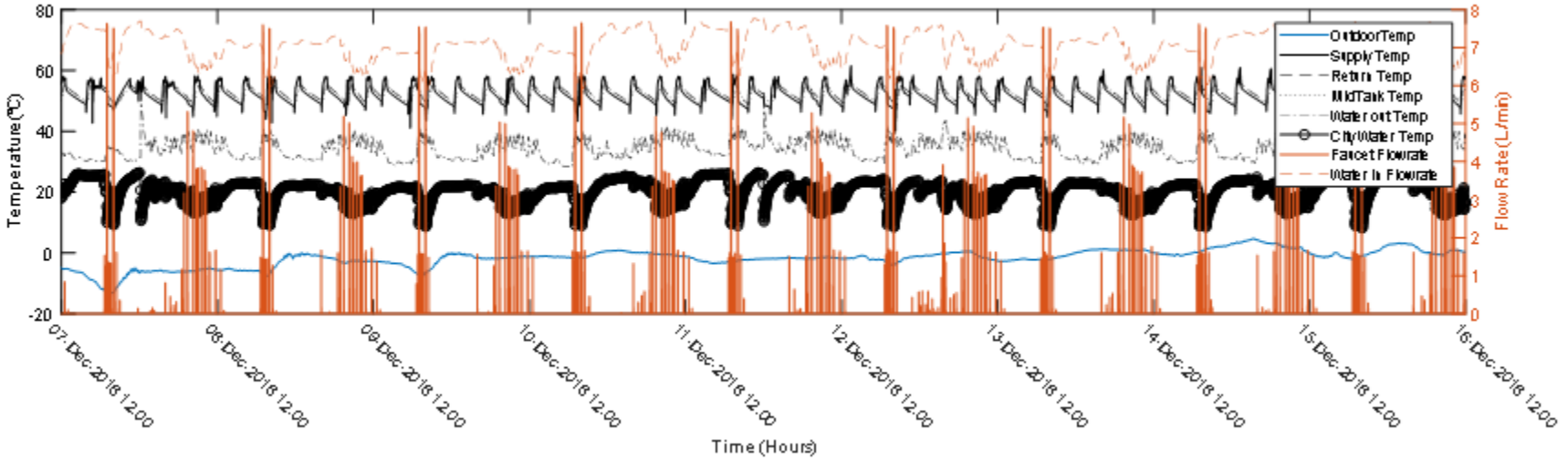

Figure B-11: Post-coil change first interval (Minutely Interval) (Dec 07, 2018 – Dec 15, 2018)

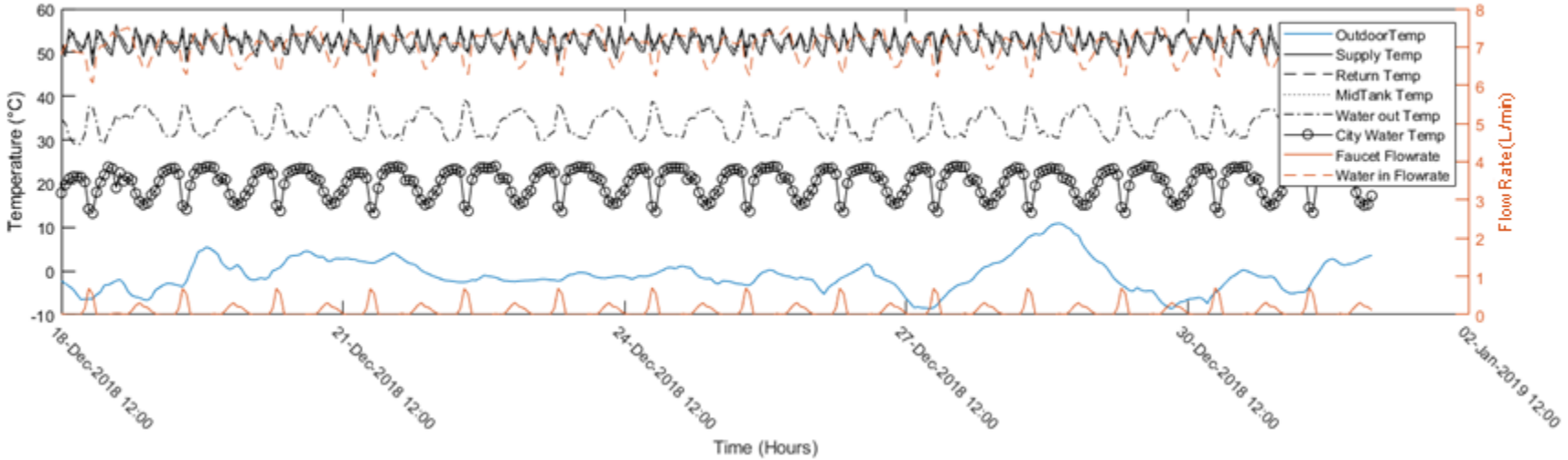

Figure B-12: Post-coil change first interval (Hourly Interval) (Dec 18, 2018 – Dec 31, 2018)

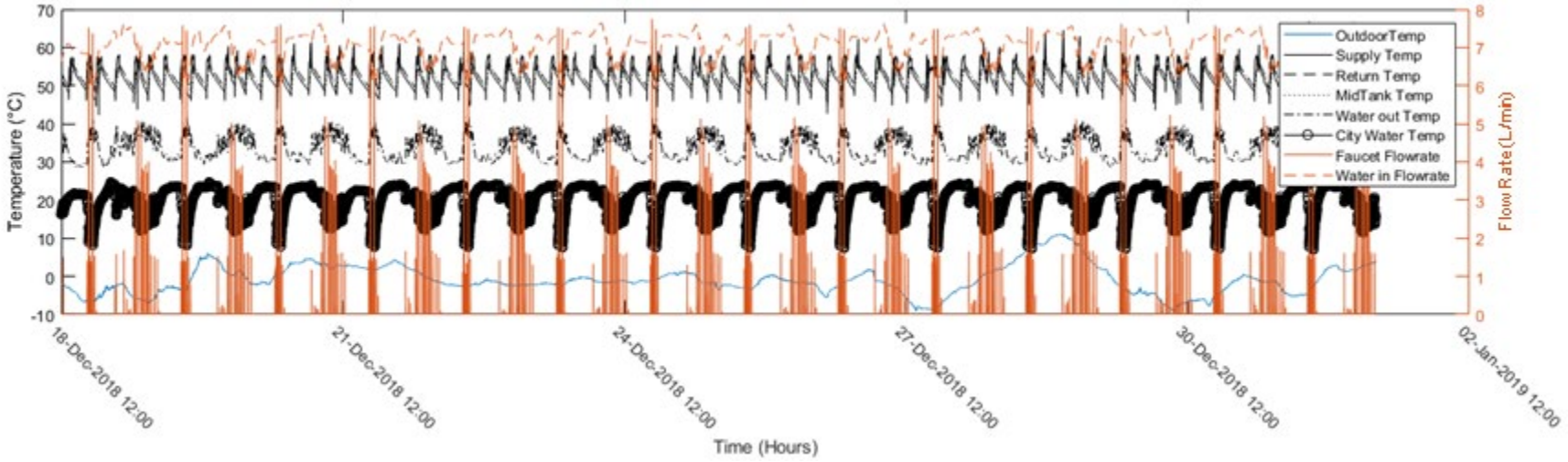

Figure B-13: Post-coil change first interval (Minutely Interval) (Dec 18, 2018 – Dec 31, 2018)

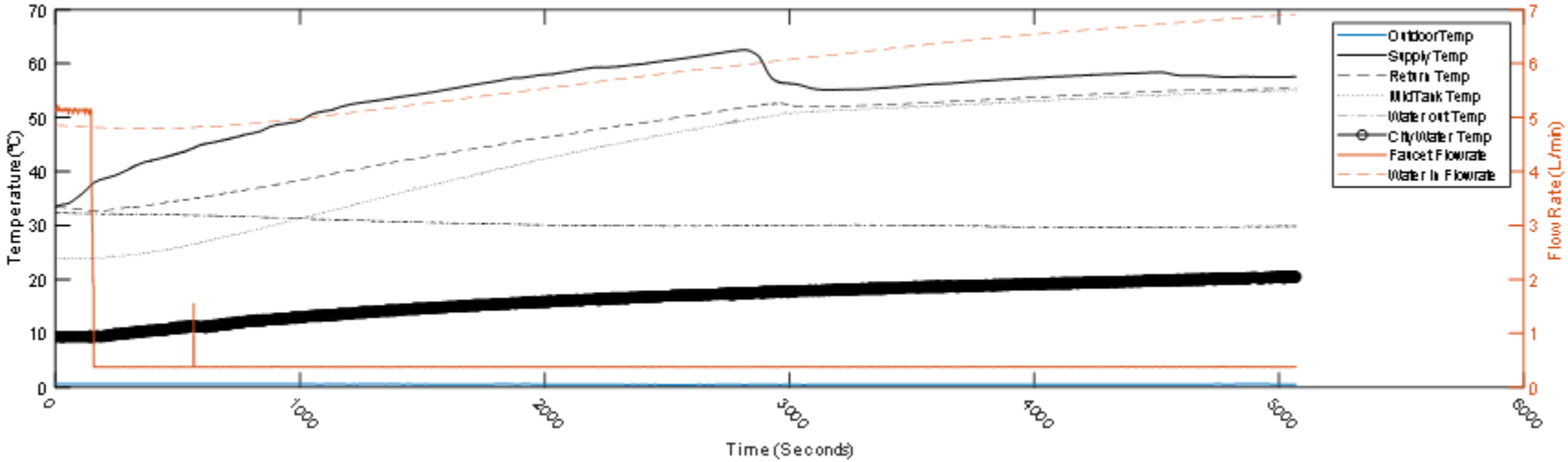

Figure B-14: Cold start test post coil change (Dec 6, 2018)

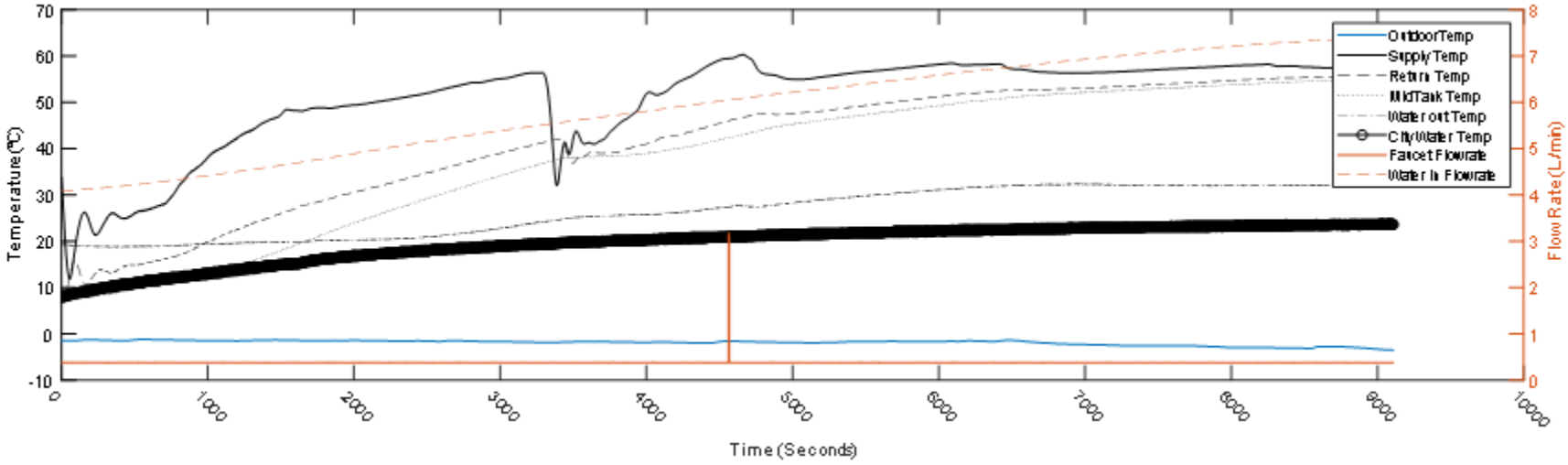

Figure B-15: Cold start test post coil change test 1 (Jan 14, 2019)

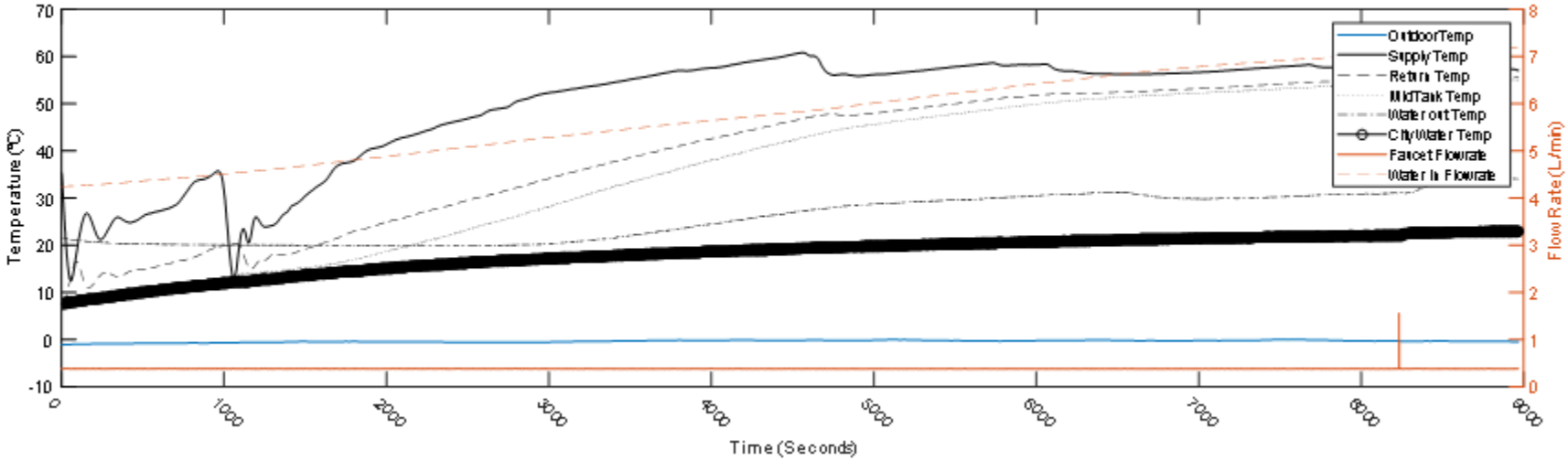

Figure B-16: Cold start test post coil change test 2 (Jan 15, 2019)

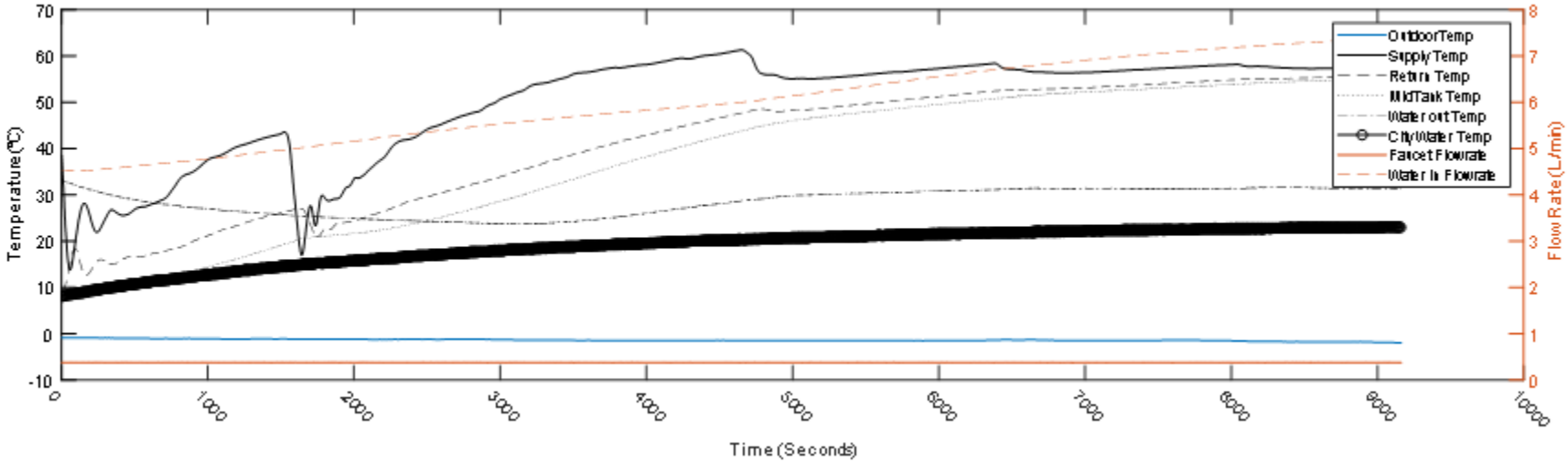

Figure B-17: Cold start test post coil change test 3 (Jan15, 2019)

References

[1] L. Pérez-Lombard, J. Ortiz, and C. Pout, "A review on buildings energy consumption information," *Energy Build.*, vol. 40, no. 3, pp. 394–398, Jan. 2008.

[2] J. Laghari, "Climate change: melting glaciers bring energy uncertainty," *Nature*, vol. 502, no. 7473, pp. 617–618, 2013.

[3] C.-F. Schleussner *et al.*, "Science and policy characteristics of the Paris Agreement temperature goal," *Nat. Clim. Change*, vol. 6, no. 9, pp. 827–835, Sep. 2016.

[4] UNFCCC, "The Paris agreement," 2018. [Online]. Available: https://doi.org/10.4324/9781351270090-20. [Accessed: 18-Aug-2019].

[5] Government of Canada, "Pan-Canadian Framework on Clean Growth and Climate Change:Canada's Plan to Address Climate Change and Grow the Economy." 2016.

[6] M. Lee, "The effects of an increase in power rate on energy demand and output price in Korean manufacturing sectors," *Energy Policy*, p. 7, 2013.

[7] P. Nejat, F. Jomehzadeh, M. M. Taheri, M. Gohari, and M. Z. Abd. Majid, "A global review of energy consumption, CO 2 emissions and policy in the residential sector (with an overview of the top ten CO 2 emitting countries)," *Renew. Sustain. Energy Rev.*, vol. 43, pp. 843–862, Mar. 2015.

[8] Natural Resources Canada, "Canada's GHG Emissions by Sector, End Use and Subsector – Including Electricity-Related Emissions," 2017. [Online]. Available: http://oee.nrcan.gc.ca/corporate/statistics/neud/dpa/showTable.cfm?type=HB&sector=aaa&juris=ca&rn=3&page=0. [Accessed: 21-Aug-2019].

[9] Government of Canada, "United Nations Framework Convention on Climate Change," *United Nation Framework Convention on Climate Change and its Paris Agreement*, 19-Feb-2015. [Online]. Available: https://www.canada.ca/en/environment-climate-change/corporate/international-affairs/partnerships-organizations/united-nations-framework-climate-change.html. [Accessed: 21-Aug-2019].

[10] Natural Resources Canada, "Residential Sector - Housing Stock by Building Type and Vintage," *Residential Sector Canada Table 21: Housing Stock by Building Type and Vintage*, 30-Nov-2018. [Online]. Available: http://oee.nrcan.gc.ca/corporate/statistics/neud/dpa/showTable.cfm?type=CP&sector=res&juris=ca&rn=21&page=3&CFID=5760273&CFTOKEN=7fd92d5546d22ec4-271F7142-FB08-DBC2-5D7D59E66B46A1B7. [Accessed: 21-Aug-2019].

[11] National Research Council, "National Building Code of Canada 2015," 2015. [Online]. Available: https://nrc.canada.ca/en/certifications-evaluations-standards/codes-canada/codes-canada-publications/national-building-code-canada-2015. [Accessed: 21-Aug-2019].

[12] Government of Ontario, "Archived - The End of Coal," *Environment and Energy*.

[Online]. Available: https://www.ontario.ca/page/end-coal.

[13] IESO, "Energy Resources: How They Work," *Ontario's Supply Mix*. [Online]. Available: http://www.ieso.ca/en/Learn/Ontario-Supply-Mix/Energy-Resources-How-They-Work.

[14] Natural Resources Canada, "Residential Sector Canada Table 27: Heating System Stock by Building Type and Heating System Type," 30-Nov-2018. [Online]. Available: http://oee.nrcan.gc.ca/corporate/statistics/neud/dpa/showTable.cfm?type=CP&sector=res&juris=ca&rn=27&page=0.

[15] Natural Resources Canada, "Residential Sector Canada Table 2: Secondary Energy Use and GHG Emissions by End-Use," 30-Nov-2018. [Online]. Available: http://oee.nrcan.gc.ca/corporate/statistics/neud/dpa/showTable.cfm?type=CP&sector=res&juris=ca&rn=2&page=0. [Accessed: 18-Aug-2019].

[16] Government of Ontario, "O. Reg. 332/12: Building Code," *Building Code Act*, 24-Jul-2014. [Online]. Available: https://www.ontario.ca/laws/regulation/120332.

[17] Natural Resources Canada, "Details of the R-2000 Standard," 05-Feb-2018. [Online]. Available: https://www.nrcan.gc.ca/homes/learn-about-professional-opportunities/become-energy-efficient-builder/details-r-2000-standard/20588.

[18] Natural Resources Canada, "ENERGY STAR® for New Homes Standard - Version 12.6," 02-Jan-2014. [Online]. Available: https://www.nrcan.gc.ca/energy/efficiency/housing/new-homes/energy-starr-new-homes-standard/energy-starr-new-homes-standard-version-126/14178.

[19] V. Delisle, "Net-Zero Energy Homes: Solar Photovoltaic Electricity Scenario Analysis Based on Current and Future Costs," p. 8.

[20] Natural Resources Canada, "Water Heater Guide." 2012.

[21] A. Szekeres and J. Jeswiet, "Heat pumps in Ontario: Effects of hourly temperature changes and electricity generation on greenhouse gas emissions," *Int. J. Energy Environ. Eng.*, vol. 10, no. 2, pp. 157–179, Jun. 2019.

[22] IESO, "Ontario Demand Forecast." IESO.

[23] IESO, "Long-Term Energy Plan." [Online]. Available: http://www.ieso.ca/en/Sector-Participants/Planning-and-Forecasting/Long-Term-Energy-Plan.

[24] IESO, "Ontario Planning Outlook." [Online]. Available: http://www.ieso.ca/sector-participants/planning-and-forecasting/ontario-planning-outlook.

[25] Government of Canada, "Canada's Mid-Century Long-Term Low-Greenhouse Gas Development Stratedy." UNFCCC.

[26] Government of Canada, "Government of Canada sets ambitious GHG reduction targets for federal operations," *gcnws*, 19-Dec-2017. [Online]. Available: https://www.canada.ca/en/treasury-board-secretariat/news/2017/12/government_of_canadasetsambitiousghgreductiontargetsforfederalop.html.

[27] Government of Canada, “Progress towards Canada’s greenhouse gas emissions reduction target,” *aem*, 20-Jul-2012. [Online]. Available: https://www.canada.ca/en/environment-climate-change/services/environmental-indicators/progress-towards-canada-greenhouse-gas-emissions-reduction-target.html.

[28] N. Alibabaei, “Effects of Intelligent Strategy Planning Models on Residential HVAC System Energy Demand and Cost During the heating and Cooling Seasons,” *Appl. Energy*, p. 15, 2017.

[29] J. Bursill and C. A. Cruickshank, “Heat Pump Water Heater Control Strategy Optimization for Cold Climates.,” *J. Sol. Energy Eng.*, vol. 138, no. 1, 2015.

[30] A. Amirirad, R. Kumar, A. S. Fung, and W. H. Leong, “Experimental and simulation studies on air source heat pump water heater for year-round applications in Canada,” *Energy Build.*, vol. 165, pp. 141–149, Apr. 2018.

[31] A. Amirirad, R. Kumar, and A. S. Fung, “Performance characterization of an indoor air source heat pump water heater for residential applications in Canada,” *Int. J. Energy Res.*, vol. 42, no. 3, pp. 1316–1327, Mar. 2018.

[32] N. Alibabaei, A. S. Fung, and K. Raahemifar, “Development of Matlab-TRNSYS co-simulator for applying predictive strategy planning models on residential house HVAC system,” *Energy Build.*, vol. 128, pp. 81–98, Sep. 2016.

[33] Canada Revenue Agency, “Carbon pollution pricing – what you need to know,” *aem*, 19-Jun-2019. [Online]. Available: https://www.canada.ca/en/revenue-agency/campaigns/pollution-pricing.html.

[34] Natural Resources Canada, “Residential Sector Ontario Table 14: Total Households by Building Type and Energy Source,” 30-Nov-2018. [Online]. Available: http://oee.nrcan.gc.ca/corporate/statistics/neud/dpa/showTable.cfm?type=CP&sector=res&juris=on&rn=14&page=0.

[35] Government of Canada, “Backgrounder: Fuel Charge Rates in Listed Provinces and Territories,” 23-Oct-2018. [Online]. Available: https://www.fin.gc.ca/n18/data/18-097_1-eng.asp.

[36] Government of Canada, “Canadian Environmental Sustainability Indicators Greenhouse Gas Emissions.pdf.” 2019.

[37] R. Z. Wang, Z. Y. Xu, Q. W. Pan, S. Du, and Z. Z. Xia, “Solar driven air conditioning and refrigeration systems corresponding to various heating source temperatures,” *Appl. Energy*, vol. 169, pp. 846–856, May 2016.

[38] Entegrus Utility, “Electricity Rates | Entegrus.” [Online]. Available: https://www.entegrus.com/electricity-rates-0.

[39] London Hydro Utility, “Electricity and Water Rates.” [Online]. Available: https://www.londonhydro.com/site/#!/residential/content?page=electricity-water-rates.

[40] Toronto Hydro Utility, “Residential electricity rates - Toronto Hydro.” [Online]. Available: https://www.torontohydro.com/for-home/rates.

[41] EnWin Utility, “Regulatory Information | ENWIN.” [Online]. Available: https://enwin.com/regulatory-information/.

[42] Synergy North Utility, “SynergyNorth Rates.” [Online]. Available: https://synergynorth.ca/residential/billing/rates/.

[43] A. A. Safa, “Performance of two-stage variable capacity air source heat pump: Field performance results and TRNSYS simulation,” *Energy Build.*, p. 11, 2015.

[44] A. A. Safa, “Heating and cooling performance characterisation of ground source heat pump system by testing and TRNSYS simulation,” *Renew. Energy*, p. 11, 2015.

[45] M. Bell *et al.*, “Development of Micro Combined Heat and Power Technology Assessment Capability at the Canadian Centre for Housing Technology,” p. 48 p., Dec. 2003.

[46] Ontario Energy Board, “Managing costs with time-of-use rates | Ontario Energy Board.” [Online]. Available: https://www.oeb.ca/rates-and-your-bill/electricity-rates/managing-costs-time-use-rates.

[47] Powerstream, “Advantage Power Pricing | Alectra Utilities.” [Online]. Available: https://www.powerstream.ca/innovation/advantage-power-pricing.html.

[48] K. Tung, A. Wang, N. Ekrami, and A. Fung, “Numerical study on smart dual fuel switching systems in net zero energy homes,” *Proceeding ESim 2018 10th Conf. IBPSA-Can.*, p. 9, 2018.

[49] EnergyPlus, “Weather Data Sources | EnergyPlus.” [Online]. Available: https://energyplus.net/weather/sources.

[50] A. A. Safa, A. S. Fung, and R. Kumar, “Comparative thermal performances of a ground source heat pump and a variable capacity air source heat pump systems for sustainable houses,” *Appl. Therm. Eng.*, vol. 81, pp. 279–287, Apr. 2015.

[51] Enbridge - Union Gas, “Current Rates - Residential - Union Gas.” [Online]. Available: https://www.uniongas.com/residential/rates/current-rates.

[52] Enbridge - Union Gas, “Conversion Factors - Business - Union Gas.” [Online]. Available: https://www.uniongas.com/business/save-money-and-energy/analyze-your-energy/energy-insights-information/conversion-factors.

[53] Government of Ontario, “Guide: Greenhouse Gas Emissions Reporting,” *Ontario.ca*, 19-Jan-2016. [Online]. Available: https://www.ontario.ca/page/guide-greenhouse-gas-emissions-reporting.

[54] C. Gordon and A. Fung, “Hourly Emission Fathers from the Electricity Generation Sector - A Tool for Analyzing the Impact of Renewable Technologies in Ontario,” *Trans. Can. Soc. Mech. Eng.*, vol. 33, no. 1, pp. 105–118, Mar. 2009.

[55] C. Gordon and A. Fung, “Analysis of Time Dependent Valuation of Emission Factors from the Electricity Sector,” in *Sustainable Growth and Applications in Renewable Energy Sources*, M. Nayeripour, Ed. InTech, 2011, pp. 295–312.

[56] A. Brookson, D. A. S. Fung, S. Saxena, P. Eng, and L. S. Hilaire, “Demonstration and Simulation of a Transactive Energy Management System for Residential Buildings,” p. 8.

[57] IESO, “Power Data Market Demand.” [Online]. Available: http://www.ieso.ca/Power-Data.

[58] Environment Canada, “Station Results - 1981-2010 Climate Normals and Averages - Climate - Environment and Climate Change Canada,” 31-Oct-2011. [Online]. Available: http://climate.weather.gc.ca/climate_normals/station_select_1981_2010_e.html?searchType=stnProv&lstProvince=ON.

[59] D. Zhang, R. Barua, and A. Fung, “TRCA-BILD Archetype Sustainable House - Overview of Monitoring System and Preliminary Results for Mechanical Systems,” *ASHRAE Trans.*, p. 17.

[60] A. Safa, A. Fung, and W. Leong, “The Archetype Sustainable House: Performance Simulation of a Variable Capacity Two-Stage Air Source Heat Pump System,” presented at the 12th Conference of International Building Performance Simulation Association, 2011, pp. 14–16.

[61] A. A. Safa, “Performance Analysis of a Two-Stage Variable Capacity Air Source Heat Pump and A Horizontal Loop Coupled Ground Source Heat Pump System,” 2009.

[62] J. L. Zhang, “Analysis and feasibility study of a multi-pass heat and energy recovery ventilator with integrated economizer for residential use.”

[63] I. Knight, N. Kreutzer, M. Manning, M. Swinton, and H. Ribberink, “European and Canadian non-HVAC Electic and DHW Load Profiles for Use in Simulating the Performance of Residential Cogeneration Systems,” *Energy Conserv. Build. Community Syst. Programme IEA Annex 42*, vol. 6, 2007.

[64] U. Jordan and K. Vajen, “Realistic Domestic Hot-Water Profiles in Different Time Scales,” 2001.

[65] E. Shaughnessy, *Introduction to Fluid Mechanics*. 1998.

[66] V. S. Kravchenko, “Empirical equation derived for temperature dependence of density of heavy water,” *Sov. At. Energy*, vol. 20, no. 2, pp. 212–212, Feb. 1966.

[67] Ministry of Municipal Affairs and Housing Building and Development Branch, “Ontario Building Code - Supplementary Standard SB-12 Energy Efficiency for Housing.” 2012.

[68] Ontario Energy Board, “Distribution Rates Application,” 2019. [Online]. Available: https://www.oeb.ca/industry/applications-oeb/electricity-distribution-rates.

[69] Enbridge, “Understanding Gas Rates | Enbridge Gas,” *Enbridge understanding gas rates*. [Online]. Available: https://www.enbridgegas.com/Understanding-gas-rates. [Accessed: 19-Aug-2019].

[70] Union Gas, “Conversion Factors - Business - Union Gas.,” 2019. [Online]. Available: https://www.uniongas.com/business/save-money-and-energy/analyze-your-energy/energy-insights-information/conversion-factors.

[71] Q. Zhang, L. Zhang, J. Nie, and Y. Li, “Techno-economic analysis of air source heat pump applied for space heating in northern China,” *Appl. Energy*, vol. 207, pp. 533–542, Dec. 2017.

[72] G. Strbac, “Demand side management: Benefits and challenges,” *Energy Policy*, vol. 36, no. 12, pp. 4419–4426, Dec. 2008.

[73] K. Klein, S. Herkel, H.-M. Henning, and C. Felsmann, “Load shifting using the heating and cooling system of an office building: Quantitative potential evaluation for different flexibility and storage options,” *Appl. Energy*, vol. 203, pp. 917–937, Oct. 2017.

[74] M. Robillart, P. Schalbart, F. Chaplais, and B. Peuportier, “Model reduction and model predictive control of energy-efficient buildings for electrical heating load shifting,” *J. Process Control*, vol. 74, pp. 23–34, Feb. 2019.

[75] M. Debbarma, K. Sudhakar, and P. Baredar, “Thermal modeling, exergy analysis, performance of BIPV and BIPVT: A review,” *Renew. Sustain. Energy Rev.*, vol. 73, pp. 1276–1288, Jun. 2017.

[76] A. Mazur and D. Słyś, “Possibility of heat recovery from gray water in residential building,” *Sel. Sci. Pap. - J. Civ. Eng.*, vol. 12, no. 2, pp. 155–162, Dec. 2017.

[77] J. Rugolo and M. J. Aziz, “Electricity storage for intermittent renewable sources,” *Energy Environ. Sci.*, vol. 5, no. 5, p. 7151, 2012.

[78] M. Aprile *et al.*, “District Power-To-Heat/Cool Complemented by Sewage Heat Recovery,” *Energies*, vol. 12, no. 3, p. 364, Jan. 2019.

[79] UNFCCC, “What is the Paris Agreement?” [Online]. Available: https://unfccc.int/process-and-meetings/the-paris-agreement/what-is-the-paris-agreement.

[80] America 2050, “America 2050.” [Online]. Available: http://www.america2050.org/about.html.

[81] F. Wang *et al.*, “Performance investigation of a novel frost-free air-source heat pump water heater combined with energy storage and dehumidification,” *Appl. Energy*, vol. 139, pp. 212–219, Feb. 2015.

[82] Y. Xu, Y. Huang, N. Jiang, M. Song, X. Xie, and X. Xu, “Experimental and theoretical study on an air-source heat pump water heater for northern China in cold winter: Effects of environment temperature and switch of operating modes,” *Energy Build.*, vol. 191, pp. 164–173, May 2019.

[83] W. Peng, Z. Hisham, and J. Pan, “Household level fuel switching in rural Hubei,” *Energy Sustain. Dev.*, vol. 14, no. 3, pp. 238–244, Sep. 2010.